FINAL REPORT

Scientific Basis for Paint Stripping Mechanism for Methylene Chloride Based Paint Removers

SERDP Project WP-1682

SEPTEMBER 2011

Young Han, Ph.D
NAVAIR Materials Engineering Division

SERDP
DOD ▪ EPA ▪ DOE

Report Documentation Page

Form Approved
OMB No. 0704-0188

1. REPORT DATE	2. REPORT TYPE	3. DATES COVERED
SEP 2011	**Final**	**-**

4. TITLE AND SUBTITLE	5a. CONTRACT NUMBER
Scientific Basis for Paint Stripping Mechanism for Methylene Chloride Based Paint Remove	5b. GRANT NUMBER
	5c. PROGRAM ELEMENT NUMBER
6. AUTHOR(S)	5d. PROJECT NUMBER
	5e. TASK NUMBER
	5f. WORK UNIT NUMBER
7. PERFORMING ORGANIZATION NAME(S) AND ADDRESS(ES) **NAVAIR Materials Engineering Division**	8. PERFORMING ORGANIZATION REPORT NUMBER
9. SPONSORING/MONITORING AGENCY NAME(S) AND ADDRESS(ES)	10. SPONSOR/MONITOR'S ACRONYM(S)
	11. SPONSOR/MONITOR'S REPORT NUMBER(S)

12. DISTRIBUTION/AVAILABILITY STATEMENT
Approved for public release, distribution unlimited

13. SUPPLEMENTARY NOTES
The original document contains color images.

14. ABSTRACT

15. SUBJECT TERMS

16. SECURITY CLASSIFICATION OF:			17. LIMITATION OF ABSTRACT	18. NUMBER OF PAGES	19a. NAME OF RESPONSIBLE PERSON
a. REPORT	b. ABSTRACT	c. THIS PAGE			
unclassified	**unclassified**	**unclassified**	**SAR**	**118**	

(This page intentionally left blank)

TABLE OF CONTENTS

1. Abstract ..... **Error! Bookmark not defined.**
2. Objective 2-1
3. Background 3-1
4. Materials and Methods 4-1
4.1 Chemicals 4-1
4.2 Coating Samples 4-1
4.2.1 Free Films 4-2
4.2.1.1 Reformulation Approach 4-2
4.2.1.2 Centrifuged Approach 4-3
4.2.1.3 Application Methods 4-4
4.2.1.4 Film Thickness 4-6
4.2.2 Clear Samples used for gravimetric solvent sorption experiment 4-6
4.2.2.1 MIL-PRF-23377 4-6
4.2.2.2 MIL-PRF-85285 4-7
4.2.2.3 MIL-PRF-85582 4-7
4.2.3 Fully Formulated Samples used for Gravimetric Solvent Sorption Experiment 4-8
4.2.3.1 MIL-PRF-85285 4-8
4.2.3.2 MIL-PRF-23377 4-9
4.3 Film Sample Exposure 4-10
4.3.1 Thermal analysis 4-10
4.3.2 Raman 4-11
4.3.3 NMR 4-11
4.4 Experimental Methods 4-11
4.4.1 Diffusion Cell Test 4-11
4.4.2 Gravimetric Solvent Sorption 4-13
4.4.3 Differential Scanning Calorimetry 4-14
4.4.4 Thermogravimetric Analysis 4-14
4.4.5 Fourier Transformed Infrared Spectroscopy-Attenuated Total Reflectance 4-14
4.4.6 Raman Spectrometry 4-15
4.4.7 Gas Chromatography – Mass Spectroscopy 4-15

4.4.8 X-ray Photoelectron Spectroscopy 4-15
4.4.9 Scanning Electron Microscopy 4-15
4.4.10 Proton (^{1}H) and Deuterium (^{2}H) Solid State NMR 4-15
4.4.11 Coating Removal 4-16
5. Results and Discussion 5-1
5.1 ARL Preparation of Clear Samples 5-1
5.2 Solvent Diffusion 5-2
5.2.1 Diffusion Cell 5-3
5.2.1.1 Diffusion Mode 5-3
5.2.1.2 Diffusion Rate and Control Factors 5-8
5.2.2 Gravimetric Solvent Sorption 5-11
5.2.2.1 MIL-PRF-23377 Clear Sample: MC vs. EtOH 5-11
5.2.2.2 Diffusion Coefficient: Diffusion Cell vs. Gravimetric Solvent Sorption 5-12
5.2.2.3 Methylene Chloride Sorption: MIL-PRF-23377 Clear vs. Fully Formulated 5-13
5.2.2.4 Methylene Chloride Sorption: Clear vs. Fully Formulated 5-14
5.2.3 Solvent Sorption Rates and Physical Changes 5-15
5.2.3.1 MIL-PRF-85285 Clear 5-15
5.2.3.2 MIL-PRF-85285 Fully Formulated 5-17
5.2.3.3 MIL-PRF-23377 Clear 5-21
5.2.3.4 MIL-PRF-23377 Fully Formulated 5-25
5.3 Thermal Analysis 5-28
5.3.1 Initial characterization 5-28
5.3.2 Clear Films 5-28
5.3.3 Color Change and Headspace Analysis 5-33
5.3.4 Fully Formulated Films 5-33
5.3.5 Comparison of clear, partially formulated and fully formulated films 5-37
5.4 Vibrational Spectrometry 5-40
5.4.1 Dilation of Polymer Hydrogen Bonding 5-41
5.4.2 Chemical Change: Hydrolysis 5-45
5.5 Solid-State NMR Analysis 5-51
5.5.1 ^{1}H Solid-state NMR of MIL-DTL-53039 Clear Film Exposed to MC 5-52

5.5.2 ^{2}H Solid-state NMR of MIL-DTL-53039 Clear Film Exposed to CD_2Cl_2 (d_2-MC) 5-56
5.5.3 ^{1}H Solid-State NMR of MIL-PRF-23377 Clear Film Exposed to Phenol/Ethanol 5-57
5.5.4 ^{2}H Solid-state NMR of Solid d_5-Phenol and of MIL-PRF-23377 Clear Film Exposed to d_5-Phenol/Ethanol Mixtures 5-59
5.6 Coating Removal 5-68
6. Conclusion 6-1
7. Literature Cited 7-1
8. Appendices 8-1
8.1 List of Scientific/Technical Publications 8-1

(This page intentionally left blank)

LIST OF TABLES

Table 4-1. List of the composition of the control solvent formulations 4-1
Table 4-2. Specifications for coatings used for the project 4-2
Table 4-3. Film Thickness 4-6
Table 5-1. Best fit linear line: MIL-PRF-85285 clear film 5-4
Table 5-2. Best fit linear line: MIL-PRF-23377 clear film 5-5
Table 5-3. Best fit linear line: MIL-PRF-85582 clear film 5-6
Table 5-4 Best fit linear line: MIL-DTL-53039 clear film 5-7
Table 5-5. Best fit linear line: MIL-DTL-53022 clear film 5-8
Table 5-6. Hansen and Hildebrandt Solubility parameters 5-9
Table 5-7. Physical properties of penetrants 5-9
Table 5-8. Diffusion coefficient obtained from the solvent sorption experiment 5-13
Table 5-9. Dimensions of sample before and after absorption test with MIL-PRF-23377 clear sample and MC 5-22
Table 5-10. Dimensions of Sample before and after Absorption Test with MIL-PRF-23377 Clear Sample and EtOH 5-24
Table 5-11. Reported glass transition values of clear coatings from DSC 5-29
Table 5-12. Glass Transition temperatures for clear and fully formulated films after a two hour exposure to control solvent solutions 5-34
Table 5-13. Glass transition temperatures of clear, partial and fully formulated coatings of MIL-85285 and MIL-53039 5-38

(This page intentionally left blank)

LIST OF FIGURES

Figure 4-1. Centrifuge and example of MIL-DTL-53039 after processing using the centrifuge 4-3
Figure 4-2. Fluid separated from MIL-DTL-53039 (Note tint from carbazole violet) 4-4
Figure 4-3. An HVLP similar to the ones pictured above was used in the spray applications of the tested coatings 4-5
Figure 4-4: Byrd film applicator used for casting a thin film 4-5
Figure 4-5. Mold used for gravimetric solvent sorption test sample preparation 4-7
Figure 4-6. Clear samples for gravimetric solvent sorption test MIL-PRF-23377 (left) and MIL-PRF-85285 (right) 4-8
Figure 4-7. MIL-PRF-85285 fully formulated samples for gravimetric solvent sorption test 4-9
Figure 4-8. MIL-PRF-23377 fully formulated in mold 4-10
Figure 4-9. MIL-PRF-23377 fully formulated samples for gravimetric solvent orption test 4-10
Figure 4-11. Top View of diffusion cell on acrylic plate 4-12
Figure 4-12. Diffusion cell experiment set-up 4-12
Figure 4-10. Schematic diagram of the diffusion cell 4-12
Figure 4-13. Micrographs (80 magnifications) 4-13
Figure 4-14. Gravimetric solvent sorption experiment set-up 4-14
Figure 4-15. Examples of T_1 and $T_{1\rho}$ data analysis each for one sample at one temperature 4-16
Figure 4-16. Coating removal experiment set-up 4-17
Figure 5-1. Examples of MIL-DTL-53039 centrifuged clear unsupported films on release paper, typical of the centrifuged samples submitted 5-2
Figure 5-2. Diffusion graph: MIL-PRF-85285 clear film 5-4
Figure 5-3. Diffusion graph: MIL-PRF-23377 clear film 5-5
Figure 5-4. Diffusion graph: MIL-PRF-85582 clear film 5-6
Figure 5-5. Diffusion graph: MIL-DTL-53039 clear film 5-7
Figure 5-6. Diffusion graph: MIL-DTL-53022 clear film 5-8
Figure 5-7. Micrograph for diffusion of aqueous solution of 5% phenol through clear MIL-PRF-85285 film for 13 hours 5-10
Figure 5-8. Percentage weight change vs. square root of minute graph for MIL-PRF-23377 clear samples 5-12
Figure 5-9. Methylene chloride solvent sorption in clear and MIL-PRF-23377 fully formulated samples 5-14
Figure 5-10. Methylene chloride solvent sorption in clear and fully formulated MIL-PRF-85285 samples 5-15
Figure 5-11 Solvent sorption of MIL-PRF-85285 clear samples 5-16
Figure 5-12. MIL-PRF-85285 clear sample exposed to MC/EtOH 5-17
Figure 5-13. MIL-PRF-85285 clear sample exposed to MC/PhOH 5-17

Figure 5-14. Solvent sorption of MIL-PRF-85285 fully formulated sample 5-18
Figure 5-15. Swelling of MIL-PRF-85285 fully formulated with MC/EtOH 5-19
Figure 5-16. Physical changes of MIL-PRF-85285 fully formulated sample exposed to MC/PhOH 5-20
Figure 5-17. Solvent sorption of MIL-PRF-23377 clear samples 5-21
Figure 5-18. Swelling of MIL-PRF-23377 clear sample with Methylene Chloride..... 5-22
Figure 5-19. Gravimetric solvent sorption test result with MIL-PRF-23377 clear sample with MC/PhOH: % weight change vs. time (minutes) 5-23
Figure 5-20. Fracture of MIL-PRF-23377 clear sample: after eighth data point (left) and three days (right) 5-23
Figure 5-21. MIL-PRF-23377 clear sample before and after absorption test with ethanol.... 5-24
Figure 5-22. Solvent sorption of MIL-PRF-23377 fully formulated samples..... 5-25
Figure 5-23. MIL-PRF-23377 fully formulated sample before and after absorption test with methylene chloride..... 5-26
Figure 5-24. Surface degradation of MIL-PRF-23377 fully formulated sample exposed to MC/PhOH 5-27
Figure 5-25. MIL-PRF-23377 fully formulated sample before and after absorption test with MC/PhOH 5-27
Figure 5-26. TGA overlay for the MIL-DTL-53039 clear film..... 5-30
Figure 5-27. TGA overlay for the MIL-PRF-85285 clear film 5-30
Figure 5-28. TGA overlay for the MIL-PRF-85582 clear film 5-31
Figure 5-29. TGA overlay for the MIL-PRF-23377 clear film 5-32
Figure 5-30. TGA overlay for the MIL-DTL-53022 clear film..... 5-32
Figure 5-31. Examples of color change of clear films after exposure to phenol solution (MIL-DTL-53039 on left, MIL-PRF-23377 on right) 5-33
Figure 5-32. TGA overlay of MIL-PRF-85582 fully formulated film 5-35
Figure 5-33. TGA overlay of MIL-PRF-85285 fully formulated film 5-35
Figure 5-34. TGA overlay of MIL-DTL-53039 fully formulated film 5-36
Figure 5-35. TGA overlay of MIL-PRF-23377 fully formulated film 5-36
Figure 5-36. TGA overlay of MIL-DTL-53022 fully formulated film 5-37
Figure 5-37. TGA overlay of the three formulations of control (unexposed) coatings of CARC polyurethane topcoat (MIL-DTL-53039)..... 5-38
Figure 5-38. TGA overlay of the three formulations of control (unexposed) coatings of NAVY topcoat (MIL-PRF-85285) 5-39
Figure 5-39. TGA overlay of Partial Formulated CARC polyurethane topcoat (MIL-DTL-53039) exposed to different solvent mixtures..... 5-39
Figure 5-40. TGA overlay of partial formulations of NAVY polyurethane topcoat (MIL-PRF-85285) exposed to different solvent mixtures 5-40
Figure 5-41. Raman spectra of the MIL-PRF-85285 clear film alone and saturated with methylene chloride (left) , zoom of C=O region (right) 5-42

Figure 5-42. Raman spectra of the MIL-DTL-53039 clear film exposed to methylene chloride (left), zoom of C=O region (right) 5-42
Figure 5-43. FTIR-ATR spectra of the MIL-DTL-53039 clear film before and after exposure to methylene chloride and MC/EtOH 5-43
Figure 5-44. Raman spectra of MIL-DTL-53039 clear film before and after exposure to MC/EtOH including an expansion to resolve the carbonyl peak 5-44
Figure 5-45. FTIR of MIL-DTL-53039 clear film before and after exposure to MC/EtOH/H_2O 5-45
Figure 5-46. XPS of carbon (1s) in MIL-DTL53039 clear film before and after exposure to MC/EtOH/H2O 5-46
Figure 5-47. XPS of Oxygen (1s) in MIL-DTL-53039 clear film before and after exposure to MC/EtOH/H2O 5-46
Figure 5-48. XPS of Nitrogen (1s) in MIL-PRF-53039 clear film before and after exposure to MC/EtOH/H2O 5-47
Figure 5-49. Electron micrographs of MIL-PRF-85285 clear film exposed to (left) methylene chloride and (right) MC/EtOH/H_2O, demonstrating significant surface changes as a result of exposure 5-48
Figure 5-50. FTIR spectra demonstrating solvent persistence in MIL-PRF-53039 clear film after drying 5-48
Figure 5-51. Raman spectra of MIL-DTL-53039 clear film before and after exposure to MC/EtOH/H_2O/PhOH 5-49
Figure 5-52. FTIR spectra of MIL-DTL-53039 clear film before and after exposure to MC/EtOH/H_2O/PhOH 5-50
Figure 5-53. Raman spectra of MIL-DTL-53039 clear film before and after exposure to phenol/water 5-51
Figure 5-54. Schematic example of polymer segmental dynamics affecting ^1H NMR relaxation through modulation of proton-proton dipolar coupling 5-53
Figure 5-55. Proton NMR T_1 vs. temperature for MIL-DTL-53039 clear film before and after 5-minute exposure to methylene chloride at 20°C. Also shown is the T_1 of neat methylene chloride 5-54
Figure 5-56. Proton NMR $T_{1\rho}$ vs. temperature for MIL-DTL-53039 clear film before and after 5-minute exposure to methylene chloride at 20°C 5-55
Figure 5-57. Wideline proton NMR spectra of MIL-DTL-53039 clear film at two different temperatures, and after exposure to methylene chloride 5-55
Figure 5-58. Deuterium quadrupole-echo NMR spectra of CD_2Cl_2 exposed MIL-DTL-53039 clear film at three different temperatures as indicated, and measurement of T_2 transverse relaxation time at 0°C 5-57
Figure 5-59. Proton NMR half-height linewidths vs. temperature for MIL-PRF-23377 clear film before and after exposure to phenol/ethanol 5-58

Figure 5-60. Proton NMR $T_{1\rho}$ relaxation times for MIL-PRF-23377 clear film vs. temperature, before and after exposure to phenol/ethanol for 10 minutes at 20°C 5-59
Figure 5-61. ^2H quadrupolar-echo NMR spectrum of solid d_5-phenol..... 5-60
Figure 5-62. ^2H quadrupolar-echo NMR spectra at 24°C of MIL-PRF-23377 clear film exposed to d_5-PhOH/EtOH (3.115/1.0) for 10 minutes, at four different echo times tau as indicated. The differing signal to noise ratios reflect differences in the number of scans acquired. The recycle delay was 0.2 s and exponential apodization (linebroadening) was 300 Hz. A wider plot of the τ = 40 μs spectrum is also depicted with a shaded region arising from the more mobile second component having a shorter T_2 5-61
Figure 5-63. ^2H quadrupolar-echo NMR spectra of MIL-PRF-23377 clear film exposed to d_5-PhOH/EtOH (3.115/1.0) for 10 minutes, at different temperatures. The recycle delay was 0.2 s, exponential apodization (linebroadening) was 300 Hz, and τ = 20 μs except as noted 5-62
Figure 5-64. ^2H quadrupolar-echo NMR spectra at 24°C of MIL-PRF-23377 epoxy primer exposed to d_5-PhOH/EtOH (3.115/1.0) for 2 hours, at four different temperatures and different echo times tau as indicated. The recycle delay was 0.2 s and exponential apodization (linebroadening) was 20 Hz. Note the expanded scale on two of the spectra at longer tau values..... 5-64
Figure 5-65. ^2H decay times at 24°C of MIL-PRF-23377 clear film exposed 2 hours to d_5-PhOH/EtOH, as measured by two different echo pulse sequences (see text). The single-exponential fit on the right is systematically lower than the experimental data points, unlike the biexponential fit..... 5-66
Figure 5-66. ^1H NMR spectra of epoxy primer MIL-PRF-23377 clear film exposed 2 hours to d_5-PhOH/EtOH at two different temperatures..... 5-67
Figure 5-67. Experimental Set-up for MIL-PRF-23377 Clear Coating Removal..... 5-68
Figure 5-68. MIL-PRF-23377 Clear Coating Exposed to MC, MC/PhOH, or MC/PhOH/H_2O..... 5-69
Figure 5-69. Separation of MIL-PRF-23377 Clear Coating Exposed to MC: At 6 Minutes and 58 Seconds (Left), 6 Minutes and 59 Seconds (Right) 5-69
Figure 5-70. MIL-PRF-23377 Fully Formulated Coating Exposed to MC/PhOH and MC/PhOH/H_2O..... 5-70

LIST OF ACRONYMS

AFM	atomic force microscopy
ARL	Army Research Laboratory
ATR	attenuated total reflectance
BzOH	benzyl alcohol
CARC	chemical agent resistant coating
CCC	chromate conversion coating
COTS	commercial-off-the-shelf
CP	cross-polarization
DFT	Dry Film Thickness
DoD	Department of Defense
DSC	differential scanning calorimetry
EDAX	energy dispersive X-ray
EM	electron microscopy
EPA	Environmental Protection Agency
EPR	electron paramagnetic resonance
ESOH	Environmental, Safety, and Occupational Health
ESR	electron spin resonance
EtOH	ethanol
FRC	Fleet Readiness Center
FRS	forward recoil spectroscopy
FTIR-ATR	Fourier transform infrared spectroscopy-attenuated total reflectance
GC/MS	gas chromatography with mass spectrometry
^{1}H	proton
^{2}H	deuterium
HDI	hexamethylene diisocyanate
HHLW	half-height linewidth
HVLP	high volume low pressure
IGC	inverse gas chromatography
MAS	magic-angle spinning
MC	methylene chloride

MRI	nuclear magnetic resonance imaging
MS	Microsoft
NAVAIR	Naval Air Systems Command
NDI	nondestructive inspection
NMR	nuclear magnetic resonance spectroscopy
NQCC	nuclear quadruple coupling constant
NRL	Naval Research Laboratory
NS	neutron scattering
OSHA	Occupational Safety and Health Administration
PALS	positron annihilation lifetime spectroscopy
PhOH	phenol
PI	Principal Investigator
PMMA	poly(methyl methacrylate)
PU	polyurethane
RBS	Rutherford backscattering spectroscopy
RCS	refrigerated cooling system
RL	radioactive labeling
SERDP	Strategic Environmental Research and Development Program
SQRT	square root
SUNY	State University of New York
T_1	spin-lattice relaxation time
$T_{1\rho}$	spin-lattice relaxation time in the rotating frame
T_2	spin-spin relaxation time
TCP	trivalent chromium pretreatment
T_g	glass transition temperature
TGA	thermogravimetric analysis
T_J	jump time
UV	ultraviolet
VOC	volatile organic compound
WFT	wet film thickness
WP	weapons program

WRS	waveguide Raman spectroscopy
XPS	X-ray photoelectron spectroscopy

(This page intentionally left blank)

ACKNOWLEDGEMENTS

The financial and programmatic support of this Strategic Environmental Research and Development Program (SERDP) project under the direction of Dr. Jeffrey Marqusee, Executive Director, and Mr. Bruce Sartwell, Manager of the Weapons Systems and Platforms, is gratefully acknowledged.

The project team supported this SERDP project consists of five technical groups led by:
Dr. Clive Clayton, Leading Professor, State University of New York (SUNY) Stony Brook, Materials Science and Engineering Department;
Dr. Young Han, Principal Investigator (PI), Naval Air Systems Command (NAVAIR), Materials Engineering Division;
Mr. John Kelley, Army Research Laboratory (ARL), Weapons and Materials Research Directorate;
Dr. James Wynne, Naval Research Laboratory (NRL), Organic Chemistry Branch; and
Dr. James Yesinowski, NRL, Materials Chemistry Branch.

Substantial contributions to the execution of the project and preparation of this report were made by:
Mr. Thomas Braswell, ARL, Weapons and Materials Research Directorate;
Mr. Dane Hanson, NAVAIR, Materials Engineering Division;
Dr. Kevin Kovaleski, NAVAIR, Materials Engineering Division;
Mr. Nick Nesteruk, ARL, Weapons and Materials Research Directorate;
Mr. Frank Pepe, NAVAIR, Materials Engineering Division;
Mr. Kyle Russell, NAVAIR, Materials Engineering Division;
Ms. Kelly Watson, NRL, Organic Chemistry Branch; and
Mr. Christopher Young, SUNY Stony Brook, Materials Science and Engineering Department.

(This page intentionally left black)

1. Abstract

Objective

The objective of this project is to determine the depaint mechanisms of methylene chloride based paint removers.

Technical Approach

Two pillars of the technical approach used to achieve the objective are (1) a study that monitors the physical changes in the paints exposed to the paint removers and identifies their causes and (2) a spectroscopic study that leads to gain a fundamental understanding of the chemical interactions between the paints and the paint removers at the molecular level.

Results

Physical changes in paints (coatings) were studied by (1) measuring solvent diffusion rates using the diffusion cell and gravimetric solvent sorption test methods and (2) monitoring sorption behavior and visual changes of the coating samples exposed to solvents. The diffusion cell study clearly indicates that methylene chloride diffuses faster than ethanol, phenol, benzyl alcohol, and methylene chloride solutions of ethanol, phenol, and benzyl alcohol. The comparison of these diffusion rates to Hansen hydrogen bonding parameters indicate that the molecules with lower Hansen hydrogen bonding parameters and molar volumes have higher diffusion rates. Another important fact found from the diffusion cell study is that the diffusion rates of ethanol, phenol, and benzyl alcohol are substantially increased when they are mixed with methylene chloride. This suggests that methylene chloride increases diffusion rates of these molecules.

The clear coating samples exposed to the methylene chloride solution of phenol (20% by weight) or ethanol (9% by weight) fractured before their sorption equilibriums were reached while the same samples exposed to methylene chloride did not. It was also found that the sample exposed to the methylene chloride solution of phenol is much stiffer than other samples. No crack developed during the solvent sorption tests for the fully formulated samples. As the case for the clear samples, weight increases of the fully formulated samples exposed to the methylene chloride solution of phenol at their sorption equilibriums were substantially higher than the same samples exposed to methylene chloride only.

Changes to the molecular-level properties of the coatings upon exposure to the components of the paint removers were studied using analytical and spectroscopic techniques; differential scanning calorimetry (DSC), thermogravimetric analysis (TGA), gas chromatography with mass spectrometry (GC/MS), solid-state proton (^{1}H) and deuterium (^{2}H) nuclear magnetic resonance spectroscopy (NMR), Raman spectroscopy, X-ray photoelectron spectroscopy (XPS), and attenuated total reflectance Fourier transform infrared spectroscopy (FTIR-ATR). DSC results of methylene chloride solutions containing water and phenol show coating degradation. FTIR-ATR and XPS results indicate a hydrolysis reaction occurring in localized regions of the coating exposed to the methylene chloride solution of ethanol and water. The DSC and TGA data show exposure to phenol containing solutions to cause the coating degradation. Deuterium NMR of d_2-methylene chloride (CD_2Cl_2) at various temperatures shows that the methylene chloride molecules present in the polyurethane (MIL-DTL-53039) clear film undergo isotropic rotational tumbling and the rate of tumbling is orders of magnitude slower than that in solvents, suggestive

of weak interactions with groups on the polymer, perhaps via electric dipoles. Variable temperature quadrupolar-echo spectra and the transverse relaxation time measurements suggest that the d_5-phenol is covalently bonded to the polymer through the substitution reaction of phenol with nucleophilic sites of the polymer chain. Reaction mechanisms for these spectroscopic findings are not yet confirmed.

The coating removal study was performed to verify the supposition that hydrogen bonding between donor hydroxides on the substrate and the epoxy groups of the primer coating is the primary adhesion strength of the substrate-epoxy interface and the hydrogen bond strength can be substantially lowered by adsorbed water working as a lubricant. Tests performed with the fully formulated epoxy primer on chromate conversion coated aluminum panels clearly indicates that water is an important component of the methylene chloride based paint stripper since methylene chloride did not remove the coating at all and the methylene chloride solution of phenol barely removed the coating. These results do not prove the supposition, but still support that the water induced interfacial delamination may be the reason for faster removal of coatings. From the same experiment, we also found that one role of water is to prevent the removed coatings from re-adhesion.

Benefits

The results from this project will help formulate a new class of paint removers. Once implemented, the process owners will realize advantages of the new paint removers such as (1) lower volatile organic compounds (VOC) emission, (2) less hazardous solid waste disposal, (3) compliance with environmental, safety, and occupational health (ESOH) regulations, (4) reduced process times, and (5) reduced corrosion-related repair time. As a result, the Department of Defense (DoD) will realize significant cost savings in the depaint and corrosion control operations.

2. Objective

The objective of the SERDP WP-1682 project is to determine the depaint mechanisms of methylene chloride based paint removers. Two pillars of the technical approach used to achieve the objective are (1) a study that monitors the physical changes in the paints exposed to the piant removers and identifies their causes and (2) a spectroscopic study that leads to gain a fundamental understanding of the chemical interactions between the paints and the paint removers at the molecular level.

(This page intentionally left blank)

3. Background

Environmental Concern

In the Department of Defense (DoD), organic coating removal operations mainly utilized chemical paint removers qualified for use under the military paint remover specification, MIL-R-81294. MIL-R-81294 paint removers provide superior performance; however, these paint removers contain methylene chloride and phenol that are under various EPA and OSHA regulations. Due to the Environmental, Safety, and Occupational Health (ESOH) reasons, non-chemical based paint removal methods have been developed and implemented. Non-chemical based paint removal methods include water-jet stripping, media blasting, and high intensity light source stripping.[2] Non-chemical based paint removal technologies have been found suitable for certain parts, yet a chemical approach is preferred over non-chemical methods for large scale maintenance work, parts of complex geometry and the paint stripping prior to nondestructive inspection (NDI).

Performance Concern

For the reasons discussed above, ESOH compliant chemical paint removers have been developed and implemented; however, these products were found to have substantially lower stripping rates as compared to MIL-R-81294 paint removers. It has been assumed that the inferior performance is primarily due to the fact that ESOH compliant chemical paint removers are formulated with less aggressive chemicals such as benzyl alcohol. The NAVAIR Jacksonville estimated 2,873 pounds (lbs) of volatile organic compound (VOC) emission from the depaint operation and $129,565 for the total cost of depaint and paint operations for one P-3 aircraft. Based on twenty-five P-3 aircraft maintenance cycles per year, an annual VOC emission of 71,825 lbs and an operation cost of $3,239,125 were estimated. Improved paint removers could substantially lower the depaint operation cost and the environmental burden by reducing operation time and eliminating regulated chemicals. The control specification for the ESOH compliant chemical paint removers is TT-R-2918. Peroxide has been found to accelerate paint stripping for TT-R-2918 paint removers. A concern is whether or not hydrogen peroxide is safe on various aluminum alloys and high strength steels commonly used as aircraft and support equipment construction materials. It was reported that severe corrosion has been found on aircraft and 2024 aluminum alloy panels depainted with a hydrogen peroxide-activated paint stripper.[3]

Military Aircraft Coatings

MIL-R-81294 includes four types of paint removers: (1) Type I for removal of epoxy and polyurethane topcoat systems (2) Type II for removal of polyurethane topcoat systems, (3) Type III for removal of polysulfide basecoat systems, and (4) Type IV for removal of polyurethane intercoat systems. Depending on the local environmental regulations and the process conditions, the Navy and the Air Force use one of two epoxy primers: (1) MIL-PRF-23377, Performance Specification, Primer Coatings: Epoxy, High-Solids and (2) MIL-PRF-85582, Performance Specification, Primer Coatings: Epoxy, Waterborne. MIL-PRF-23377 epoxy primer is a two component system that consists of an epoxy resin component and a polyamide catalyst component. Upon application and drying of the mixed components, a highly crosslinked film forms on the substrate. The waterborne epoxy primer chemistry is different from the solvent borne counterpart.[4] Maintenance personnel in the Navy Fleet Readiness Centers (FRC) have

stated that the MILPRF-85582 primer is more difficult to remove chemically than the MIL-PRF-23377 primer. However, the energy dispersive X-ray (EDAX) spectra from a MIL-PRF-23377 primer and a MIL-PRF-85582 primer show identical patterns and intensities. The epoxy resin component contains corrosion inhibitors, pigments, and/or extenders. The epoxy binder and these additives are important determining factors for the efficiency of chemical paint strippers.

The Navy and the Air Force use a polyurethane topcoat conforming to MIL-PRF-85285 for aircraft and support equipment. MIL-PRF-85285 includes two classes; (1) Class H for high solid formulation and (2) Class W for waterborne formulation. Class H is a two component system that provides a flexible, durable, weather and chemical resistant coating upon curing. Aliphatic isocyanates such as hexamethylene diisocyanate (HDI) are used for the military application because of their ultraviolet light stability. Aliphatic isocyanates react with another component, polyester polyols, forming the polyurethane topcoat. The polyurethane topcoat also contains color pigments and silicone dioxide filler. Two-component water borne polyurethane coatings, Class W, are based on an acrylic polyol emulsion and a water dispersible polyisocyanate.[5] The Navy is considering using Class W on support equipment. The Army developed the two component waterborne polyurethane chemical agent resistant coating (CARC) and tested its chemical strippability. This new waterborne polyurethane coating was stripped in five minutes using a commercial-off-the-shelf (COTS) methylene chloride based paint remover. The same product also stripped MIL-P-46168, two-component solvent-borne polyurethane CARC, in five minutes.[6] MIL-DTL-64159 is the control specification for the two-component waterborne polyurethane CARCs.

The Navy aircraft organic coating system is typically applied on the substrate treated with chromate conversion coating (CCC) or trivalent chromium pretreatment (TCP). These pretreatments provide (1) corrosion protection and (2) enhanced paint adhesion. The corrosion protection property of CCC has been extensively studied; as a result, we have a good understanding of the structure and composition of CCC. A study of the interfacial region between a metal substrate and an organic polymer has been another active research area in an attempt to prevent coating delamination, which can lead to corrosion. However, we have not found any study on the nature of the binding between CCC and coating primer, which might be an important factor in chemical paint stripping.

The military coating systems described above are designed to withstand extreme weather conditions and chemical attacks; as a consequence, removal is exceptionally difficult. A systematic study to understand how each component of the methylene chloride paint removers chemically and physically affects the coating components would provide important data to help understand how the coating system is removed and eventually help improve the performance of existing products or formulate new paint strippers.

4. Materials and Methods

4.1 Chemicals

All chemicals, except NMR solvents, were reagent grade and used without further purification. The d_2-methylene chloride and d_5-phenol (98% atom % D on aromatic ring) were obtained from Cambridge Isotopes Laboratory. The d_5-phenol was stored in a freezer to prevent its decomposition when it is not in use.

Solutions and mixtures were prepared by weight according to the ratios listed in Table 4-1. The selection of solutions or mixtures for this study was made to investigate how the performance of methylene chloride is influenced by other components. The solution of phenol and ethanol was used to compare its performance to the methylene chloride solutions. The ratios of the components in the solutions or mixtures are based on the ratio of the control formulation components.

Table 4-1. List of the composition of the control solvent formulations

		Component Weight Percent			
		Methylene chloride	Ethanol	Water	Phenol
Solution	MIL-R-81294 control formulation[a]	60.6	5.8	7.8	15.8
	Methylene chloride and ethanol	91	9	---	---
	Methylene chloride, ethanol and water[b]	82	8	10	---
	Methylene chloride, ethanol, water and phenol[b]	67	6	9	18
	Phenol and methylene chloride	79	---	---	21
	Phenol and ethanol	---	27	---	73
	Methylene chloride, phenol and ethanol[c]	74	7	---	19
	Methylene chloride, phenol and water[c]	78	---	1	21

Notes: [a] Also contains Methocel (1.2%), toluene (1.3%), sodium petroleum sulfonate (5.5%) and paraffin wax (1.9%),
[b] Methocel added to emulsify into a single phase, and
[c] Used only for diffusion, solvent sorption, and coating removal tests.

4.2 Coating Samples

Currently employed, most common military coatings were selected for this study. These included two polyurethane topcoats and three epoxy primers as shown in Table 4-2. Thin unsupported coating samples (free films) were used for DSC, TGA, GC/MS, solid-state ^{1}H and deuterium ^{2}H NMR, Raman spectroscopy, XPS, FTIR-ATR, and the diffusion cell study. Thicker samples, prepared utilizing a mold, were used for the gravimetric solvent sorption study.

Table 4-2. Specifications for coatings used for the project

Specification	Title
MIL-PRF-85285	Performance Specification, Coating: Polyurethane, Aircraft and Support Equipment
MIL-DTL-53039	Detail Specification, Coating, Aliphatic Polyurethane, Single Component, Chemical Agent Resistant
MIL-PRF-23377	Performance Specification, Primer Coatings: Epoxy, High-Solids
MIL-PRF-85582	Performance Specification, Primer Coatings: Epoxy, Waterborne
MIL-DTL-53022	Detail Specification, Primer, Epoxy Coating, Corrosion Inhibiting Lead and Chromate Free

To eliminate confusion for readers, the terminology of "film sample", "sample", "clear", "partially formulated", and "fully formulated" used in this report are defined here. Most of the experiments we performed require thin unsupported coating samples. So, ARL prepared thin coating samples for these experiments. These thin unsupported coating samples are called "films" or "film samples". The gravimetric solvent sorption experiments require substantially thicker samples than "films" because a thin "film" used in a solvent sorption test reaches its equilibrium sorption too quickly, which only allows us to obtain a limited number of data points. The thicker coating samples prepared for the gravimetric solvent sorption tests are called "samples". Some samples were prepared of polymeric binders with or without a small amount of organic additives. These samples are much clearer than the samples prepared of the product components received from the coating manufacturer. The samples prepared of organic binders only are called "clear". Limited studies were performed on partial formulations of the specified coatings, which are formulations containing all of the full formulation components except the flattening agents and are called "partially formulated". The samples prepared of the product from the coating manufacturer are called "fully formulated".

4.2.1 Free Films

ARL used two approaches to forming films without pigmentation (clear films); a reformulation approach and a centrifuged approach. The films prepared utilizing these two approaches were used for evaluating the efficacy of various paint stripping systems.

4.2.1.1 Reformulation Approach

Specific details of the formulations will not be presented in this report due to current non-disclosure agreements ARL has with coatings suppliers. General information can be obtained by reviewing the published information on the specific coatings.

Nearly 60 ingredients were required to assemble the coatings and produce films without prime pigments and extenders. Each was formulated to minimize the amount of flow-modifiers, surfactants, dispersants, or other additives that would confound the study with extraneous variables to the fundamental resin systems. As each formula was tested for application, films were cast onto paint test charts (commonly called "Leneta charts") using a film applicator.

4.2.1.2 Centrifuged Approach

In an effort to save time and simplify the process, the alternate approach using a centrifuge was employed to remove the opaque pigments and extenders. This would leave the flow modifiers and additives intact and could enhance the film integrity to help render clear films. The samples were centrifuged 3 times each @18,000 RPMs for 30 minutes to stratify the components and yield a nearly clear colored supernatant (Figures 4-1 and 4-2)

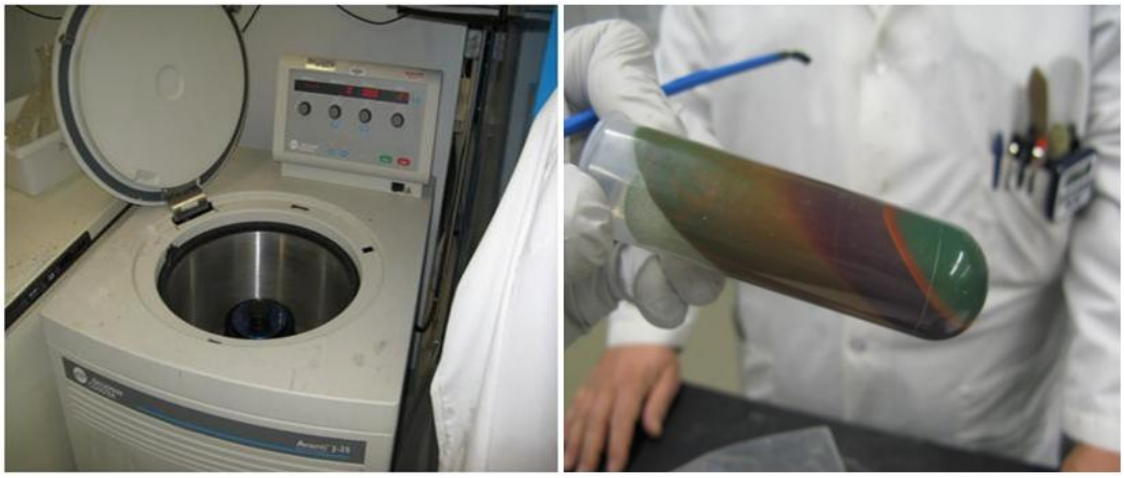

Figure 4-1. Centrifuge and example of MIL-DTL-53039 after processing using the centrifuge

Figure 4-2. Fluid separated from MIL-DTL-53039 (Note tint from carbazole violet)

4.2.1.3 Application Methods

Two application methods were used for producing the coatings: spray and casting. For the paint spray applications, an Air Atomizing Spray Gun application High Volume Low Pressure (HVLP) external mix spray gun was used (illustrated in Figure 4-3.). External-mix air atomizing guns are the most common spray guns used for applying high quality paint finishes. Where regulated to the tougher air emission standard, HVLP air atomizing guns are required. When charged with compressed air, the turbulent flow breaks up the liquid stream or atomizes it, causing it to break up into droplets that form a spray. Most external-mix guns have controls to regulate fluid flow, atomizing air, and spray patterns. These adjustments allow the guns to meet the finishing requirements of a variety of sizes and shapes.

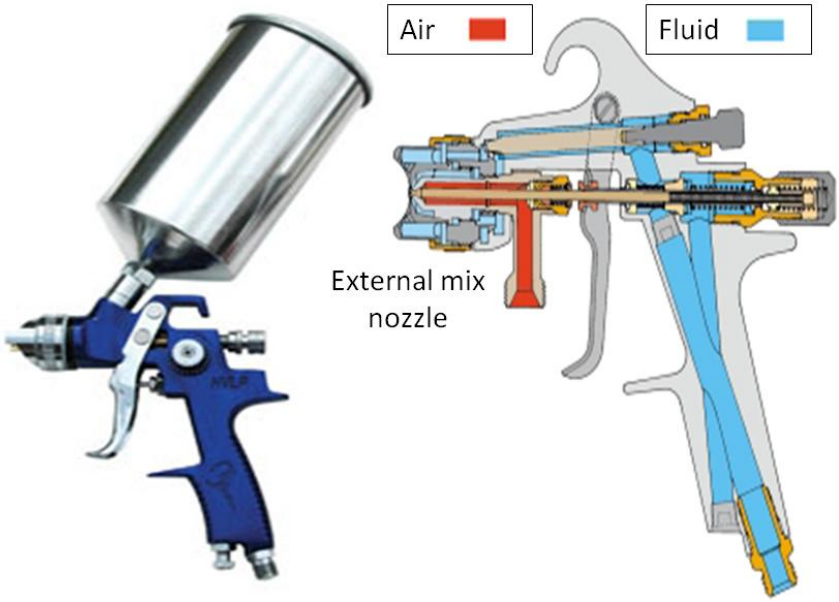

Figure 4-3. An HVLP similar to the ones pictured above was used in the spray applications of the tested coatings

A Byrd film applicator (illustrated in Figure 4-4.) was used to cast some of the films for this report to assist the formulator in making flow adjustments to the formulations. It is a precision-machined stainless steel bar that has a measured elevation to cast a wet paint film to a precise Wet Film Thickness (WFT) which will cure to a corresponding Dry Film Thickness (DFT) as the resin cures and solvents evaporate. This device aids the formulator in making quick modifications to the formula because results can be obtained in minutes.

Figure 4-4: Byrd film applicator used for casting a thin film

4.2.1.4 Film Thickness

The thickness of the free films used for DSC, TGA, GC/MS, solid-state ^{1}H and ^{2}H NMR, Raman spectroscopy, XPS, and FTIR-ATR was measured and found to be approximately 5 mils (0.127 mm or 127 μm), as shown in Table 4-3.

Table 4-3. Film Thickness

Military Specification	Clear Films (mm)	Partially Formulated Films (mm)	Fully formulated Films (mm)
MIL-DTL-53039	0.13	0.06	0.14
MIL-PRF-85285	0.13	0.07	0.20
MIL-PRF-23377	0.13	N/A	0.17
MIL-PRF-85582	0.17	N/A	0.15
MIL-DTL-53022	0.12	N/A	0.16

Notes: N/A – Not Applicable

The targeted thickness of the sample for the diffusion cell experiment was 4 mils (101.6 μm). However, the thickness variation was found to be ± 1 mil (± 25.4 μm) due to the limitation of hand spray painting on the thickness control. All clear films were aged at 150°F for seven days as specified in TT-R-2918 prior to diffusion cell experiments.

4.2.2 Clear Samples used for gravimetric solvent sorption experiment

Clear samples were prepared in the NAVAIR Materials Organic Coating Laboratory with aid from the ARL. Resin components of the clear samples are same to those of clear films.

4.2.2.1 MIL-PRF-23377

A mold (illustrated in Figure 4-5), which can produce 0.09 inch (2.286 mm) thick coating samples, was built using two tempered glass plates (10 inches by 10 inches) on the exterior, a right-angled U-shaped metal frame (1 inch wide) on the interior, and a dozen metal binder clips along the edges. Silicon oil was applied to the insides of the glass plates and the metal frame prior to assembly. The mold was assembled to produce a 4 inch by 8 inch sheet of coating sample. Coating part A was prepared by mixing component A (9.60 grams), component B (1.38 grams), and component C (3.10 grams) in a 100 mL plastic paint mixing cup. The mixing cup containing part A was covered with a piece of aluminum foil to minimize solvent loss. Part A was kept in an oven at 150°F until no air bubbles were observed. Likewise, part B was prepared by mixing component D (20.60 grams) and plasticizers (0.6 grams) in a 50 mL plastic paint mixing cup. Then, part B was slowly added to part A while the mixture was gently stirred with a glass rod. Air bubbles in the mixture were removed by heating at 150°F. The mixture was slowly poured into the mold until the mold was filled. The mold was then placed in an oven preheated to 150°F. The coating was cured at 150°F for 12 hours. At the completion of curing, the mold was allowed to cool in the oven to room temperature to avoid thermal shock. The clips were removed from the edges and the coating was removed from the mold by carefully

separating the glass plates from the cured coating. Circular samples illustrated in Figure 4-6 were punched out using a die of 1-inch diameter. The samples were aged at 150°F for seven days. The average diameter of the ten cured samples is 23.636 mm (0.9305 inch) with the standard deviation of 0.140 mm (0.0055 inch). The average thickness of the ten samples is 2.246 mm (0.0884 inch) with the standard deviation of 0.056 mm (0.0022 inch).

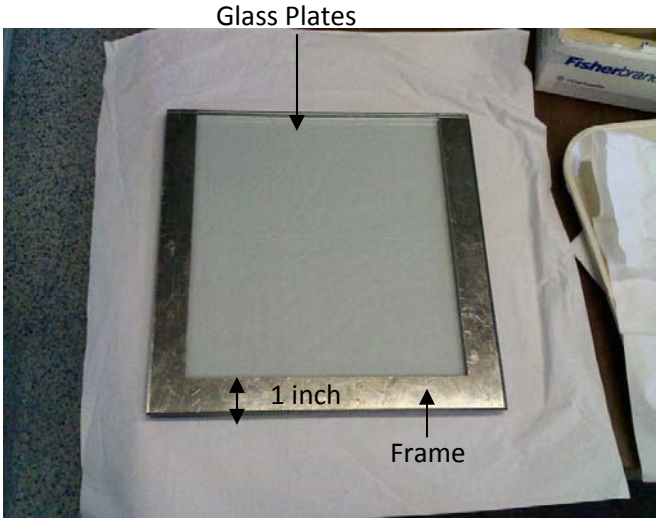

Figure 4-5. Mold used for gravimetric solvent sorption test sample preparation

4.2.2.2 MIL-PRF-85285

MIL-PRF-85285 samples (illustrated in Figure 4-6) were prepared by mixing component A (42.7 grams) and component B (36.9 grams). The sample preparation was the same as that of MIL-PRF-23377 except that the mold was assembled to produce a 9 inch by 8 inch sheet. The average diameter of ten cured die-cut samples is 24.926 mm (0.9813 inch) with the standard deviation of 0.100 mm (0.0039 inch). The average thickness of the ten cured sample is 2.302 mm (0.0906 inch) with the standard deviation of 0.049 mm (0.0019 inch).

4.2.2.3 MIL-PRF-85582

Attempts to prepare MIL-PRF-85582 clear samples using the same sample preparation technique described above were unsuccessful. Numerous attempts resulted in inhomogeneous, curled samples with unacceptably deep cracks.

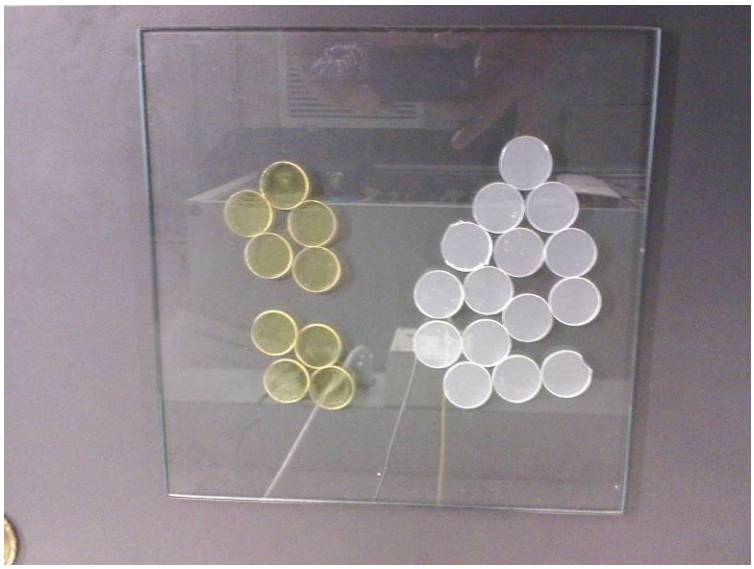

Figure 4-6. Clear samples for gravimetric solvent sorption test MIL-PRF-23377 (left) and MIL-PRF-85285 (right)

4.2.3 Fully Formulated Samples used for Gravimetric Solvent Sorption Experiment

4.2.3.1 MIL-PRF-85285

To 80 mL of part A in a 250 mL plastic paint mixing cup, 20 mL of part B was slowly added while the mixture was gently stirred using a glass rod as recommended in the manufacturer technical data sheet. The mixture in the cup was put inside of a vacuum desiccator connected to a faucet aspirator vacuum pump. Then the faucet was turned on and the mixture was kept in the desiccator until formation of bubbles ceased (approximately 30 minutes). Upon removal from the desiccator, the mixture was poured into the mold and cured at room temperature for 4 days at room temperature inside the fume hood and further cured at 150°F for 2 hours inside a temperature controlled oven. The mold was cooled down to room temperature and the sheet of cured coating was removed from the mold. Seven round samples were cut from the cured coating using a 1-inch hollow-punch and a hammer. The samples were aged at 150°F in an oven for 7 days. Figure 4-7 illustrates the aged fully formulated MIL-PRF-85285 samples.

Figure 4-7. MIL-PRF-85285 fully formulated samples for gravimetric solvent sorption test

4.2.3.2 MIL-PRF-23377

The methods used to prepare other samples for the gravimetric solvent sorption tests were found unsuitable for preparation of fully formulated MIL-PRF-23377 samples because the additive(s) (e.g. chromates) that are heavier than the resin precipitated during curing. The method described in the following paragraph provides samples with acceptable thickness and visually uniform composition.

A release film was affixed to a glass plate (10 x 10 inches) using double sided tape. The edges of the plate were covered with an aluminum frame (1 inch wide, 0.1 inch thick) and the frame was secured to the glass plate using metal binder clips. Then, this mold was laid on a flat surface. To 20 ml of part A in a 50 ml paint mixing cup, 5 ml of part B was slowly added while stirring using a glass rod as . The mixture was poured into the mold and spread evenly by tilting the mold side to side as recommended in the manufacturer technical data sheet. The mixture was allowed to partially cure at ambient temperature for 5 hours. Six (6) more layers were laid and allowed to partially cure in the same manner to build the thickness of the coating to the thickness of the aluminum frame. After the 7^{th} layer was partially cured, the coating was allowed to further cure for 3 days at ambient temperature as illustrated in Figure 4-8. Round samples were punched out of the cured coating using a 1-inch diameter hollow punch and a hammer after the coating was removed from the release film. Then, the round samples were aged at 150°F for 7 days. Figure 4-9 illustrates the aged fully formulated MIL-PRF-23377 samples.

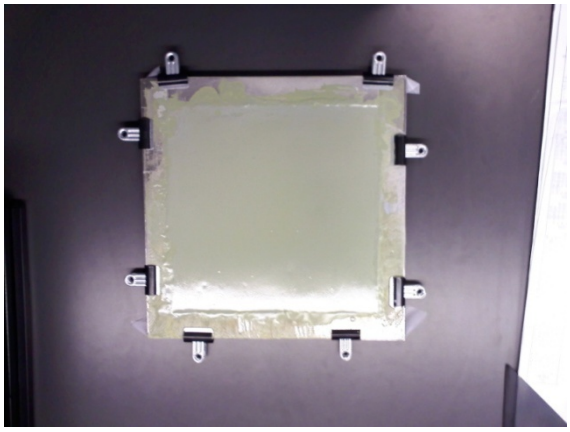

Figure 4-8. MIL-PRF-23377 fully formulated in mold

Figure 4-9. MIL-PRF-23377 fully formulated samples for gravimetric solvent sorption test

4.3 Film Sample Exposure

4.3.1 Thermal analysis

For thermal analysis, the film samples were exposed as follows. Approximately 2 cm square coupons of each film were cut and placed into individual scintillation vials. To each vial was added the respective solvent or solvent mixture (Table 4-1) until the film was completely covered (~10 mL). After exposure periods of two hours and two days, respectively, the liquid was decanted, rinsed with absolute ethanol and the film allowed to air dry in the vial. A rinse with ethanol ensured that no remaining chemicals were adhered to the surface of the film prior to analysis. Caution was taken to ensure the film was completely dry before testing.

4.3.2 Raman

For Raman spectroscopy the film samples were exposed for times ranging from 15 minutes to 2 hours. The films were then air dried thoroughly, for times ranging from 2 hours to 2 weeks, to reduce spectral contamination from residual solvent. Solvents systems used included liquid phenol (89:11 phenol/water) as well as a selection of the solvent mixtures listed in Table 4-1.

4.3.3 NMR

The ^{1}H NMR studies were performed on MIL-DTL-53039 films before and after a five minute room-temperature exposure to methylene chloride and on MIL-PRF-23377 films before and after a ten minute room-temperature exposure to a phenol:ethanol (2.724:1 weight ratio) solution. The exposures were performed by immersing squares of the cut film in the solvent in a beaker, removing, and blotting dry before placing into a 5 mm glass NMR tubes loosely sealed with Teflon tape to minimize evaporation.

Film samples for ^{2}H NMR were prepared similarly. The MIL-DTL-53039 film was exposed to d_2-methylene chloride (d_2-MC or CD_2Cl_2) for 10 minutes at 21°C, and after blotting dry showed a 34.9 wt.% increase in weight (that very slowly dropped on the balance, before being placed in the NMR tube). Two samples of the MIL-PRF-23377 film were prepared with different exposure times to deuterated phenol/ethanol solvent. Because of the slightly higher formula weight (F.W.) of the deuterium-substituted phenol, the d_5-PhOH/EtOH solvent was prepared with a somewhat higher weight ratio of 3.115:1 than used for the all-proton solvent mixture above. The mole ratio of the two components in the deuterated mixture was very similar (only 8.6% higher) to that in the protonated mixture. One MIL-23377 sample exposed to the deuterated solvent mixture for 10 minutes at 21°C showed a 21.4 % weight gain. A second sample exposed at 21°C for two hours showed a 124.5% weight gain, with the film crumbling into some fragments when handled with tweezers.

4.4 Experimental Methods

4.4.1 Diffusion Cell Test

A diffusion cell, illustrated in Figures 4-10 and 4-11, similar to the one used by Vesely was fabricated.[7] A test sample (approximately 5 mm by 5mm) cut from the sheet of clear film prepared by the ARL team was placed between two glass plates. Then, the diffusion cell was assembled as illustrated in Figure 4-10. To prevent unintentional disruption during experiments, the diffusion cell was fixed to an acrylic plate that was fixed to a stand using screws. Then, the stand was placed on the stage plate of an optical microscope equipped with a digital camera and a computer with imaging software, IrfanView, as illustrated in Figure 4-12. Approximately one hundred (100) digital micrographs of the progressing diffusion front were taken per experiment.

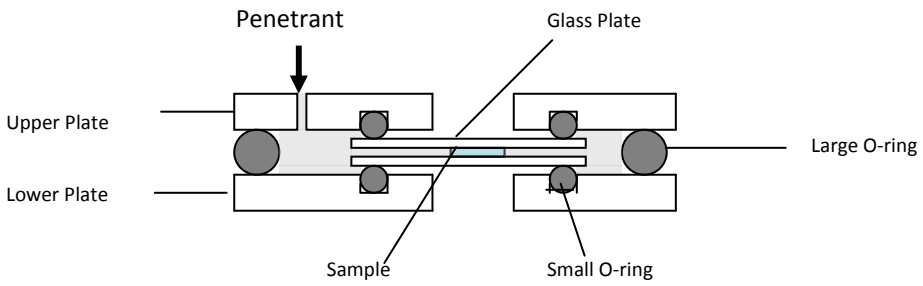

Figure 4-10. Schematic diagram of the diffusion cell

Figure 4-11. Top View of diffusion cell on acrylic plate

Figure 4-12. Diffusion cell experiment set-up

Once all micrographs were taken, diffusion distances were measured using the imaging software at pre-determined time intervals. Diffusion distances and times when micrographs were taken were entered into Microsoft (MS) Excel and manipulated to produce plots of diffusion distance

vs. square root of time. Figure 4-13 shows the micrographs from the diffusion cell experiment performed with the MIL-DTL-53039 clear film and methylene chloride.

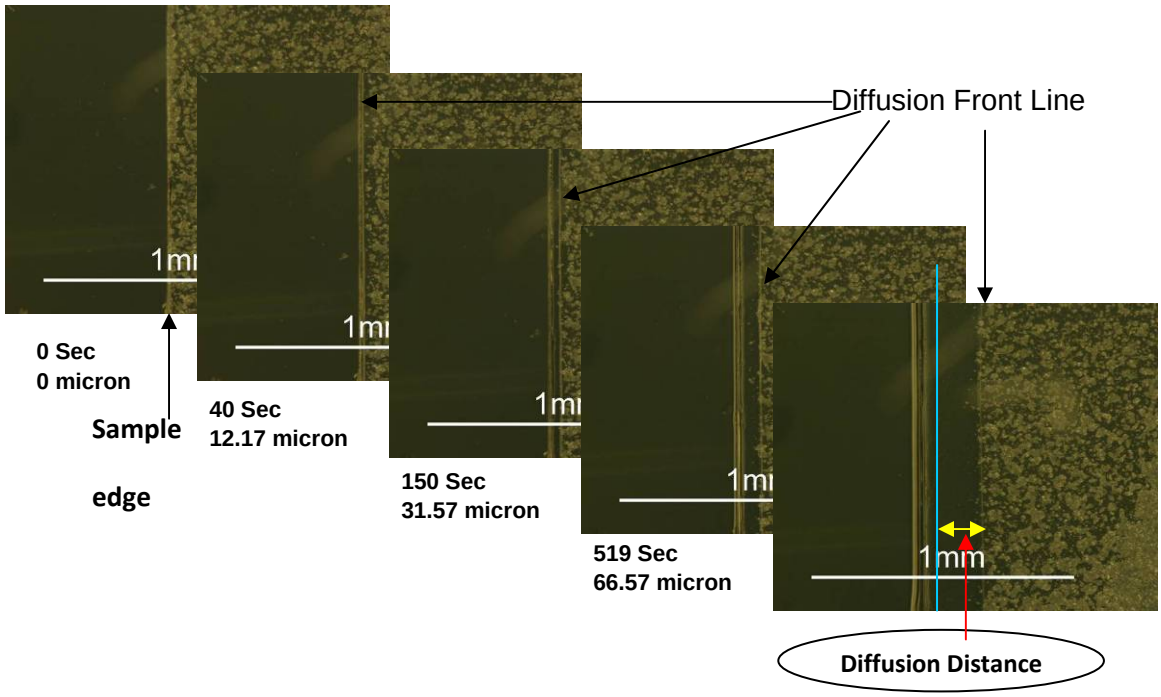

Figure 4-13. Micrographs (80 magnifications)

Not all micrographs appeared as sharp as the micrographs shown above. Solvent front lines on some micrographs appeared wavy, so the diffusion rate may change slightly depending on where on the diffusion distance was measured on the micrograph. On some of the micrographs, solvent front lines could not be found at all. We believe that variations in sample thickness, surface roughness, and morphology of samples contribute to diffusion and solvent front line formation. Based on our experience, the diffusion rates determined using the aforementioned method for this project should be used qualitatively, not quantitatively.

4.4.2 Gravimetric Solvent Sorption

An analytical balance connected to a laptop computer installed with laboratory automation software, WinWedge by Taltech, as illustrated in Figure 4-14 was used for accurate reading and fast recording of the weights of the sample and the times when the weight were measured. WinWedge automatically saved the weight and time data into MS Excel spreadsheets. Weight measurements were taken until the weight stabilized. Data analysis was performed using MS Excel.

Figure 4-14. Gravimetric solvent sorption experiment set-up

4.4.3 Differential Scanning Calorimetry

DSC was performed on a TA Instruments Q20 DSC with the DSC Refrigerated Cooling System (RCS) and a purge gas of nitrogen set to 50 mL/min. Film samples of approximately 1-2 mg were placed into TA Instrument Tzero Aluminum pans and an empty aluminum pan was used as reference. Samples were analyzed from -90°C to 150°C at the temperature ramp rate of 20°C/min twice to demonstrate hysteresis. All data reported were taken from the second cycle. Glass transition temperatures (T_g) were determined using TA Universal Analysis software.

4.4.4 Thermogravimetric Analysis

TGA was performed on a TA Instruments Q50 TGA using a platinum sample pan. The analysis was carried out in the presence of oxygen with breathing air used as the sample gas. Nitrogen was used as the purge gas for the balance. Data were recorded from ambient temperature to 700°C at a 5°C/min ramp. Plots of percent weight loss versus temperature were constructed to analyze the data.

4.4.5 Fourier Transformed Infrared Spectroscopy-Attenuated Total Reflectance

FTIR spectra were recorded on a Thermo Scientific Nicolet 6700 FTIR spectrometer equipped with a Smart Performer ATR attachment with a Germanium crystal at 32 scans. Spectra were recorded from 4000 – 500 cm^{-1} with a resolution of 2 cm^{-1}, and were analyzed using the Nicolet OMNIC software suite.

4.4.6 Raman Spectrometry

Film samples were analyzed using either a Nicolet Almega dispersive Raman spectrometer with 10x objective lens and 785 nm or 532 nm excitation laser; or a WiTec Alpha 500 confocal Raman spectrometer with 20x objective and 532 nm laser, at Brookhaven National Laboratory's Center for Functional Nanomaterials; the incident laser spot sizes of these instruments are less than 3 μm.

4.4.7 Gas Chromatography – Mass Spectroscopy

The GC/MS system was an Agilent 7890A gas chromatograph equipped with an Agilent 5975C mass selective detector operating in electron ionization mode and an Agilent 7693A auto-injector. The column utilized was an Agilent HP-5MS (5 % phenyl) methylpolysiloxane film. The carrier gas was helium with a flow rate of 1 mL/min^{-1}. The injection temperature, MS quad temperature, and source temperature were 250°C, 150°C and 230°C, respectively. The detector was set to scan with a mass range of 15 to 250 *m/z*. The temperature program has an initial temperature of 35°C for one minute, then 0.5°C per minute ramp to 37°C followed by a 5°C per minute ramp to 80°C and then a 20°C per minute ramp to 110°C with a two minute post run hold at 250°C.

4.4.8 X-ray Photoelectron Spectroscopy

XPS spectra were obtained using a VG ESCA-3 Mk. II system at ultra-high vacuum (10^{-9} torr). A pass energy of 20eV was used across 50 scans of the sample for each element, in combination with a magnesium K (alpha) anode operating at 120W. Spectra were calibrated using a reference value of 284.0 eV for adventitious carbon.

4.4.9 Scanning Electron Microscopy

SEM Micrographs were obtained using an FEI Helios Nanolab dual-beam scanning electron microscope with a secondary electron detector.

4.4.10 Proton (^1H) and Deuterium (^2H) Solid State NMR

Solid State ^1H NMR experiments were performed on a Bruker Avance DMX-500 NMR spectrometer using a non-spinning high-power ^1H probe with a horizontal 5 mm solenoidal coil containing the glass sample tube with film. The ^1H NMR spectra and ^1H relaxation times were obtained at 500 MHz (11.7 T field).

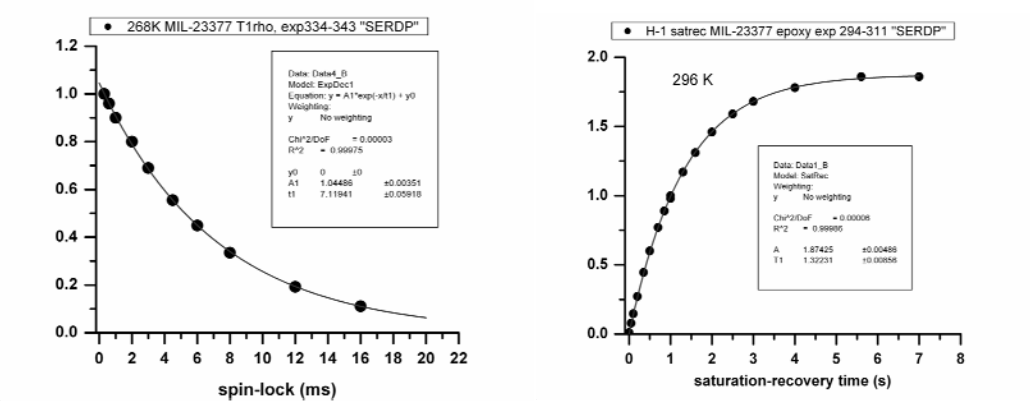

Figure 4-15. Examples of T_1 and $T_{1\rho}$ data analysis each for one sample at one temperature

The ^{1}H spin-lattice relaxation times ($T_{1)}$ were measured using a saturation-recovery pulse sequence with typically a dozen different recovery delays, and by fitting the recovery curve of the peak intensity using OriginPro 7.0 to a single-exponential recovery curve with time constant T_1. The intensities of static ^{1}H NMR peaks vs. spin-lock times (typically nine values) in a spin-locking pulse sequence were fit using Origin to a single-exponential decay curve with a decay time constant ($T_{1\rho}$). Measurements (shown in Figure 4-15) were repeated at different temperatures and for different samples.

All of the ^{2}H NMR spectra (nuclear spin I=1) were acquired at 76 MHz on a Varian/Agilent NMR spectrometer at 11.7 T, using a high-power static probe with a 5 mm horizontal solenoidal coil. Spectra of the isotopically-labeled materials were obtained using a quadrupolar-echo pulse sequence ("ssecho1d" provided by Varian) in order to be able to detect the extremely wide (>200 kHz) "powder-pattern" spectra characteristic of ^{2}H in the absence of molecular motions. An error was discovered in the phase-cycling of this manufacturer-supplied program after all experiments were completed. The phases of the last two (out of eight) phase cycles had the phases of the second pulse interchanged from the correct values, which produced two phase cycles where the two pulses were not orthogonal to each other as they should be. However, because the spectra were obtained exactly on-resonance, the net effect of this error was relatively minimal: a reduction of the acquired signal amplitude to 75% of what it should have been, and some loss in the artifact-removal properties of the phase-cycling. These effects do not affect the data analysis and conclusions presented later.

4.4.11 Coating Removal

Coated test panels aged at 150°F for 7 days were used for this test. Glass columns were fixed to the coated surface using spring clips as illustrated in Figure 4-16. Test solutions were added into the columns, which were loosely closed with cork stoppers. Changes of the coating were observed and recorded using a video recorder.

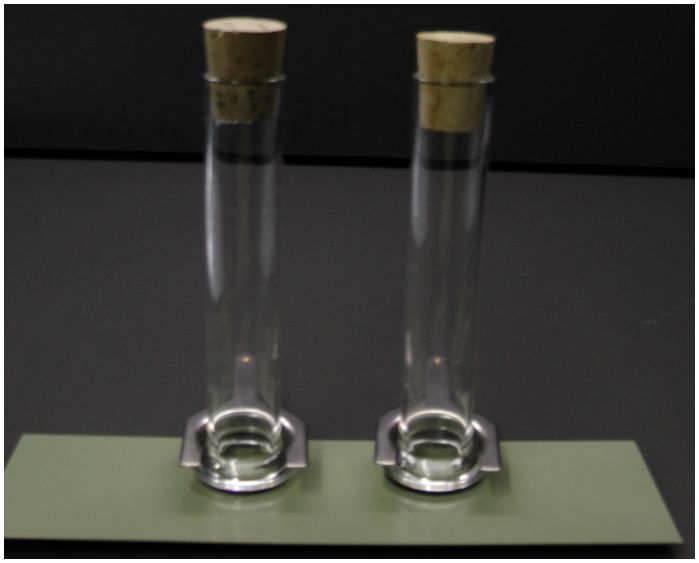

Figure 4-16. Coating removal experiment set-up

(This page intentionally left blank)

5. Results and Discussion

5.1 ARL Preparation of Clear Samples

ARL chose to reformulate all of the selected military coatings because no resin-only attempts could be formed properly without significant adjustments to the mixes. All of these military coatings have been formulated by dozens of formulators spending hundreds of hours to achieve the characteristics desired in our military coatings for ultraviolet (UV) light resistance, corrosion resistance, agent resistance, and more. Reformulating by removing the opaque pigments and other additives to achieve a continuous clear film that behaves similarly to the pigment-containing film is not an arbitrary task. This became apparent as soon as prime pigments and additives were removed to obtain the clear films required for this SERDP study.

For reformulation, flow modifiers were extracted from the initial formulations to eliminate their influence on the effects of the methylene chloride strippers. Without flow modifiers and other additives that help induce flow or suppress flow characteristics, most resin systems will exhibit some form of film anomaly like crawling, fisheyes, and foaming. Moderate success was achieved with all of the original formulation of the specified military coatings that were either sprayed or cast.

It was found that centrifuging complete formulations to remove the pigments is a far more efficient way of producing clear films than reformulation. After centrifuging the samples, the clear films were cast as supported and unsupported films using metal substrates and release paper respectively. The films were sprayed onto the metal substrates and Tedlar, polyvinyl fluoride release film using the HVLP spray gun. Several thin coats had to be applied to allow the solvents to flash-off and promote the coatings to "set" to avoid pinholing, cratering, and other films anomalies (Figure 5-1). The coatings formed using centrifuged paint were also used as bases to reintroduce the prime pigments without extenders for study. Using the centrifuged clear bases, additional formulations were assembled to produce films free of the silica extenders. This approach proved much more fruitful than the formulation approach and easily yielded viable films free of defects for this study. When there are no other specific requirements that can only be replicated with reformulation, the centrifuge approach is a faster, simpler, and more cost effective way to produce the clear films. Through repeated efforts of formulation, subtle application techniques, and trial and error, the clear films were eventually produced successfully.

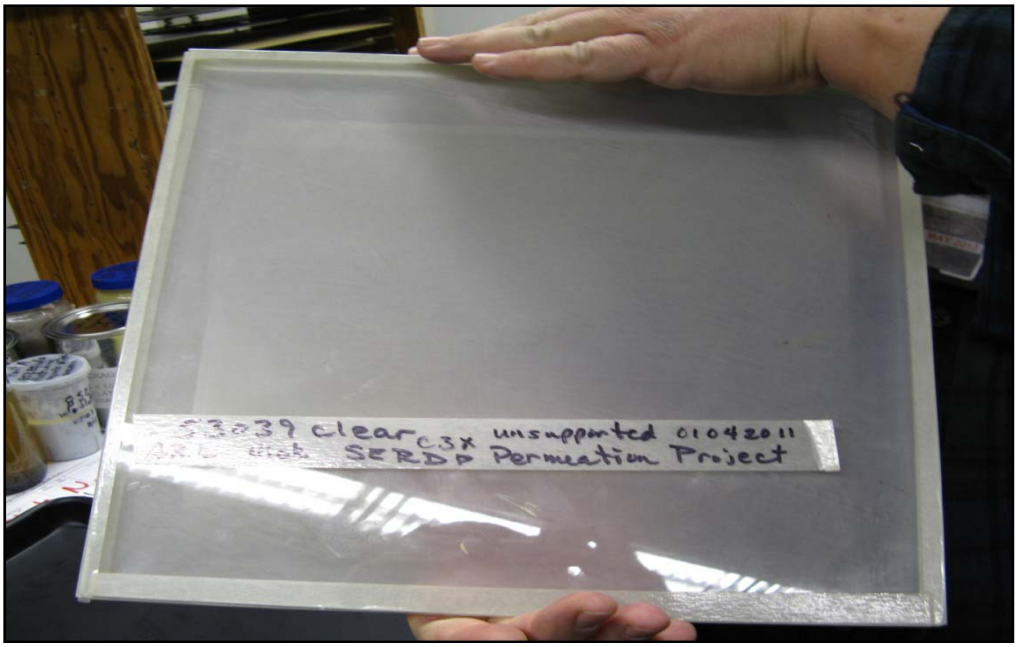

Figure 5-1. Examples of MIL-DTL-53039 centrifuged clear unsupported films on release paper, typical of the centrifuged samples submitted

5.2 Solvent Diffusion

Solvent diffusion is believed to be one of the major factors in paint stripping. However, no solvent diffusion study regarding paint stripping has been performed to our knowledge, while the results of abundant diffusion studies for packaging, structural engineering, membrane filtration, drug delivery, corrosion protection and electronics appear in peer reviewed journals. Gravimetric solvent sorption is the most widely used technique for diffusion studies due to its simplicity, but other techniques are also known to be employed. These include light microscopy, electron microscopy (EM), nuclear magnetic resonance imaging (MRI), Rutherford backscattering spectroscopy (RBS), forward recoil spectroscopy (FRS), FTIR, FTIR-ATR, waveguide Raman spectroscopy (WRS), electron spin resonance (ESR), radioactive labeling (RL), inverse gas chromatography (IGC), and neutron scattering (NS).[8] A new technique to measure the diffusion rate of methanol through a thin film of poly(methyl methacrylate) (PMMA) accurately in situ was recently introduced.[7] The clear films that we prepared are not as clear as PMMA, but the initial diffusion tests indicated that the clear films are suitable for this new technique, diffusion cell technique. For these reasons, we decided to use diffusion cell and gravimetric solvent sorption techniques for our diffusion study.

Some minor modification was made to the coating binder formulation in the production of clear films in order to achieve the proper spray-ability and/or bubble-free samples, but we expect that the physical and chemical properties of the polymer in the clear samples are similar to those of the binders in the target coatings. However, the structural property could be different because the polymer chains in the fully formulated sample are arranged differently from the same polymers in clear films as the case for proteins that can be folded in different ways, but no

attempt has been made to verify their structural similarities or differences. There are techniques, such as atomic force microscopy (AFM)[9] and positron annihilation lifetime spectroscopy (PALS)[10], which can be used to identify microstructures and free volume properties of organic coatings and, thus, structural similarities.

5.2.1 Diffusion Cell

As discussed in the materials and methods section, data manipulation and plotting for the diffusion cell study were performed using MS Excel. This process produced the graphs of diffusion distance vs. square root of time and the slopes of the best fit straight lines, which are provided in Figures 5-2, 5-3, 5-4, 5-5 and 5-6 and Tables 5-1, 5-2, 5-3, 5-4 and 5-5 respectively.

5.2.1.1 Diffusion Mode

For the MIL-PRF-85285 clear film as illustrated in Figure 15-2, methylene chloride and the methylene chloride solution of ethanol (MC/EtOH) show a linear relationship, which suggests these diffusions fit either Vesely's molecular sorption theory or Fick's theory. Vesely's molecular sorption theory assumes that molecular interactions are the major driving forces for diffusion and there exists a resistance to flow of penetrant.[11] Fick's theory is based on the assumption that the concentration gradient is the driving force for diffusion. Other plots for the MIL-PRF-85285 clear film are slightly deviated from a linear relations ship. The reason for the deviation is not clearly understood. The graphs for all five test penetrants tested with the MIL-PRF-23377 clear film (illustrated in Figure 5-3) show a linear relationship between square root of time and distance. Other graphs illustrated in Figures 5-4, 5-5, and 5-6 also show linear or slightly deviated linear relationship.

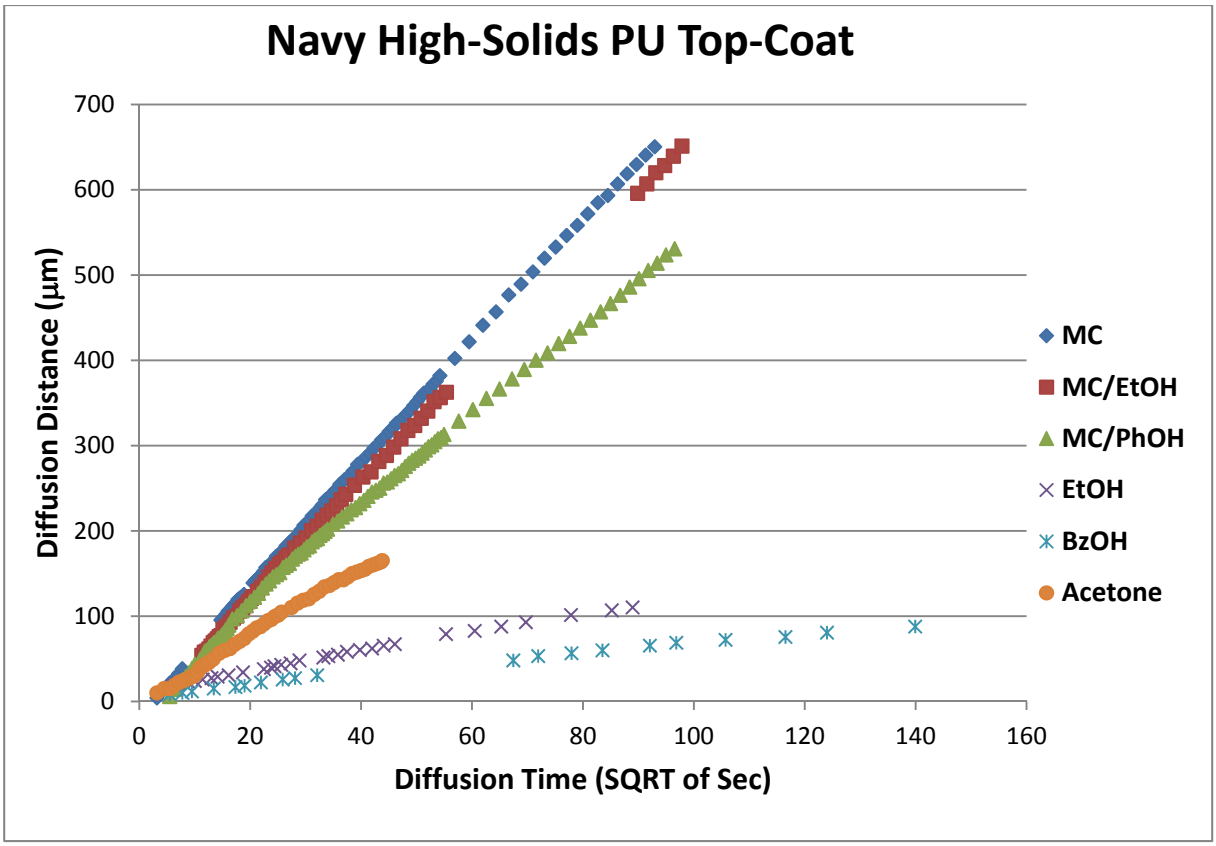

Figure 5-2. Diffusion graph: MIL-PRF-85285 clear film

Table 5-1. Best fit linear line: MIL-PRF-85285 clear film

Penetrant	Slope	R^2
Methylene Chloride (MC)	7.211	0.999
MC & Ethanol	6.870	0.999
MC & Phenol	7.577 (lower portion) 5.233 (higher portion)	0.998 0.999
Ethanol	1.130	0.996
Benzyl Alcohol	0.599	0.992
Acetone	4.003	0.994

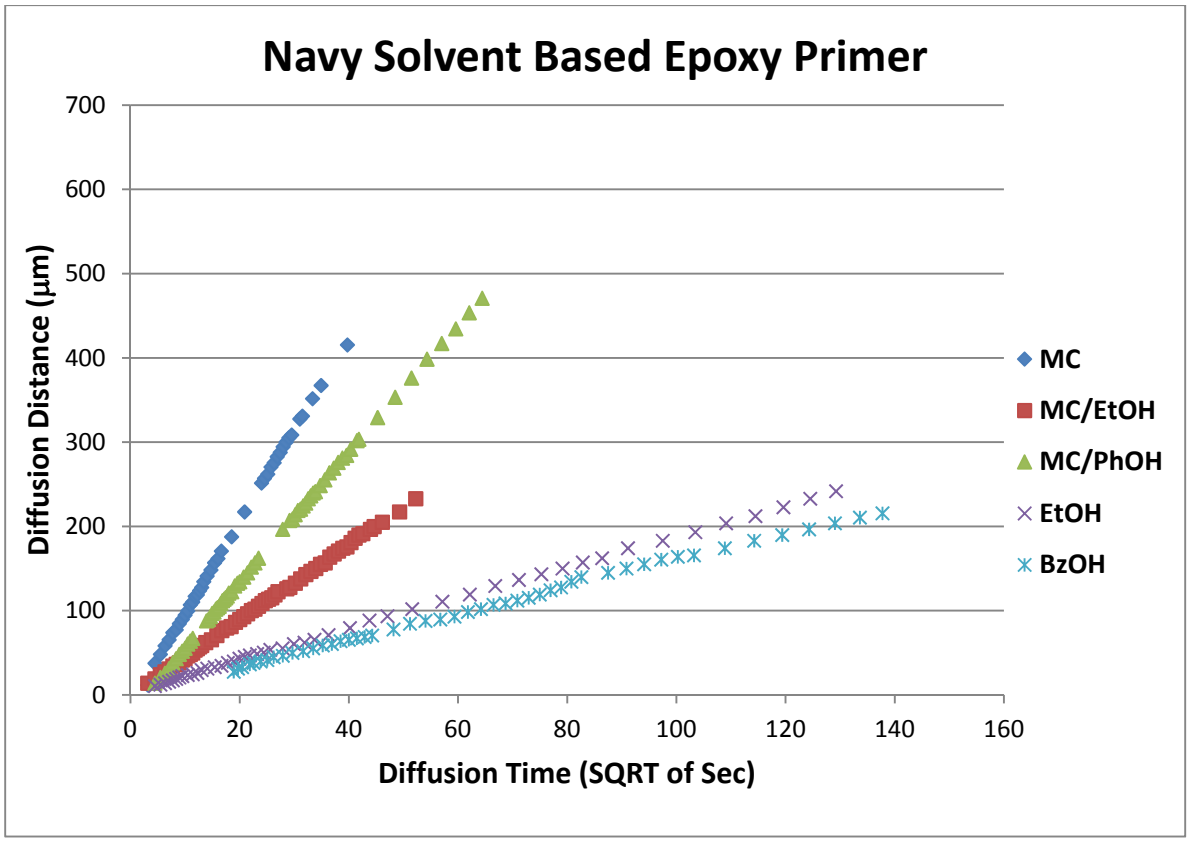

Figure 5-3. Diffusion graph: MIL-PRF-23377 clear film

Table 5-2. Best fit linear line: MIL-PRF-23377 clear film

Penetrant	Slope	R^2
Methylene Chloride (MC)	10.897	0.999
MC & Phenol	7.657	0.999
MC & Ethanol	4.473	0.999
Ethanol	1.837	0.999
Benzyl Alcohol	1.585	0.998

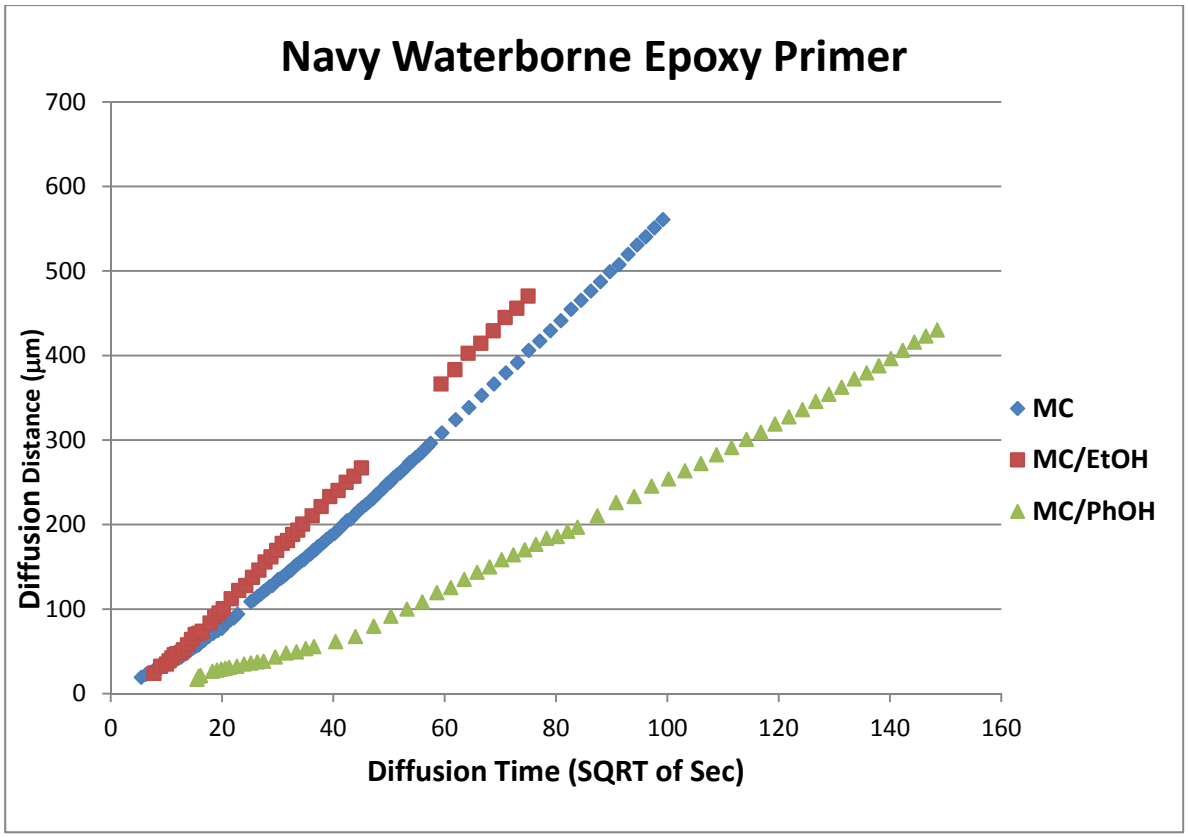

Figure 5-4. Diffusion graph: MIL-PRF-85582 clear film

Table 5-3. Best fit linear line: MIL-PRF-85582 clear film

Penetrant	Slope	R^2
MC	6.177 (between 120 and 560 microns)	0.999
MC & Ethanol	6.727	0.999
MC & Phenol	3.410 (between 50 and 150 microns)	0.998
Benzyl Alcohol	No diffusion observed for 7 hours	Not Applicable

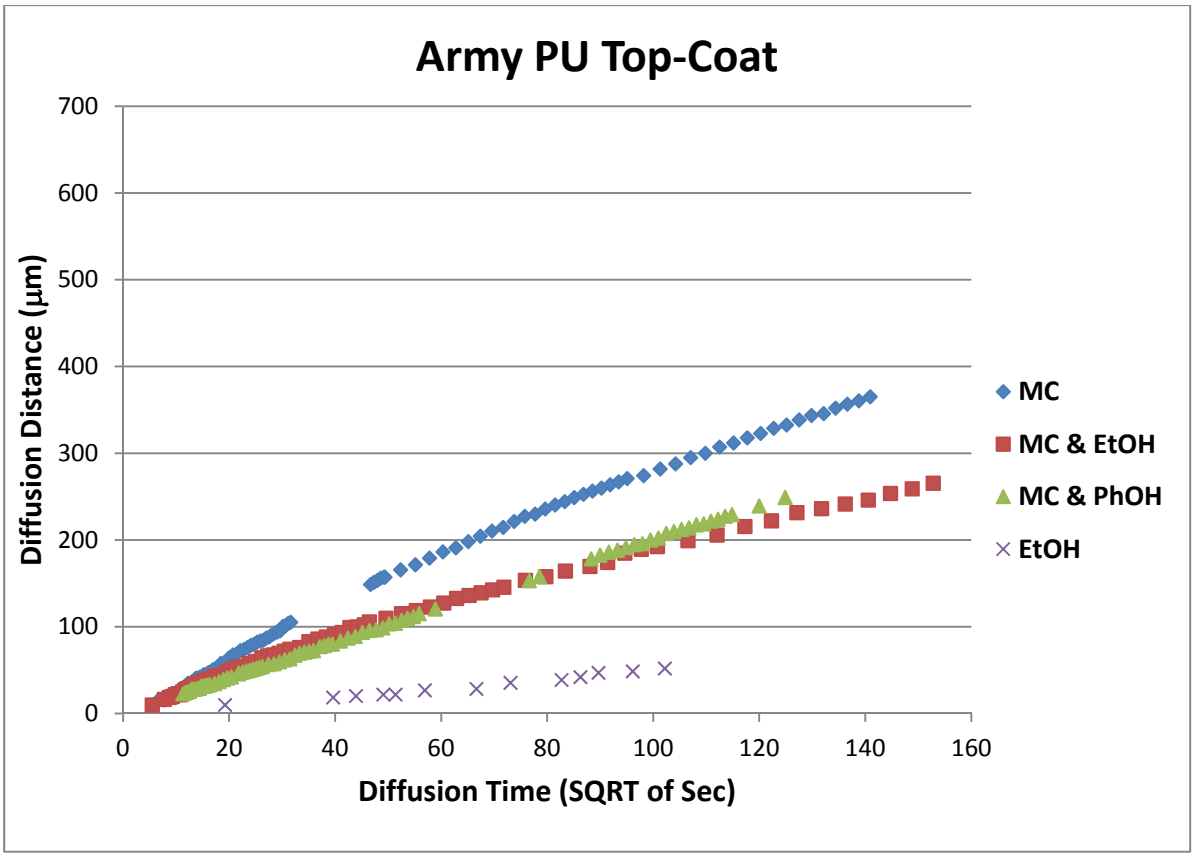

Figure 5-5. Diffusion graph: MIL-DTL-53039 clear film

Table 5-4 Best fit linear line: MIL-DTL-53039 clear film

Penetrant	Slope	R^2
Methylene Chloride (MC)	2.662	0.990
MC & Ethanol	1.917	0.990
MC & Phenol	2.230	0.999
Ethanol	0.539	0.980

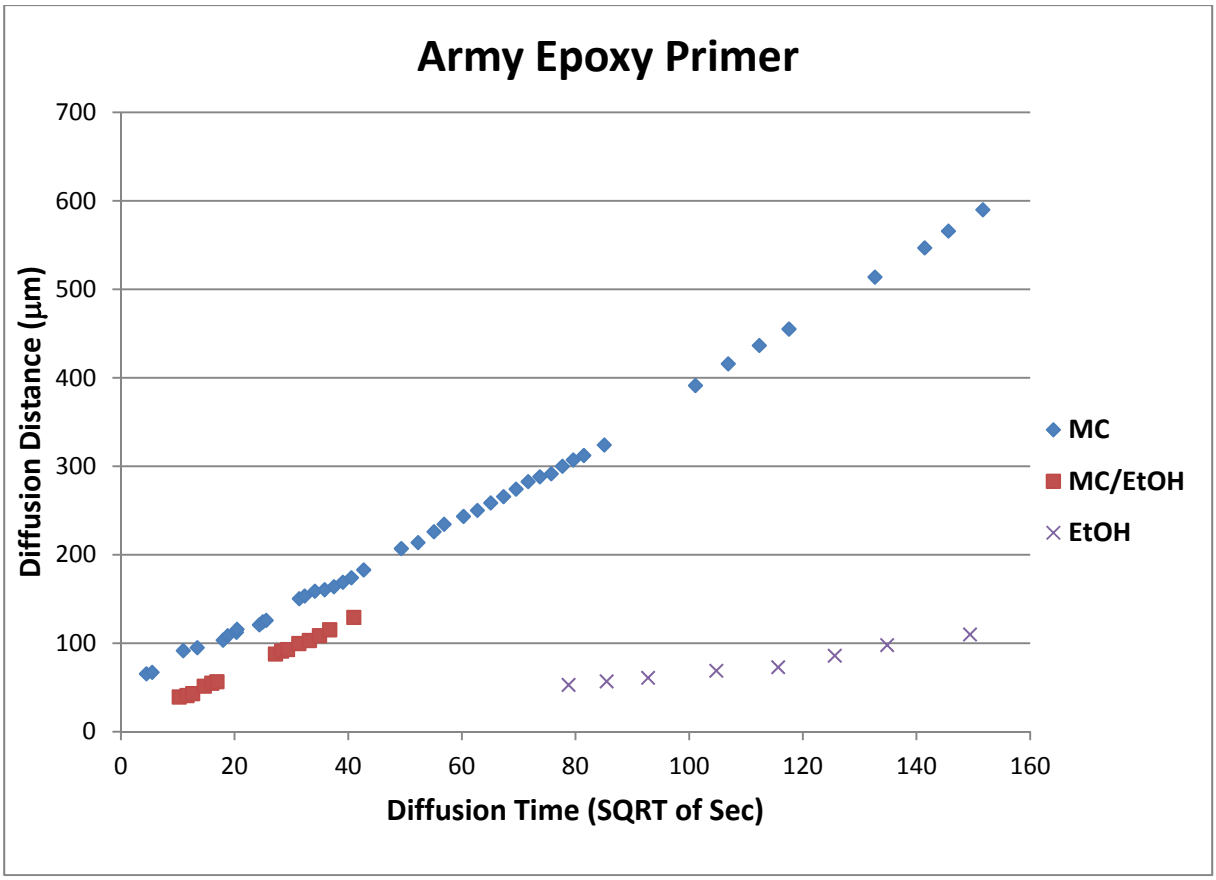

Figure 5-6. Diffusion graph: MIL-DTL-53022 clear film

Table 5-5. Best fit linear line: MIL-DTL-53022 clear film

Penetrant	Slope	R^2
MC	3.566	0.995
MC & Ethanol	3.018	0.997
Ethanol	0.849	0.989

5.2.1.2 Diffusion Rate and Control Factors

Methylene chloride diffuses fastest for all clear films except the MIL-PRF-85582 clear film. Ethanol and benzyl alcohol diffuse substantially slower than methylene chloride. Methylene chloride solutions of ethanol and benzyl alcohol diffuse faster than ethanol and benzyl alcohol, but slower than methylene chloride.

For the MIL-PRF-85582 clear film, the methylene chloride solution of ethanol (MC/EtOH) diffuses slightly faster than methylene chloride. The chemistry and microstructure of the water based MIL-PRF-85582 are different from solvent based primers[3], which may be the reason for faster diffusion of MC/EtOH than methylene chloride.

The diffusion of ethanol is substantially slower than methylene chloride in all cases. As shown in Table 5-6, the Hansen hydrogen bonding parameter (δ_h) of ethanol is substantially higher than that of methylene chloride, which suggests that ethanol is chemically less compatible[11] to the diffusion channels in the sample than methylene chloride. Benzyl alcohol is not a component of the methylene chloride based paint stripper. Yet, a diffusion test was performed with benzyl alcohol to prove the supposition that diffusion is a key factor in paint stripping as discussed in the introduction section. As illustrated in Figures 5-2 and 5-3, benzyl alcohol diffuses substantially slower than methylene chloride. Hildebrandt solubility parameters for benzyl alcohol and methylene chloride are close each other, 11.64 $MPa^{1/2}$ and 9.88 $MPa^{1/2}$ respectively. However, the Hansen hydrogen bonding parameter for benzyl alcohol (6.70 $MPa^{1/2}$) is substantially greater than that of methylene chloride (2.98 $MPa^{1/2}$). This result further supports the idea that hydroxyl group of penetrants lowers the diffusion rate, which ultimately lowers the paint stripping rate. One may then ask why the diffusion rate of benzyl alcohol is lower than ethanol considering the fact that benzyl alcohol has lower hydrogen bonding contribution. This can be explained by the size difference between ethanol and benzyl alcohol. There are two primary competing factors, the size of penetrant and its hydrogen bonding property. In this case, the size of benzyl alcohol contributes more than its hydrogen bonding property resulting in slightly slower diffusion of benzyl alcohol than ethanol. As shown in Table 5-7, the molar volume of ethanol is almost a half of benzyl alcohol.

Table 5-6. Hansen and Hildebrandt solubility parameters

Penetrants	δ_d ($MPa^{1/2}$)	δ_p ($MPa^{1/2}$)	δ_h ($MPa^{1/2}$)	δ_H ($MPa^{1/2}$)
Methylene chloride	8.90	3.08	2.98	9.88
Ethanol	7.72	4.30	9.48	12.96
Benzyl alcohol	9.00	3.08	6.70	11.64
Acetone	7.58	5.08	3.42	9.75

Note: Data from http://www.stenutz.eu/chem/solv24.php?sor=2

δ_d – Hansen dispersion parameter

δ_p – Hansen polar parameter

δ_h – Hansen hydrogen bonding parameter

δ_H – Hildebrandt solubility parameter

Table 5-7. Physical properties of penetrants

Penetrants	Molar volume (cm^3/mol) @ 25°C	Boiling Point (°C)	Density (g/cm^3) @ 25°C
Methylene chloride	64.5	42	1.324
Ethanol	58.7	78	0.785
Benzyl alcohol	103.8	205	1.042
Acetone	74.0	56.5	0.785

Acetone has a similar molar volume as well as Hansen hydrogen bonding parameter (7.1 $Mpa^{1/2}$) to methylene chloride even though the dispersion and polarity parameters are more deviated than benzyl alcohol from methylene chloride. So, we tested acetone to see if it diffuses faster than

ethanol and benzyl alcohol. The diffusion distance versus square root of time graph for the MIL-PRF-85285 clear film, Figure 5-2, shows a linear relationship with a slop of 4.003 for acetone, which is lower than that of methylene chloride, 10.89, but substantially higher than either benzyl alcohol (0.599) or ethanol (1.130).

The diffusion rates of methylene chloride solutions of phenol, benzyl alcohol, and ethanol fall between those of methylene chloride and ethanol (or benzyl alcohol). Another word, methylene chloride solutions of phenol, benzyl alcohol, and ethanol diffuse faster than phenol, benzyl alcohol, and ethanol alone. This result suggests that methylene chloride creates diffusion channels that did not exist for ethanol, benzyl alcohol, and phenol to pass through. Considering a large amount of methylene chloride absorption into coating samples that is discussed in Sections 5.2.2 and 5.2.3, it is possible that co-solvents or activators diffuse through methylene chloride absorbed in coatings.

Even though phenol diffusion is not reported in any of the diffusion charts, we experimented with an aqueous solution of 5% phenol by weight and the MIL-PRF-85285 clear film. It was difficult to determine the diffusion distances from the micrographs taken for this experiment due to the uneven diffusion line, although the section of the sample penetrated by 5% phenol looks substantially darker than intact section as illustrated in Figure 5-7. That is one reason that the diffusion of 5% phenol is not included in the diffusion graphs. Another reason is that we do not know the chemical species that diffuses through the test film. Phenol is well known to exist as clusters with water.[12] Even though it is impossible to measure the exact diffusion distance on Figure 5-7, a rough estimate can be made, which is approximately 100 μm. The 100 μm diffusion for 13 hours is slower than benzyl alcohol, which diffuses almost the same distance for 5.44 hours. So, it is not unrealistic to say that methylene chloride solution of phenol diffuses substantially faster than phenol alone.

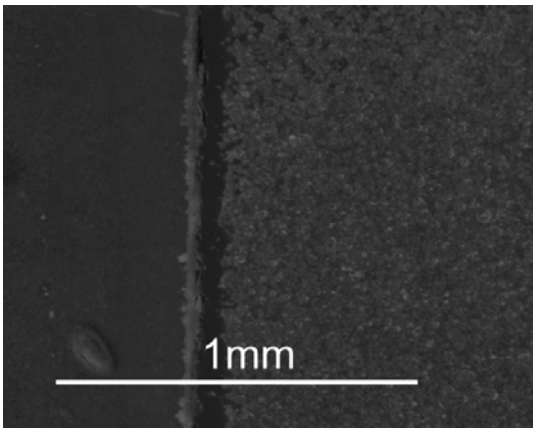

Figure 5-7. Micrograph for diffusion of aqueous solution of 5% phenol through clear MIL-PRF-85285 film for 13 hours

It is believed that benzyl alcohol was selected as an alternative to methylene chloride because the solubility of benzyl alcohol is close to that of methylene chloride. As we have learned from

the depot level depaint work, benzyl alcohol based paint strippers work substantially slower than methylene chloride based paint strippers. Our diffusion tests suggest that the low hydrogen bonding property of methylene chloride provides methylene chloride faster diffusion as compared to benzyl alcohol. Yet, the low hydrogen bonding is not the only property that makes methylene chloride an effective solvent. The small size of methylene chloride and its ability to increase the mobility of other components such as ethanol and phenol are also important properties of methylene chloride as a paint stripper solvent.

5.2.2 Gravimetric Solvent Sorption

Diffusion cell experiments were attempted with fully formulated films, but fully formulated films did not exhibit solvent front line due to their opacity. The gravimetric solvent sorption technique allows measuring and comparing diffusion rates of clear and fully formulated samples quantitatively. However, the gravimetric solvent sorption technique also has its own limitation for this study. Test samples buckled (saddle shaped) and fractured when they were exposed to the methylene chloride solutions of alcohols. For this reason, our discussion in this section is limited to the results from the experiments performed with methylene chloride or ethanol.

5.2.2.1 MIL-PRF-23377 Clear Sample: MC vs. EtOH

The MIL-PRF-23377 clear sample reached its sorption equilibrium with methylene chloride in 6 hours and 37 minutes and then lost its weight as illustrated in Figure 5-8. The weight decrease may be due to extraction of a component of the sample by methylene chloride. Evaporation of methylene chloride from the glass bottle used for immersion of the sample left small amount of non-volatile liquid. Identification of this liquid was not attempted, but it is most likely a plasticizer. At the sorption equilibrium, the sample weight increase is 165%. Ethanol reached its sorption equilibrium in 6 days 21 minutes, which is substantially slower compared to methylene chloride. The sample weight increase at the sorption equilibrium is 30%. These data suggest that the methylene chloride diffusion is substantially faster than ethanol, which is corresponding to the result of the diffusion cell experiment performed with the MIL-PRF-23377 clear film.

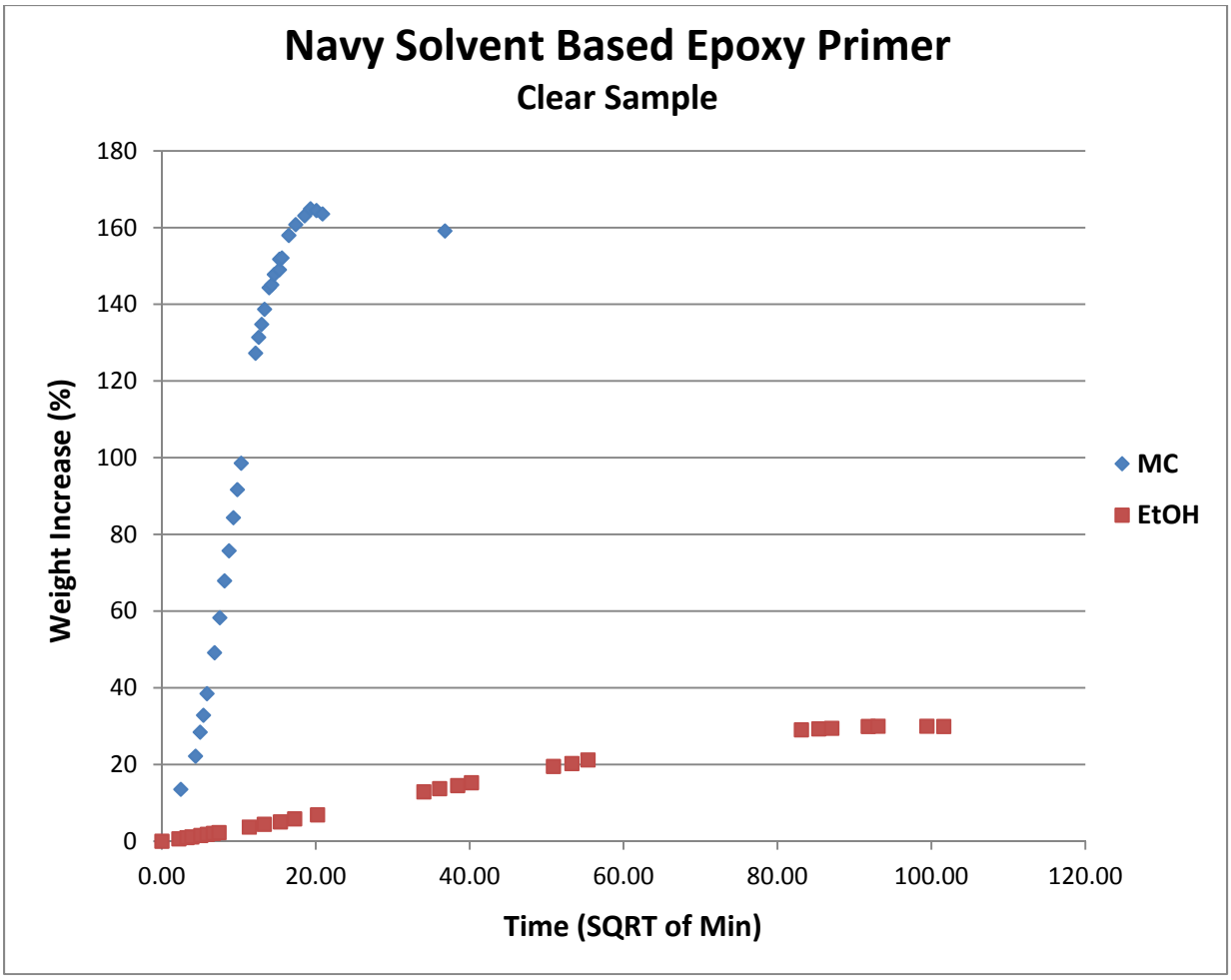

Figure 5-8. Percentage weight change vs. square root of minute graph for MIL-PRF-23377 clear samples

5.2.2.2 Diffusion Coefficient: Diffusion Cell vs. Gravimetric Solvent Sorption

Both plots in Figure 5-8 are sigmoidal, which suggests that both diffusions are Fickian. Assuming both diffusions are one dimensional, the diffusion coefficients are calculated using equation (1);[13]

$$D = \pi \left[\frac{h\theta}{4M_\theta}\right]^2 \qquad (1)$$

where h is thickness of the sample, θ is the slope of the plot of the weight change as a function of time$^{1/2}$, and M_θ is the mass uptake at infinite time. As shown in Table 5-8, the diffusion coefficients for two solvents calculated using the equation (1) correlate well with the diffusion

rates obtained from the diffusion cell experiments, 118.74 μm^2/sec (10.897 $\mu m/sec^{1/2}$) and 3.37 μm^2/sec (1.837 $\mu m/sec^{1/2}$) for methylene chloride and ethanol respectively. This result allows us to extend the use the diffusion cell data for the solvent sorption data analysis. Slight differences in the diffusion coefficient may be due to the deviation of the solvent sorption from the theoretical model of one dimensional diffusion. The deviation is evidenced by our observation of the continuing increase in diameter during sorption and swelling of the sample edges before other areas for both samples.

Solvent sorption experiments with methylene chloride solution of phenol and ethanol were performed. However, both of MIL-PRF-85285 and MIL-PRF-23377 clear samples broke into pieces before reaching their sorption equilibriums. One-dimensional diffusion cannot be assumed for this case. Physical changes of these samples during the sorption tests are discussed in Section 5.2.3.

Table 5-8. Diffusion coefficient obtained from the solvent sorption experiment

	Methylene Chloride	Ethanol
h	2.760 x 10^3 μm	2.421 x 10^3 μm
θ	2.355 x 10^{-2} $g/sec^{1/2}$	6.971 x 10^{-4} $g/sec^{1/2}$
M_∞	2.2261 g	0.4157 g
D	167.3 μm^2/sec	3.2 μm^2/sec
D (Diff. Cell)	118.74 μm^2/sec	3.37 μm^2/sec

5.2.2.3 Methylene Chloride Sorption: MIL-PRF-23377 Clear vs. Fully Formulated

The plot for the sorption of methylene chloride through the MIL-PRF-23377 fully formulated sample is also sigmoidal as illustrated in Figure 5-9. The fully formulated sample reached the sorption equilibrium in approximately 6 hours and 18 minutes, which is slightly faster than through the clear sample, 6 hours and 37 minutes. This result indicates that the diffusion rate of methylene chloride through the MIL-PRF-23377 fully formulated sample is almost same to the diffusion rate through the MIL-PRF-23377 clear sample since the thicknesses of the clear and fully formulated samples are almost same.

The weight increase at the sorption equilibrium for the fully formulated sample, 33%, is substantially less than the clear sample, 165%, which suggests that absorption of methylene chloride by additives in the fully formulated sample is limited or negligible and the additive loading in the fully formulated sample is high. The high loading of impermeable additives should create tortuous paths for methylene chloride to diffuse. Yet, the times for methylene chloride to reach its sorption equilibriums for both samples are almost equal. So, there should be a new path, most likely free volume, in the fully formulated sample for methylene chloride diffuses quickly.

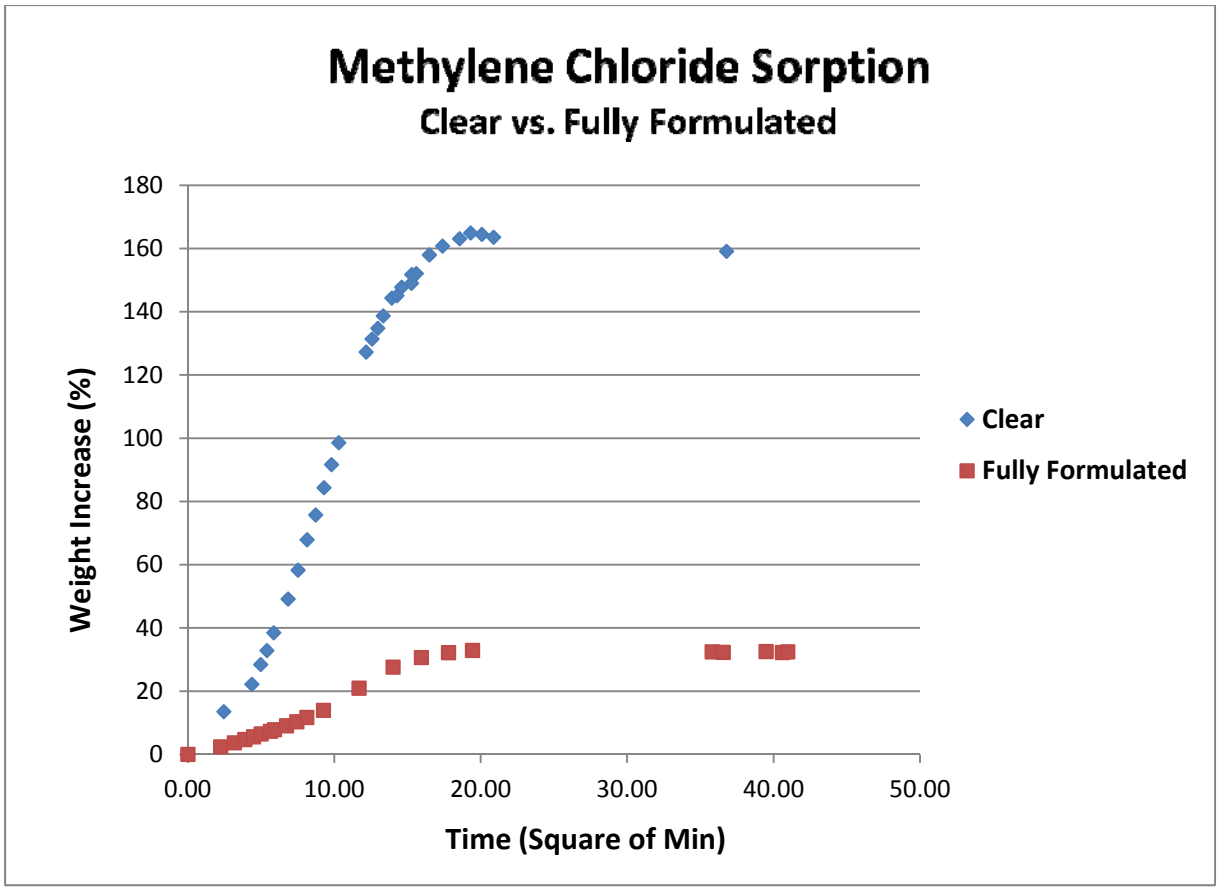

Figure 5-9. Methylene chloride solvent sorption in clear and MIL-PRF-23377 fully formulated samples

5.2.2.4 Methylene Chloride Sorption: Clear vs. Fully Formulated

The plots for the methylene chloride solvent sorption through the MIL-PRF-85285 clear and fully formulated samples are sigmoidal as illustrated in Figure 5-10. Data interpolation for the fully formulated sample indicates that the solvent reaches its sorption equilibrium in approximately 15 hours, which is slower than the fully formulated sample, 3 hours. However, the plots in Figure 5-10 indicate that the θ/M_θ for both samples are almost same, so diffusion rates of methylene chloride through the MIL-PRF-23377 clear and fully formulated sample should not be too much different. The weight increase at the sorption equilibrium for the fully formulated sample is 20% higher than the clear sample, which is not clearly understood. These two results suggest that the interface between the binder and inorganic additives absorbs a large quantity of methylene chloride.

As demonstrated in Sections 5.2.2.3 and 5.2.2.4, it is difficult to predict the solvent sorption behavior of fully formulated coating based on the sorption behavior of the binder of the coating.

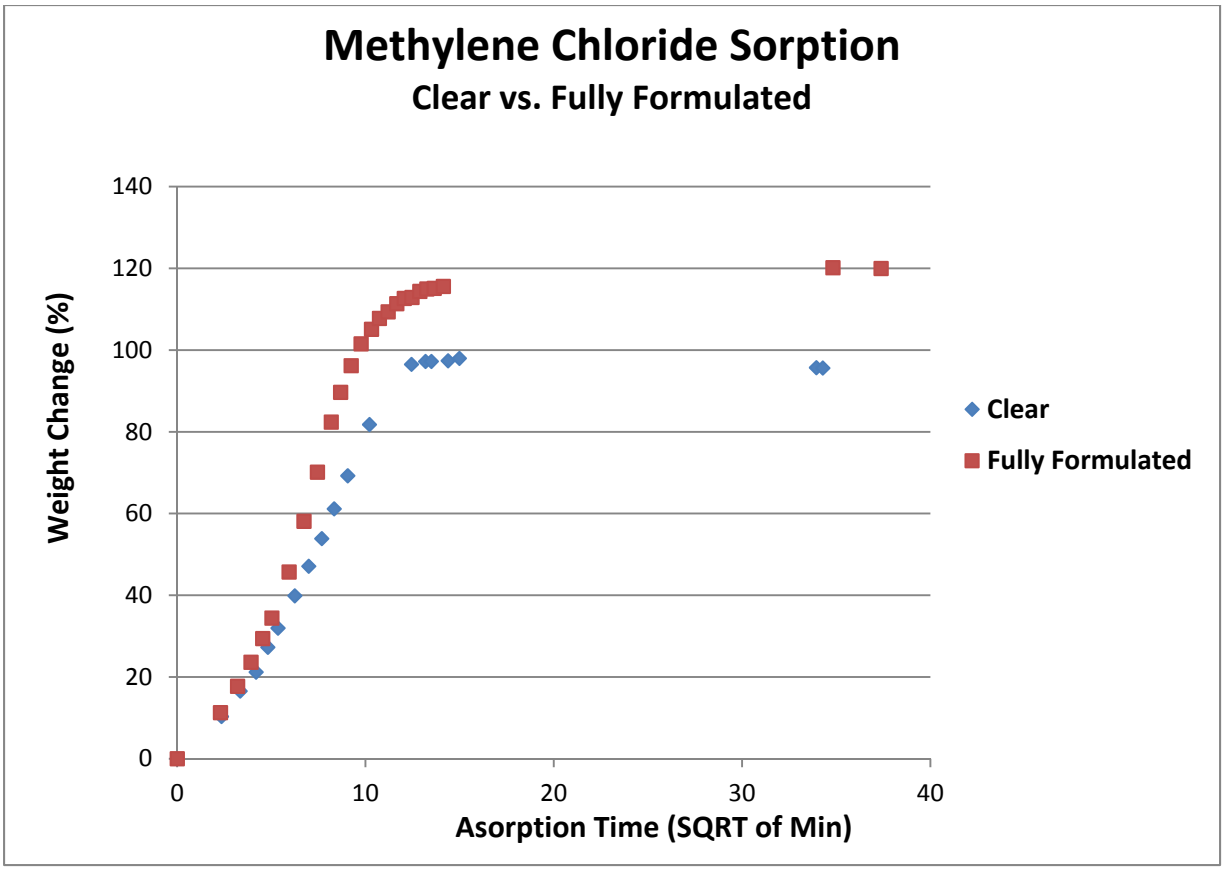

Figure 5-10. Methylene chloride solvent sorption in clear and fully formulated MIL-PRF-85285 samples

5.2.3 Solvent Sorption Rates and Physical Changes

This section describes the observations made during sorption experiments. This section also discusses possible explanations for unusual findings.

5.2.3.1 MIL-PRF-85285 Clear

As illustrated in Figure 5-11, the MIL-PRF-85285 clear sample immersed in methylene chloride reached its sorption equilibrium at 3 hours and 44 minutes. The weight increase at the sorption equilibrium is 98%. Then, the weight decreased slightly. The weight increase at 19 hours and 35 minutes is 95.6%, which is 2.4% decrease from the maximum weight. No crack was observed on the sample immersed in methylene chloride during the absorption experiment.

The sample in the MC/EtOH solution broke into three pieces in 12 minutes. The broken sample is shown in Figure 5-12. The largest piece further broke into two pieces in 1 hour and 19 minutes. The broken pieces were assembled and placed in MC/EtOH solution for three days. The sample was then filtered and weighed. The weight increase of the sample in the MC/EtOH solution for three days was 96.8%.

The sample exposed to the methylene chloride solution of 20% phenol by weight (MC/PhOH) started buckling (saddle-shaped) after 30 minutes of immersion. It is believed that the saddle-shape formed to relieve the stress built up due to solvation of the absorbed layer over the unaffected core.[14] After 45 minutes, the sample in the MC/PhOH broke into three pieces like the sample exposed to MC/EtOH solution. The broken pieces were placed in the MC/PhOH for 2 days and 18 hours. The sample broken into small pieces as illustrated in Figure 5-13. The sample was then filtered and weighed. The weight increase of the sample in MC/PhOH was 173%.

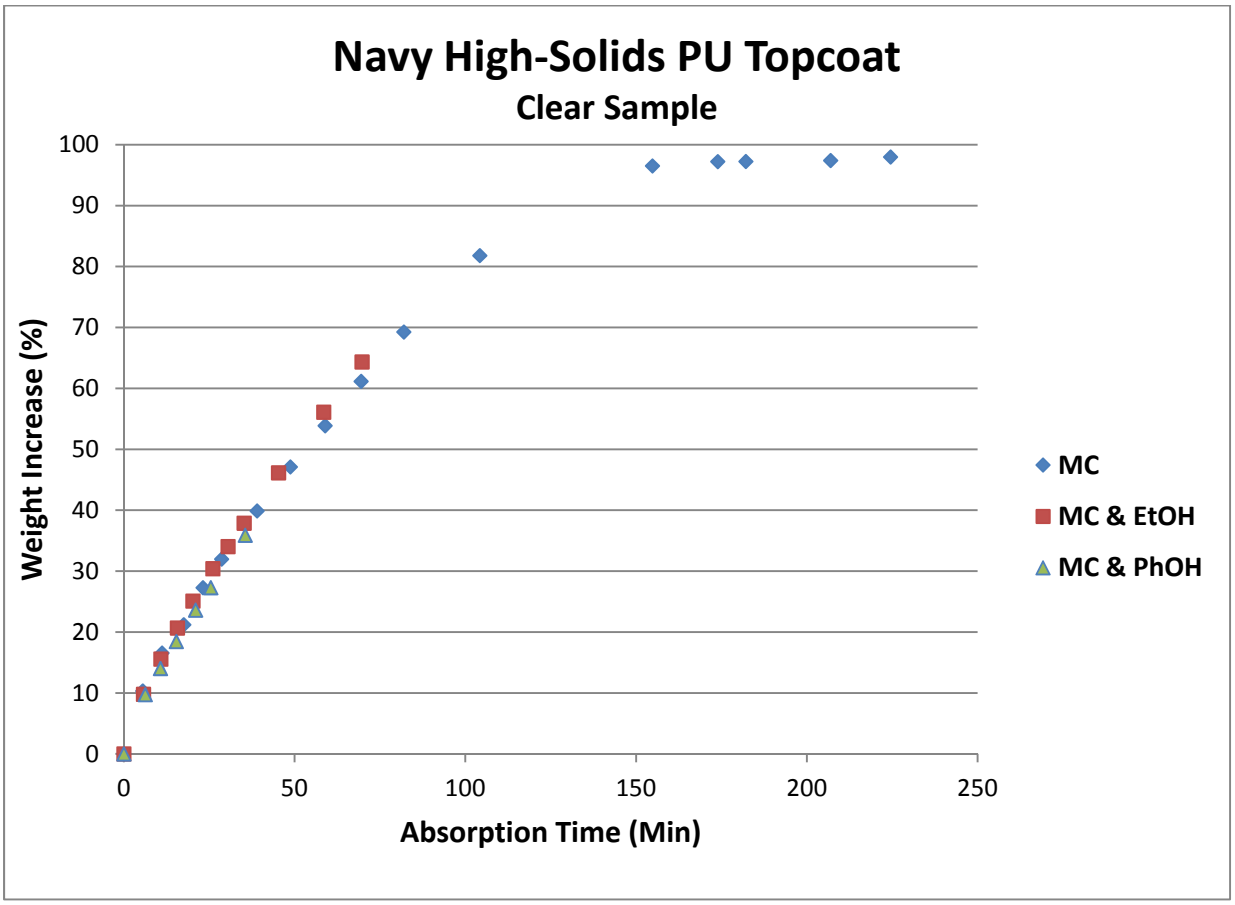

Figure 5-11 Solvent sorption of MIL-PRF-85285 clear samples

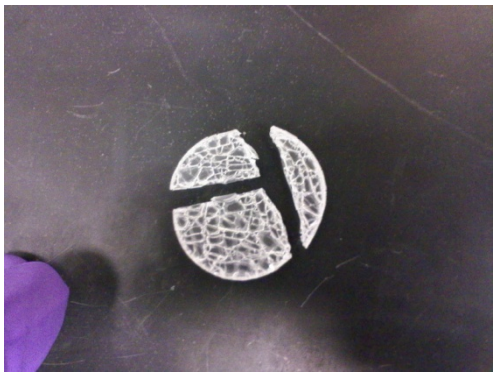

Figure 5-12. MIL-PRF-85285 clear sample exposed to MC/EtOH

Figure 5-13. MIL-PRF-85285 clear sample exposed to MC/PhOH

Unlike the methylene chloride experiment, the samples exposed to MC/EtOH or MC/PhOH broke into pieces before the sorption equilibriums were reached. As shown in Figure 5-11, weight increases for methylene chloride, MC/EtOH, and MC/PhOH are comparable. The diffusion cell study shows that methylene chloride diffuse slightly faster than MC/EtOH and substantially faster than MC/PhOH. Therefore, the weight increase in a unit volume of the solvated layer of sample is highest for MC/PhOH and lowest for methylene chloride. The layer of sample with higher weight increase is expected to experience higher internal stress, which causes fracture of the sample. The sample exposed to MC/PhOH is substantially stiffer than one exposed to methylene chloride. The stress built in an inflexible polymer is not as easily removed, which may be another reason for the fractures of the samples exposed to MC/PhOH. The weight increase of the sample exposed to MC/PhOH for 2 days is 173%, which is 75% higher than the weight increase of the same sample at the sorption equilibrium with methylene chloride alone. This suggests that a large quantity of phenol is absorbed. Absorbed phenol is likely binding with polar groups of the polymer binder, which indicates that hydrogen bond between polymer chains are broken or weakened by phenol. These unique properties of phenol, once absorbed into the polymer binder, may be the reason for the quick fracture of the sample exposed to MC/PhOH into small pieces.

5.2.3.2 MIL-PRF-85285 Fully Formulated

A continuous increase in volume of the MIL-PRF-85285 fully formulated sample immersed in methylene chloride was observed until the sample reached the sorption equilibrium. The sample seemed to soften substantially as the sample absorbed methylene chloride. However, no instrumental measurement on hardness was attempted because current available techniques would have precluded maintenance of the sample intact. The weight vs. time plot, illustrated in Figure 5-14, prepared using the experimental data, indicates that the weight of the sample increased linearly (0.015 g/min, R^2= 0.975) for 80 minutes. After this point the rate of weight increase continuously decreased until the sample reached the sorption equilibrium. At the absorption equilibrium, the weight increase of the sample is 120%.

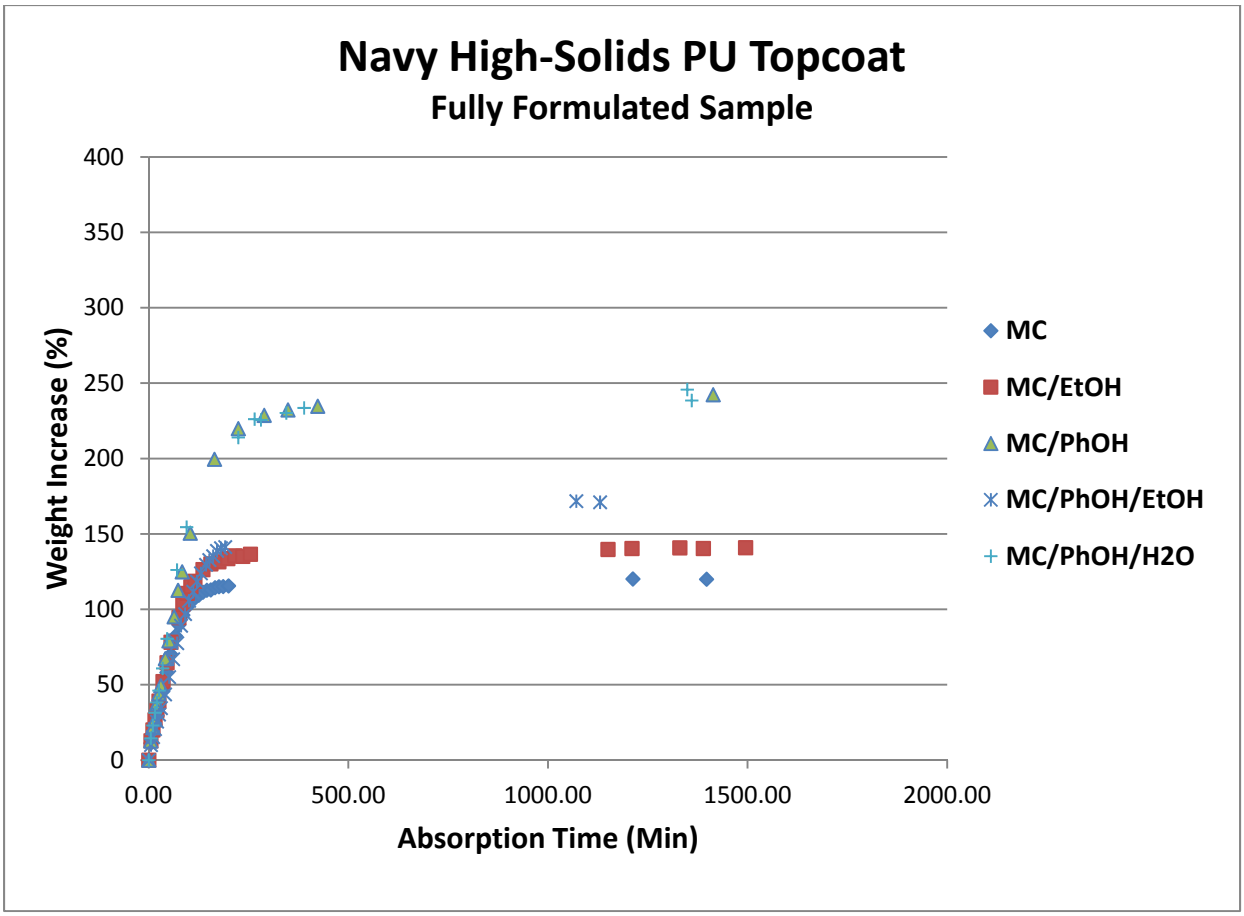

Figure 5-14. Solvent sorption of MIL-PRF-85285 fully formulated sample

Our observation on physical changes of the MIL-PRF-85285 fully formulated sample exposed to MC/EtOH was very similar to the same sample exposed to methylene chloride. The weight of the sample increased linearly (0.017 g/min, R^2= 0.975) for 80 minutes. After this point the rate of weight increase continuously decreased until the sample reached the sorption equilibrium. At the sorption equilibrium, the weight increase of the sample is 140%. The weight increase of the sample used for this experiment is 20% greater than the weight increase of the sample used for the methylene chloride experiment. The increase in size of the sample at the sorption equilibrium is illustrated in Figure 5-15. No fracture was observed unlike the MIL-PRF-85285 clear sample. Cracks shown on Figure 5-15 were developed while the picture was being taken. No attempt was made to find the reason for the different observation. One possible reason may be that the unsolvated core of the MIL-PRF-85285 fully formulated sample is more flexible than that of the MIL-PRF-85285 clear sample.

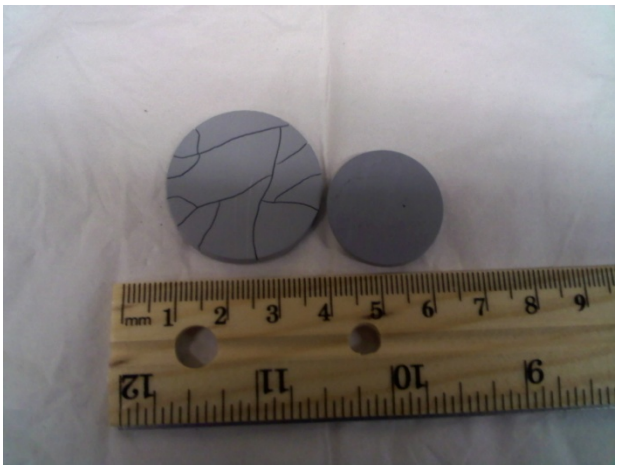

Figure 5-15. Swelling of MIL-PRF-85285 fully formulated with MC/EtOH

Degradation of the surface of the sample exposed to MC/PhOH was observed immediately after the sample was immersed into the test solution. Small coating particles removed from the surface were observed on the bottom of the glass bottle and in the solution as suspended. The sample started to turn to a saddle shape at 19 minutes of immersion and broke into two pieces at 53 minutes. The sample exposed to MC/PhOH was much stiffer than the sample exposed to methylene chloride only. This indicates that the microstructure of the sample absorbed the MC/PhOH is different from that of the sample absorbed methylene chloride. At the completion of the experiment, the coating particles were collected by filtering the test solution through a filter paper and subsequent washing with acetone. The particles were dried and weighed. The weight of the particles was 0.028g that is only 2.18% of the weight of the unexposed sample. The weight of the sample increased linearly (0.019 g/min, R^2= 0.990) for 100 minutes. After this point the rate of weight increase continuously decreased until the sample reached the sorption equilibrium. At the sorption equilibrium, the sample weight had increased by 240%. The weight increase is 120% greater than the weight increase of the sample used for the methylene chloride experiment and 67% higher than the weight increase of the MIL-PRF-85285 clear sample exposed to MC/PhOH. Figure 5-16 illustrates changes of the sample exposed to MC/PhOH.

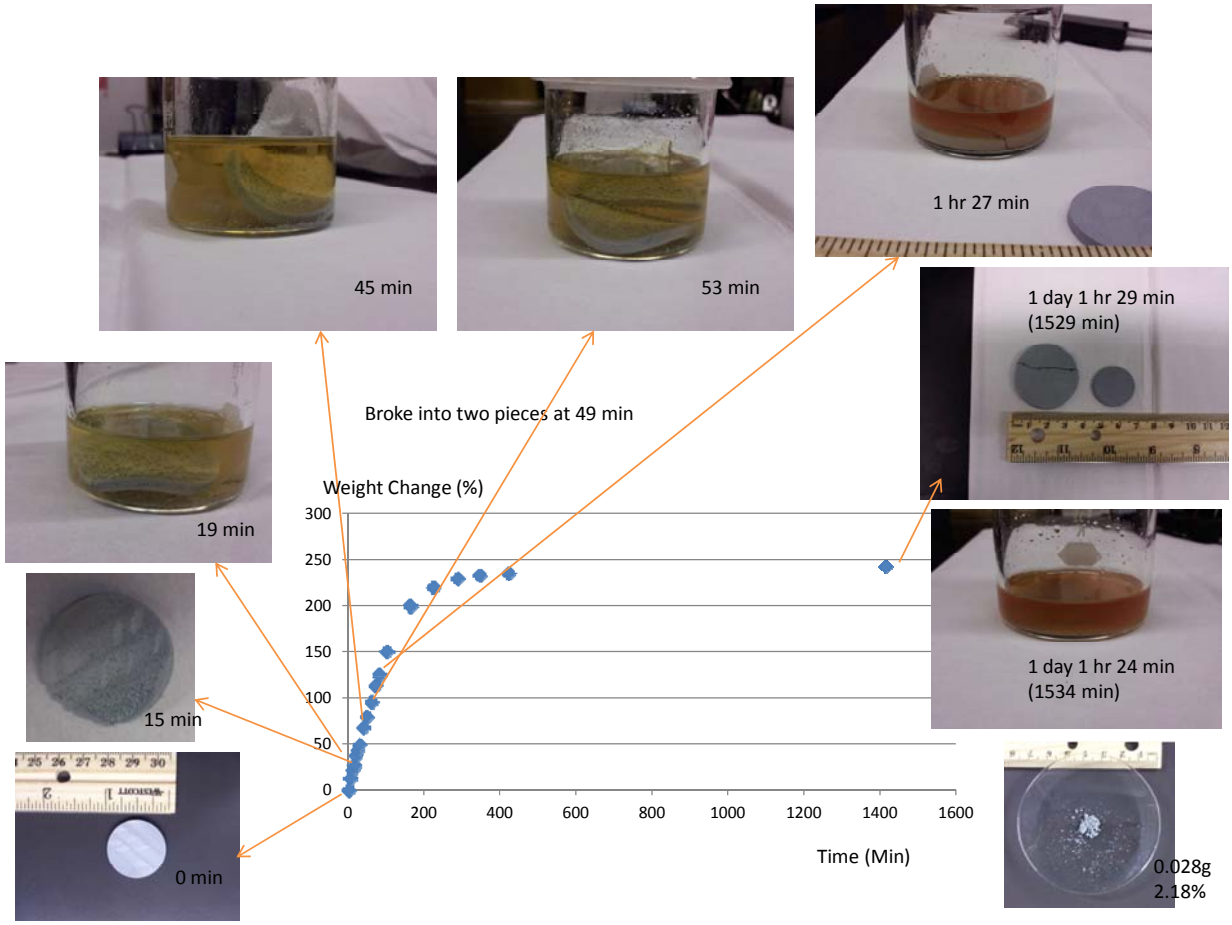

Figure 5-16. Physical changes of MIL-PRF-85285 fully formulated sample exposed to MC/PhOH

The MC/PhOH/EtOH solution is composed of 74% of MC, 19% of PhOH, and 7% of EtOH. No surface degradation was observed for the MIL-PRF-85285 fully formulated sample exposed to this solution. A crack in the middle of the sample was observed at 51 minutes and the sample broke into 2 pieces at 61 minutes. A crack at one corner of the larger piece was also observed at 61 minutes. The weight of the sample increased linearly (0.014 g/min, R^2= 0.994) for 100 minutes. At this point the weight increase slowed. At the absorption equilibrium, the weight increase of the sample is 170% which is 50% greater than the weight increase of the sample exposed to MC alone, but 70% less than the sample exposed to MC/PhOH.

Decomposition of the MIL-PRF-23377 clear film was reported when it was exposed to the MC/PhOH/H_2O mixture listed in Table 4-1.[15] An increase in depaint efficiency was also reported when water was added to MC/PhOH.[16] So, we wanted to see how water in MC/PhOH would change the absorption behavior of the MIL-PRF-85285 fully formulated sample. The test solution was prepared by adding 1 gram of water to the solution of 79 g of MC and 21 g of PhOH. Water didn't dissolve into the solution immediately and water droplets were observed on

the surface of the solution. Gently swirling the solution helped to dissolve water into the solution. This may indicate that swirling helps to form water-phenol clusters[12] that dissolve in methylene chloride. Our observation of physical changes and the solvent absorption behavior of the sample exposed to MC/PhOH/H_2O were very similar to the sample exposed to MC/PhOH; no evidence of chemical decomposition was observed. The weight of the sample increased linearly (0.021 g/min, R^2= 0.991) for 95 minutes. After this point the rate of weight increase continuously decreased until the sample reached the sorption equilibrium. At the absorption equilibrium, the weight increase of the sample is 245%.

5.2.3.3 MIL-PRF-23377 Clear

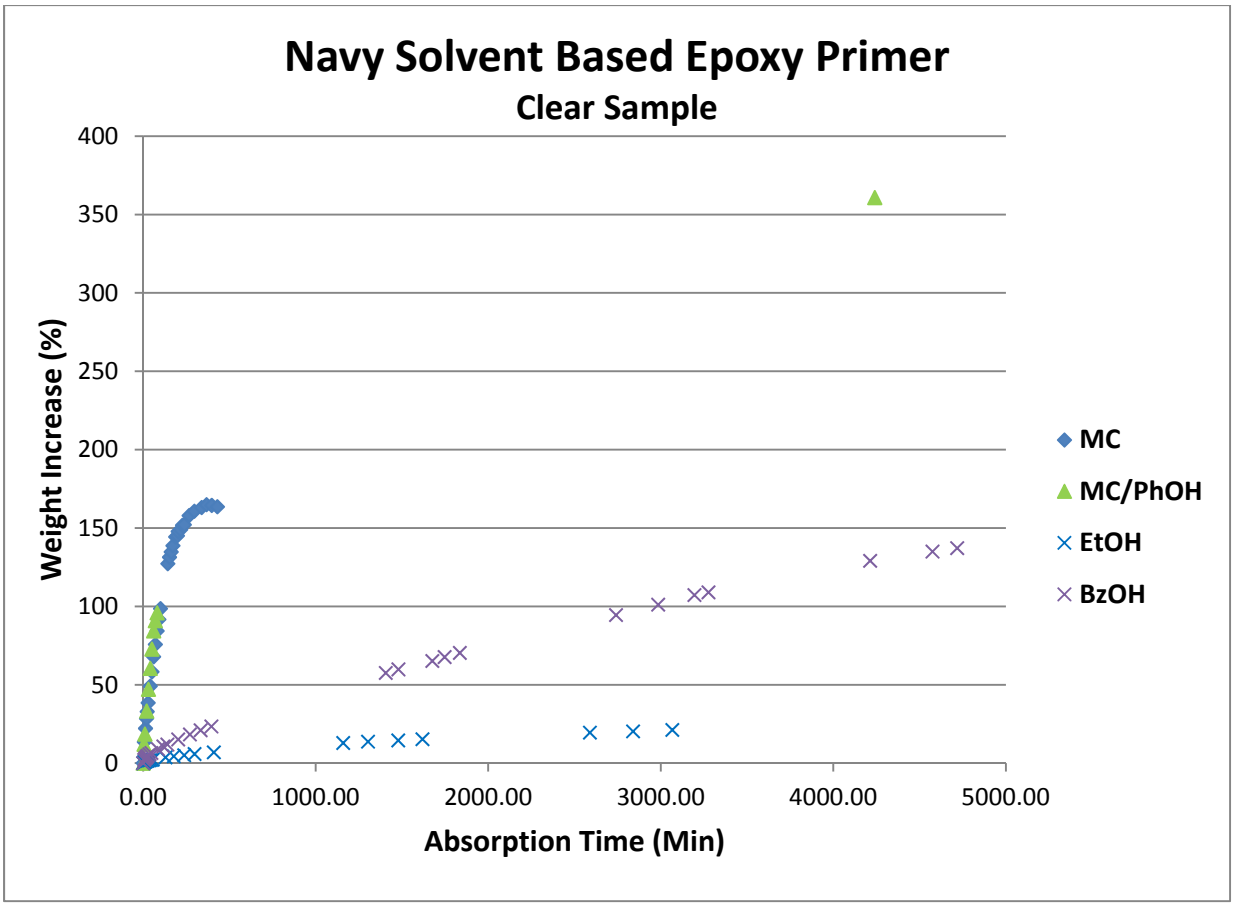

Figure 5-17. Solvent sorption of MIL-PRF-23377 clear samples

The plot of percent mass uptake of methylene chloride vs. time for the MIL-PRF-23377 clear sample is illustrated in Figure 5-17. The weight increase at the sorption equilibrium, which was reached in 6 hours and 7minutes, is 165%. The weight decreased slightly after reaching the sorption equilibrium. The development of cracks in the sample during the absorption test was observed. The picture (illustrated in Figure 5-18) of the sample taken right after completion of absorption test shows the cracks developed during absorption and the size difference relative to

the unexposed sample. Measured dimensions of the sample before and after absorption are provided in Table 5-9. At the sorption equilibrium, the volume increase was 1.525 cm^3 without regard to the volume increase due to cracks and the weight increase was 2.208 grams. If the increased volume was occupied by methylene chloride, the density of methylene chloride in that volume is 1.448 g/ml, which is higher than the density of methylene chloride at ambient condition of 1.327 g/ml. This may imply that (1) the free volume which existed in the sample was filled with methylene chloride and/or (2) methylene chloride has strong dipole-dipole interactions with the polymer chains.

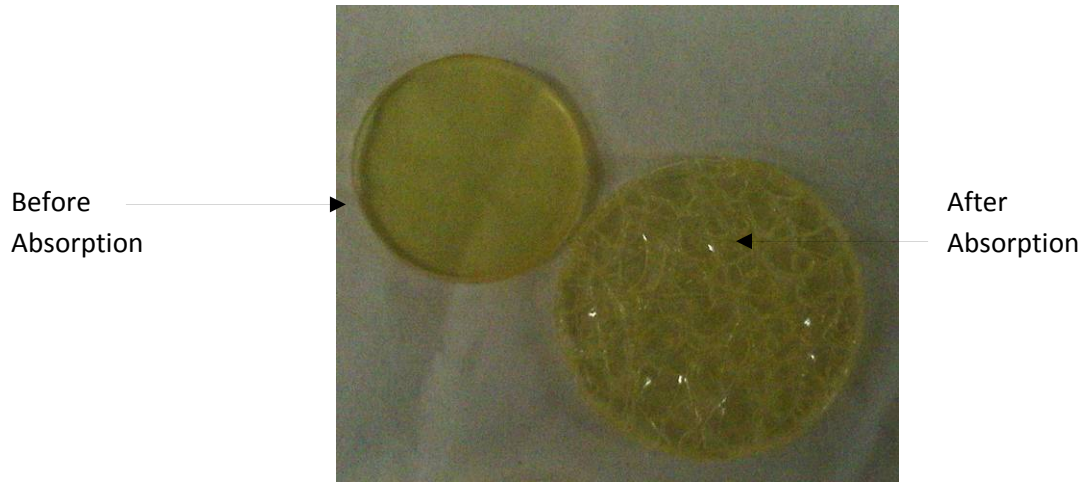

Figure 5-18. Swelling of MIL-PRF-23377 clear sample with methylene chloride

Table 5-9. Dimensions of sample before and after absorption test with MIL-PRF-23377 clear sample and MC

	Before Testing	After Testing	% Increase
Diameter	2.410 cm	3.121 cm	29.5 %
Thickness	0.276 cm	0.364 cm	31.9 %
Volume	1.258 cm^3	2.783 cm^3	121.2 %

For the absorption test performed with MC/PhOH, a 95% weight increase was measured for the sample exposed for 1 hour and 20 minutes as illustrated in Figure 5-19. After that weight measurement, the sample broke into small pieces. It was impossible to collect all pieces for weighing; however, those data gathered clearly indicate that the weight increase of the sample in the MC/PhOH was faster than in methylene chloride. The broken pieces were exposed to the MC/PhOH for three days, which was deemed more than enough time for the sample to reach its equilibrium of sorption. The sample was then filtered and weighed. The weight increase of the sample in the MC/PhOH for three days was 360 %. The picture of the broken sample after 3 day exposure to the MC/PhOH is illustrated in Figure 5-20.

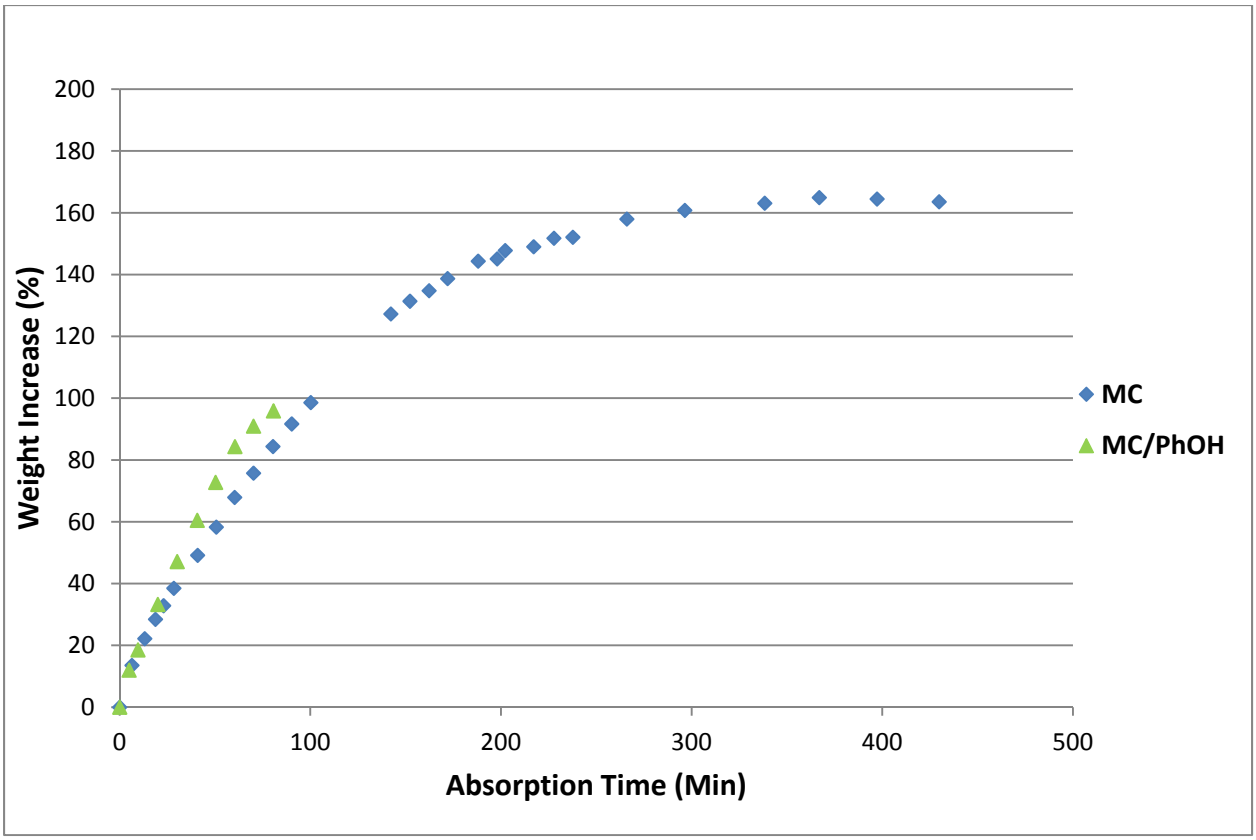

Figure 5-19. Gravimetric solvent sorption test result with MIL-PRF-23377 clear sample with MC/PhOH: % weight change vs. time (minutes)

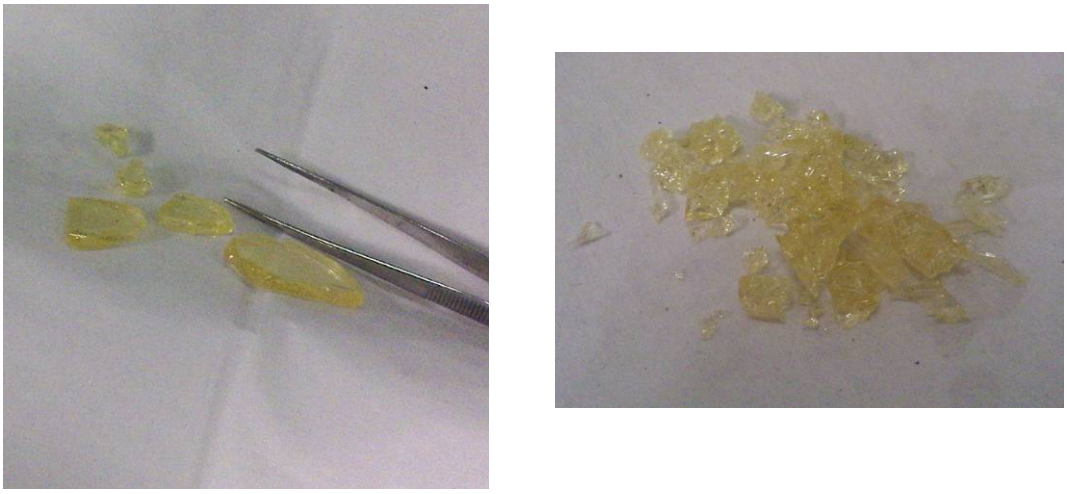

Figure 5-20. Fracture of MIL-PRF-23377 clear sample in MC/PhOH: after 70 minutes (left) and three days (right)

For the absorption test performed with the MIL-PRF-23377 clear sample with ethanol, the sorption equilibrium was reached at 16 hours. The weight increase at the sorption equilibrium is 30%. No cracks or weight decreases were observed with ethanol. Figure 5-21 shows the size difference of the sample after the absorption test relative to an unexposed sample. The measured dimensions of the sample before and after absorption are provided in Table 5-10. The difference between the increases in diameter and thickness is substantial, which indicates that swelling of MIL-PRF-23377 clear sample in ethanol is anisotropic. The weight increase at the equilibrium of sorption is 0.4157 gram. The calculated density of the ethanol absorbed is 0.828 g/ml what is slightly higher than the density of ethanol at ambient condition, 0.789 g/ml.

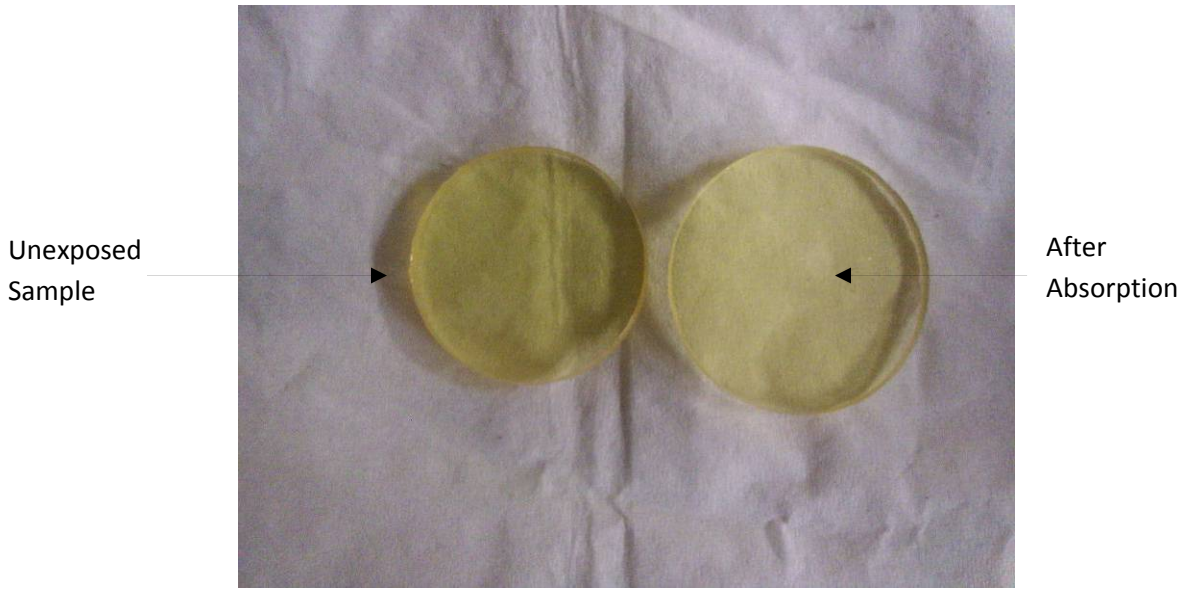

Figure 5-21. MIL-PRF-23377 clear sample before and after absorption test with ethanol

Table 5-10. Dimensions of Sample before and after Absorption Test with MIL-PRF-23377 Clear Sample and EtOH

	Before Testing	After Testing	% Increase
Diameter	2.421 cm	2.675 cm	10.5 %
Thickness	0.272 cm	0.313 cm	15.1 %
Volume	1.251 cm^3	1.758 cm^3	40.5 %

The sorption equilibrium for the sample exposed to benzyl alcohol was reached in 6 days (not all data points are shown in Figure 5-17), which is substantially slower than the time that the same sample exposed to methylene chloride reaches its sorption equilibrium, 6 hours and 40 minutes. However, at the sorption equilibrium the weight increase of the sample immersed in benzyl alcohol is almost identical: 160% for methylene chloride and 164% for benzyl alcohol. These

results indicate that benzyl alcohol would eventually remove a coating that methylene chloride can remove, but the depaint process would be more than 20 times slower.

5.2.3.4 MIL-PRF-23377 Fully Formulated

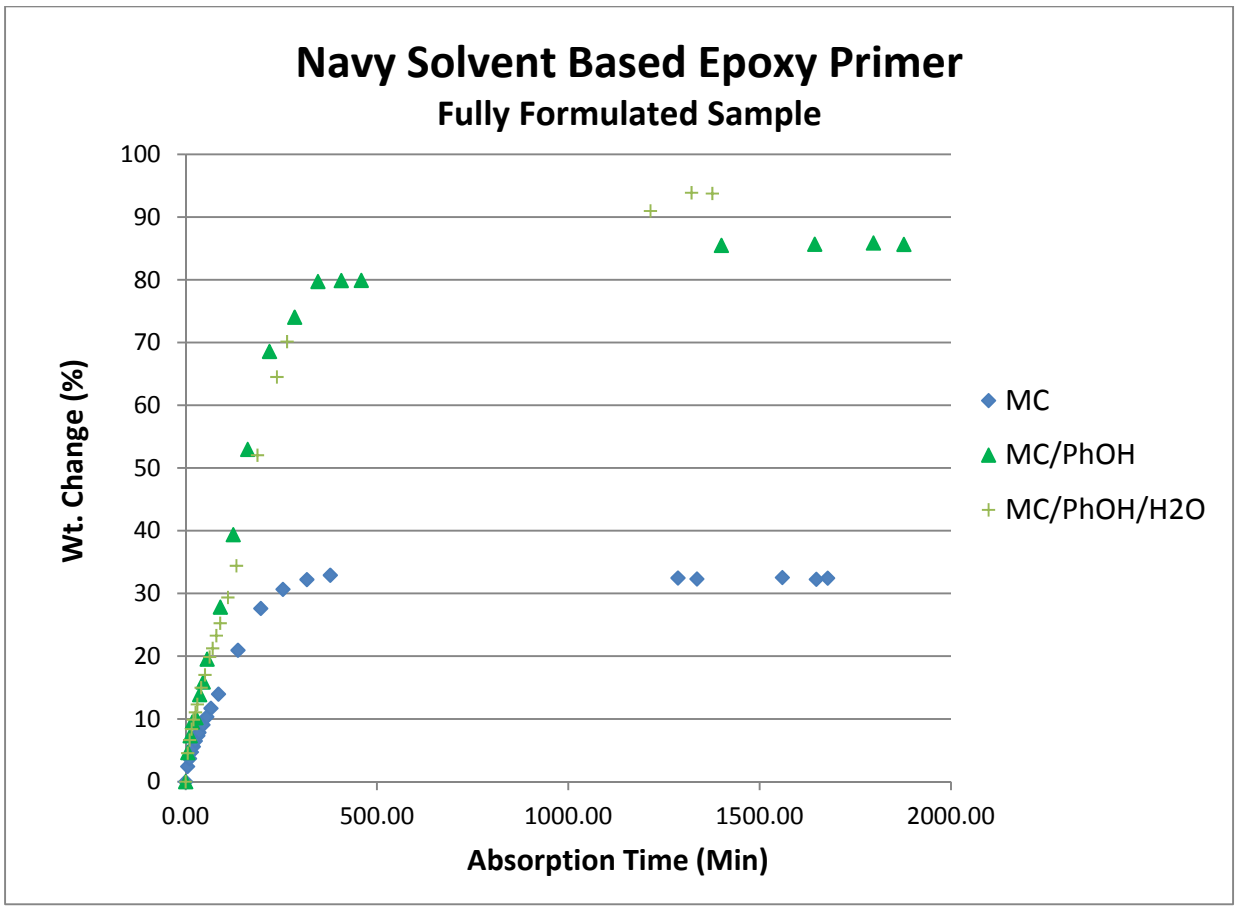

Figure 5-22. Solvent sorption of MIL-PRF-23377 fully formulated samples

The weight of the sample exposed to methylene chloride continuously increased until the sample reached the sorption equilibrium as illustrated in Figure 5-22, but no crack or fracture was observed. Continuous softening of the sample as the sample absorbed methylene chloride was sensed when the tips of the tweezers touched the sample to remove it from the test solvent for weighing. However, no instrumental measurement on hardness was attempted because the attempt would damage the sample. Both the weight vs. time and weight vs. square root of time plots prepared using the experimental data slightly deviate from linearity, which indicates that the methylene chloride absorption mechanism of the fully formulated MIL-PRF-23377 coating is more complicated than that of the clear MIL-PRF-23377 sample. Even though the weight does not increase linearly with respect to time, the weight vs. time plot clearly indicates that the weight increase rate starts dropping significantly at 3 hours and 16 minutes. After this point the rate of weight increase continuously decreased until the sample reached the sorption equilibrium

at 6 hours and 18 minutes. At the absorption equilibrium, the weight increase of the sample is 33%, which is substantially lower than the weight increase of the clear MIL-PRF-23377 exposed to methylene chloride, 165%. The increase in volume is approximately 31.7%. The picture (illustrated in Figure 5-23) of the sample taken right after completion of absorption test, shows the size difference relative to the unexposed sample. The increases in diameter and thickness of the sample are 11.44% and 18.14% respectively.

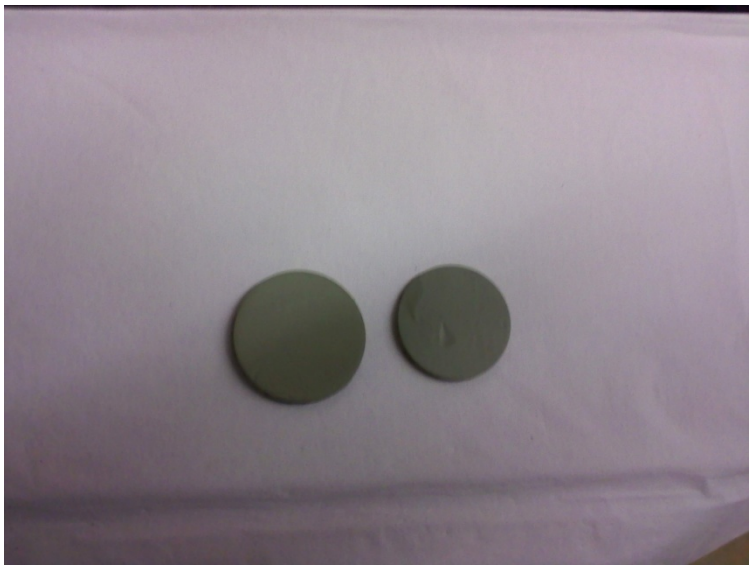

Figure 5-23. MIL-PRF-23377 fully formulated sample before and after absorption test with methylene chloride

Surface degradation of the MIL-PRF-23377 fully formulated sample (illustrated in Figure 5-24) was first observed 20 minutes after the sample was immersed in MC/PhOH. It appears that degradation only occurs on the surface of the sample. Similar degradation was also observed on the MIL-PRF-85285 fully formulated sample exposed to MC/PhOH. The weight of the sample increased linearly (rate = 0.318 gram/minute, $R^2 = 0.989$) for 3 hours and 39 minutes. After this point the rate of weight increase continuously decreased until the sample reaches the equilibrium sorption at 10 hours. At the sorption equilibrium, the weight increase of the sample is 85%. As we observed for the MIL-PRF-85285 fully formulated sample and MC/PhOH, the weight increase is substantially higher than the weight increase of the sample exposed to MC alone. The picture (illustrated in Figure 5-25) of the sample taken immediately after completion of absorption test, shows the size difference relative to the unexposed sample. No crack was observed during the absorption test. The crack shown on Figure 5-25 was developed while the picture was taken. The increases in diameter and thickness of the sample are 33.55% and 29.70% respectively. The increase in volume is approximately 73%.

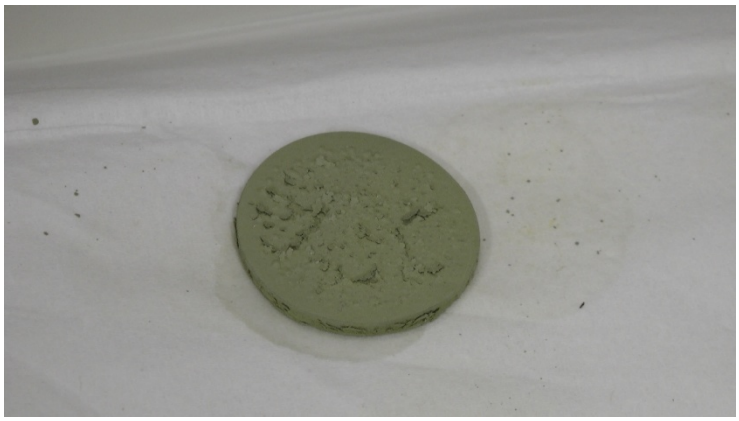

Figure 5-24. Surface degradation of MIL-PRF-23377 fully formulated sample exposed to MC/PhOH

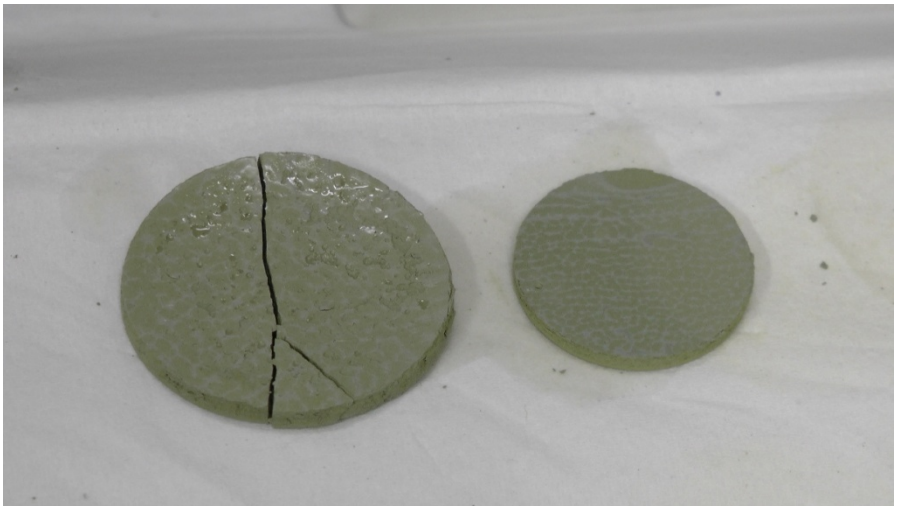

Figure 5-25. MIL-PRF-23377 fully formulated sample before and after absorption test with MC/PhOH

An experiment was conducted with MC/PhOH/H_2O to examine how water in MC/PhOH changes the absorption behavior of the MIL-PRF-23377 fully formulated epoxy primer. Unlike the experiment with MC/PhOH, no degradation of the sample surface was observed. The weight of the sample increased linearly (rate = 0.265 gram/minute, $R^2 = 0.979$) for 4 hours and 25 minutes. Interpolation of the data points suggests that the absorption equilibrium was reached at approximately 10 hours. At the absorption equilibrium, the weight and volume increases of the sample are 93% and 85% respectively. These results indicate that water added to MC/PhOH slightly changed the absorption behavior of the fully formulated MIL-PRF-23377 sample.

5.3 Thermal Analysis

Thermal analysis of the coatings before and after exposure to control solvent mixtures of individual components typically found in commercial paint stripper can give insight into the degradation caused by the paint stripper. By studying the change in glass transition temperature, T_g, the specific solvent mixtures that were responsible for significant degradation of the coatings were identified. DSC scans taken of coatings after exposure to the control solvent mixtures show decreases of the glass transition temperature by as much as 100°C. Changes in the TGA curve can also illustrate a solvent mixture's activity and suggest both the physical and chemical degradation mechanism.

5.3.1 Initial characterization

Film samples of fully formulated CARC (MIL-DTL-53039) and Navy/Air Force topcoat (MIL-PRF-85285) were prepared on release paper and characterized for baseline measurements using FTIR-ATR, TGA, and DSC. The purpose of this preliminary study was to determine that the method and instrumental technique were not only compatible with the individual instrument, but also to determine that the sample thickness was sufficient to perform under the specified method once the control formulation coatings become available.

Upon receiving the clear control films, characterization by FTIR-ATR ensured the correct functionalities were present and to provide a snapshot of the degree of curing by examining free unreacted functional groups. After observing satisfactory results, TGA analysis was performed to ensure the absence of nontraditional species such as inorganic additives. All coatings demonstrated less than 1 wt. % incombustible material in a breathing air atmosphere, which was acceptable for subsequent analyses.

5.3.2 Clear Films

In an attempt to find evidence of chemical and physical changes, DSC was employed on each of the clear films upon exposure to controlled combinations of the depaint ingredients as seen in Table 5-11. This was followed by analysis of the exposed clear film using TGA. The control solutions of phenol with methylene chloride and separately with ethanol were tested for the effect on the films after observation of the significant change to the films exposed to the mixture containing phenol. DSC was performed on all exposed coatings while TGA was only performed on films exposed to solvent for two hours. The solutions used for thermal studies are shown in Table 4-1.

Table 5-11. Reported glass transition values of clear coatings from DSC

		MIL-DTL-53039	MIL-PRF-85285	MIL-PRF-85582	MIL-PRF-23377	MIL-PRF-53022
Control		87	51	62	40	67
2 hour exposure	**MC**	67	46	74	49	81
	MC/ EtOH	67	44	76	48	85
	MC/EtOH/Water	70	45	77	48	75
	MC/EtOH/H_2O/PhOH	-11	decomp	decomp	17	61
	MC/PhOH	-4	-30	-18	-22	73
	EtOH/PhOH	-9	-25	-33	-19	41
Two day exposure	**MC**	72	44	70	51	70
	MC/EtOH	65	41	76	49	69
	MC/EtOH/H_2O	70	43	82	51	75
	MC/EtOH/H_2O/PhOH	-4	decomp	decomp	-5	62

For the MIL-DTL-53039 clear film, it is also noted that exposure to EtOH/PhOH caused the coating to separate into two layers with different physical properties, although each layer had similar T_g values. Exposure to MC/PhOH resulted in the onset of delamination; however, no other solvent(s) caused such separation, making it unreasonable to assume that the separation results from film preparation. The TGA for the MIL-DTL-53039 clear film before and after exposure can be seen in Figure 5-26. The TGA of the coatings exposed to the mixtures without phenol are all similar to that of methylene chloride alone. All of these mimic the shape of the TGA control coating except a larger weight loss by 150°C. The TGA of the coatings exposed to the mixtures containing phenol show immediate weight loss and a different graph shape including a more severe (~50%) weight loss by 200°C. Measurement of the TGA of the EtOH/PhOH exposed coating was preempted by the coating's separation into two layers.

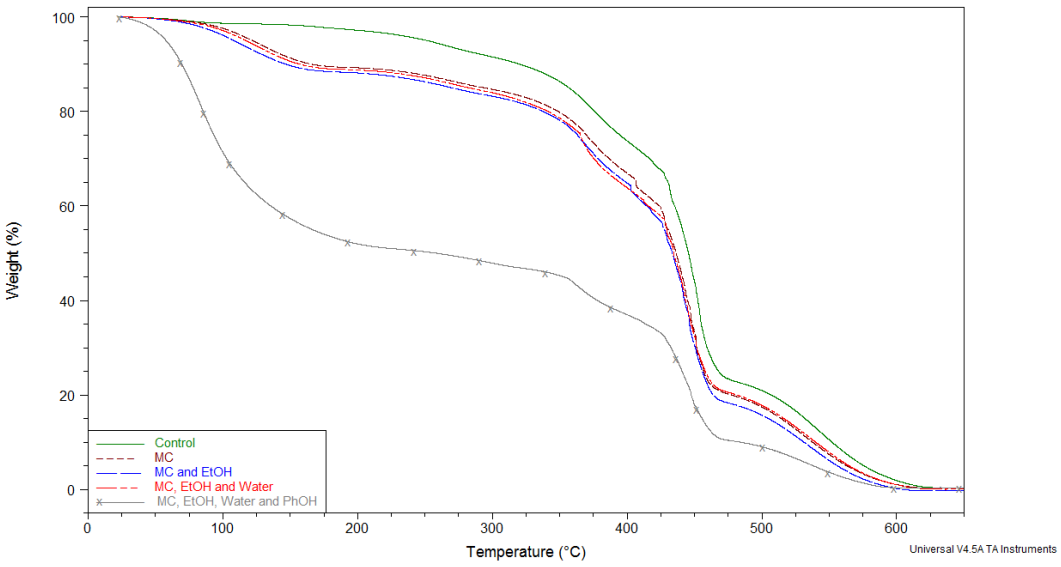

Figure 5-26. TGA overlay for the MIL-DTL-53039 clear film

For MIL-PRF-85285, the clear film of this coating that was exposed to MC/EtOH/H_2O/PhOH decomposed into small pieces preventing DSC or TGA analyses. The TGA results for this MIL-PRF-85285 clear film can be seen in Figure 5-27. They follow the same patterns as the TGAs of MIL-DTL-53039.

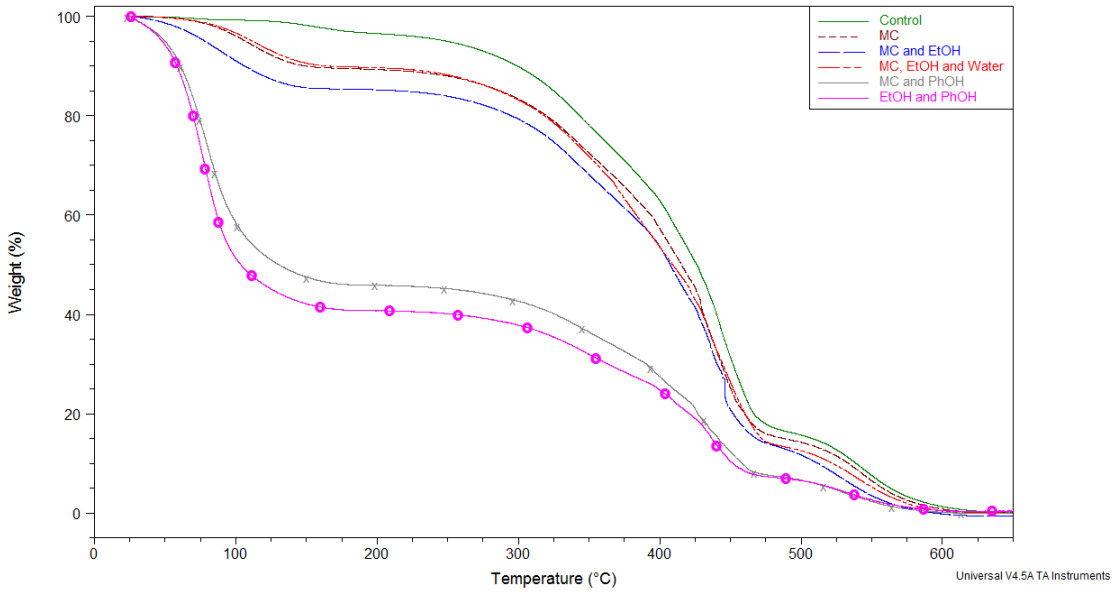

Figure 5-27. TGA overlay for the MIL-PRF-85285 clear film

For MIL-PRF-85582, the clear film of this coating that was exposed to MC/EtOH/H_2O/PhOH decomposed into small pieces, like the MIL-PRF-85285 clear film, preventing DSC and TGA analysis. The TGA of the MIL-85582 coatings can be seen in Figure 5-28.

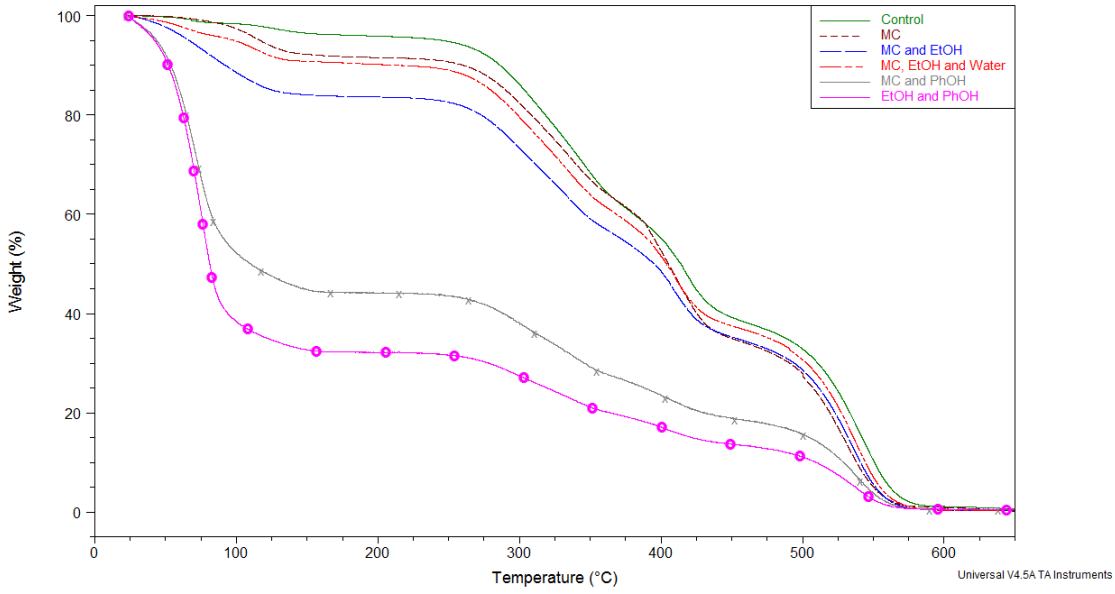

Figure 5-28. TGA overlay for the MIL-PRF-85582 clear film

For MIL-PRF-23377, it appears that the analysis process is most likely resulting in additional cross-linking of the already highly cross-linked system. The TGA of the MIL-23377 clear film can be seen in Figure 5-29.

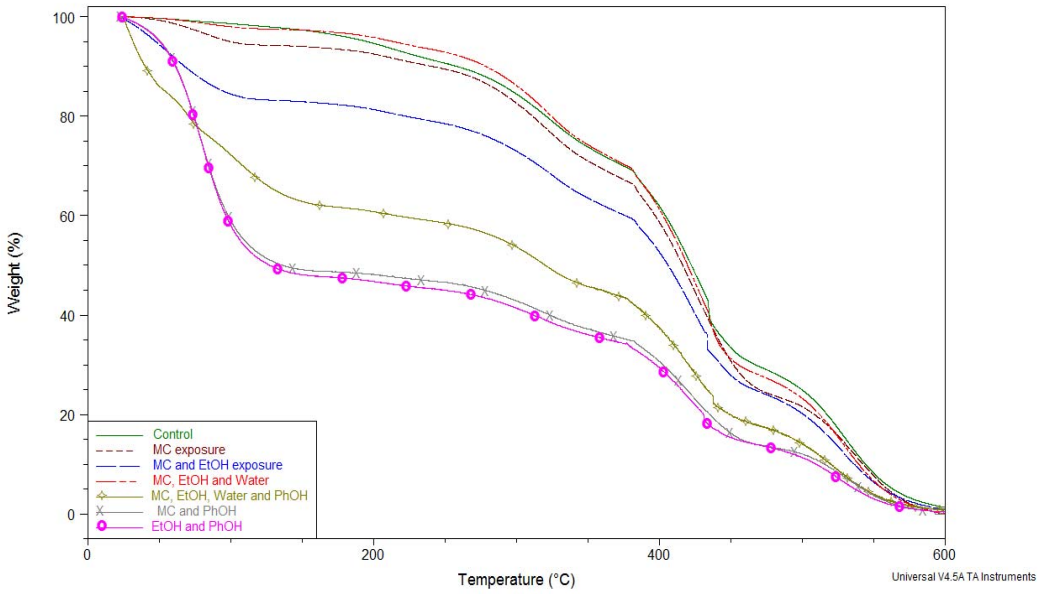

Figure 5-29. TGA overlay for the MIL-PRF-23377 clear film

For MIL-DTL-53022, the degradation profile is unchanged by exposure. Exposures to the solvent mixtures have a limited effect, primarily increasing the weight loss at low temperatures. The MC/EtOH/H_2O/PhOH exposure does not dramatically change the TGA profile as shown in other clear films. The TGA for the MIL-DTL-53022 clear film is shown in Figure 5-30.

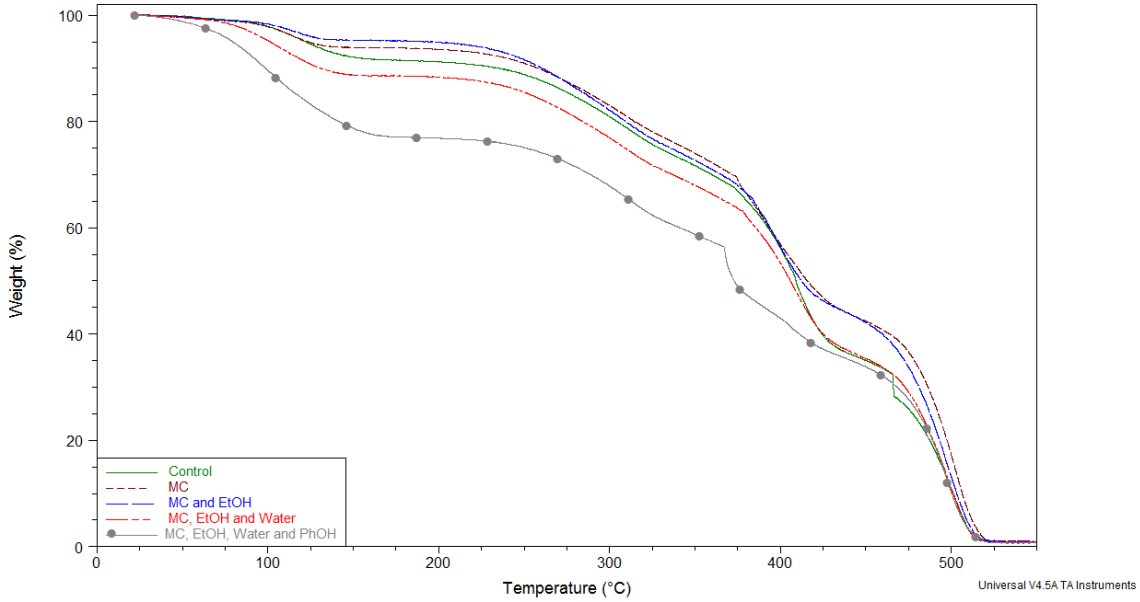

Figure 5-30. TGA overlay for the MIL-DTL-53022 clear film

5.3.3 Color Change and Headspace Analysis

It was noted, some weeks after testing the samples, that clear films which had been exposed to solvent mixtures containing phenol exhibited color changes. The original coating samples are clear or slightly opaque. MIL-DTL-53039 and MIL-PRF-85285 clear films turned pink after exposure to phenol while MIL-PRF-85582 and MIL-PRF-23377 clear films turned orange. Figure 5-31 shows an example of the color changes. The left is MIL-DTL-53039 clear film (the CARC polyurethane topcoat) after exposure to MC/EtOH/H_2O/PhOH and the right is MIL-PRF-23377 clear film (the polyamide epoxy primer) after exposure to MC/PhOH.

Figure 5-31. Examples of color change of clear films after exposure to phenol solution (MIL-DTL-53039 on left, MIL-PRF-23377 on right)

A weight loss is seen in the TGA at temperatures lower than 100°C for the clear films exposed to solvent mixtures containing methylene chloride, ethanol, water and phenol in any combination. This weight loss was not seen in the unexposed coatings. A method was devised to determine if the exposure solvents were trapped in the clear coatings at room temperature. Small portions of exposed coatings were heated in small air-tight vials and then the head space vapors were injected into the GC/MS. The resulting chromatograms show that methylene chloride, ethanol and phenol are being trapped in the clear coatings at room temperature and released upon heated. Methylene chloride and ethanol are seen weeks after drying while phenol is seen months after drying.

5.3.4 Fully Formulated Films

Fully formulated coatings were also examined by thermal analysis. The first difference noted between the fully formulated and clear films was that the DSC of unexposed coating (control) gave a lower glass T_g for the fully formulated films than for the clear films in all formulations except MIL-PRF-23377. Two of the coatings, MIL-DTL-53022 and MIL-PRF-85285, have T_g below room temperature and are somewhat rubbery/flexible at room temperature.

Fully formulated films were exposed for two hours to five separate solvent mixtures previously used with the clear films: methylene chloride alone (MC); a methylene chloride and ethanol solution (MC/EtOH); a methylene chloride, ethanol and water (MC/EtOH/H_2O); a methylene chloride, ethanol, water and phenol (MC/EtOH/H_2O/PhOH); a methylene chloride and phenol solution (MC/PhOH); and an ethanol and phenol solution (EtOH/PhOH) listed in Table 4-1. It was observed that the fully formulated films react somewhat differently than the clear films upon solvent exposure, as can be seen in Table 5-12. The exposure of the first three solvent mixtures does not significantly change the T_g of the clear coatings. However these exposures cause large

increases in T_g for the fully formulated films. The exposure to the phenol containing solutions causes severe decreases in T_g for most of the fully formulated coatings. The MC/EtOH/H_2O/PhOH solution gives the greatest decrease in T_g from the control for all of the fully formulated films. The other two phenol containing solutions decrease the T_g to a lesser extent except in MIL-DTL-53022. For all of the fully formulated films the EtOH/PhOH solution has a less pronounced effect than the MC/PhOH solution.

Table 5-12. Glass Transition temperatures for clear and fully formulated films after a two hour exposure to control solvent solutions

	MIL-PRF-23377 epoxy primer		MIL-PRF-85582 epoxy primer		MIL-DTL-53039 Polyurethane topcoat		MIL-PRF-85285 Polyurethane topcoat		MIL-PRF-53022 epoxy primer	
	clear	fully formulated	clear	fully formulated	clear	fully formulated	clear	fully formulated	clear	fully formulated
Control	40	65	62	50	87	60	51	0	67	10
MC	49	91	74	102	67	76	46	15	81	83
MC/EtOH	48	93	76	100	67	76	44	22	85	81
MC/EtOH/ Water	48	103	77	103	70	81	45	26	75	93
MC/EtOH/ Water/PhOH	17	-2	DECOMP	-12	-11	-8	DECOMP	-38	61	-20
EtOH/PhOH	-19	56	-33	4	-9	-13	-25	-45	41	38
MC/PhOH	-22	36	-18	21	-4	-2	-30	-54	73	15

TGA of the fully formulated coatings were performed before (control) and after exposure to the same solvent solutions used to test the clear coatings. For the fully formulated films exposed to methylene chloride, MC/EtOH, or MC/EtOH/H_2O, the TGA differ from those of the clear films, but in general do not differ from the control. In all of the fully formulated film samples the exposed samples show less weight loss than the controls as illustrated in Figures 5-32 through 5-36, which is opposite of what was seen with the clear coatings. The MIL-PRF-23377 fully formulated film shows little difference after exposure compared to the control. The shape of the TGA curve after exposure looks very similar to the controls for MIL-PRF-23377, MIL-PRF-85285 and MIL-DTL-53022. The TGA curves for MIL-PRF-85582 vary somewhat depending upon exposure. The thermograms of MIL-DTL-53039 fully formulated film look similar in shape to each other, but different from the control.

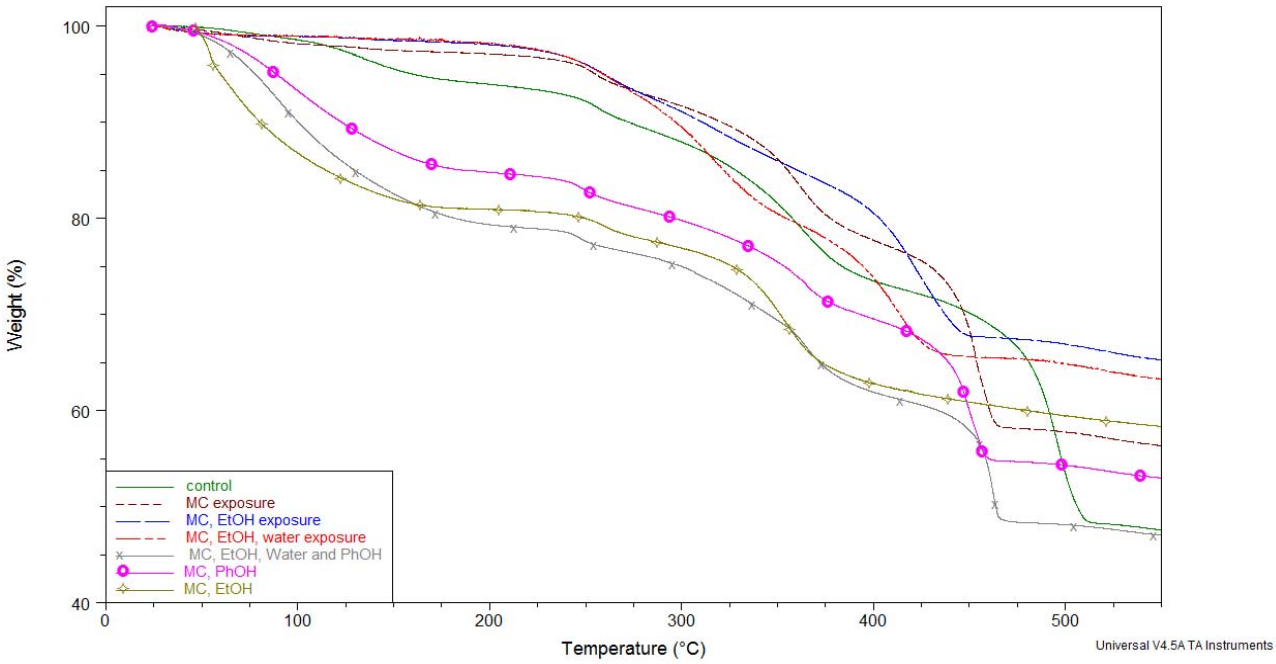

Figure 5-32. TGA overlay of MIL-PRF-85582 fully formulated film

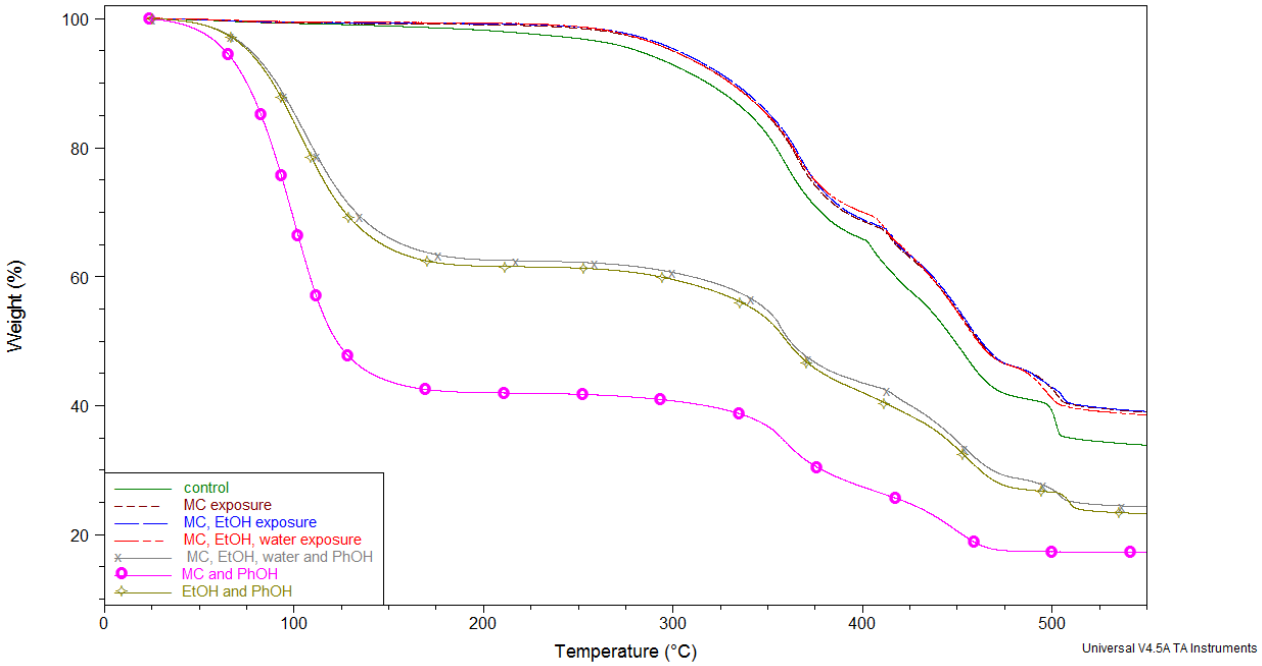

Figure 5-33. TGA overlay of MIL-PRF-85285 fully formulated film

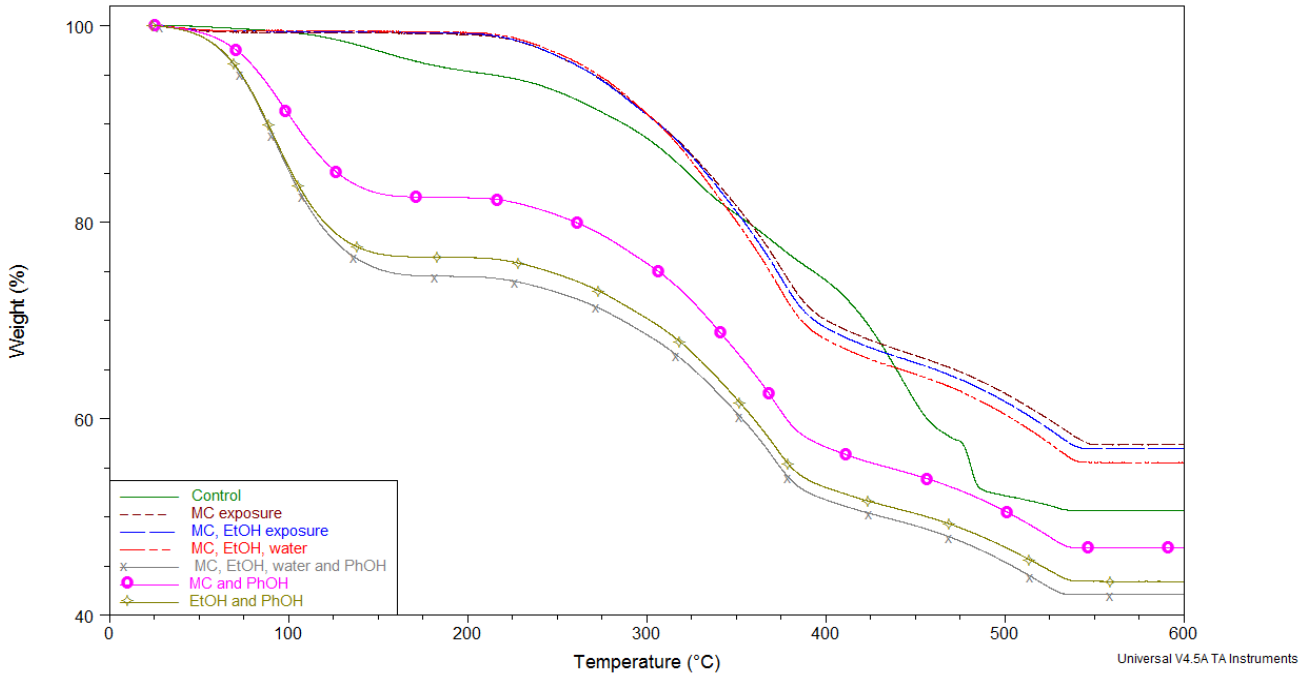

Figure 5-34. TGA overlay of MIL-DTL-53039 fully formulated film

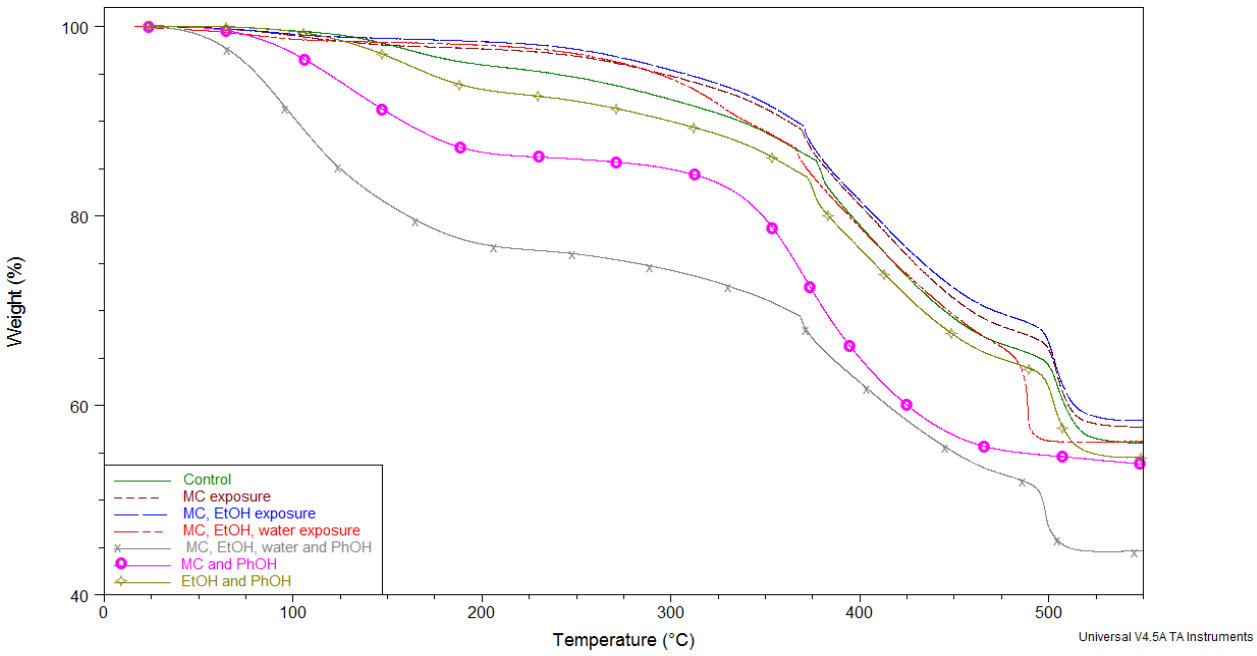

Figure 5-35. TGA overlay of MIL-PRF-23377 fully formulated film

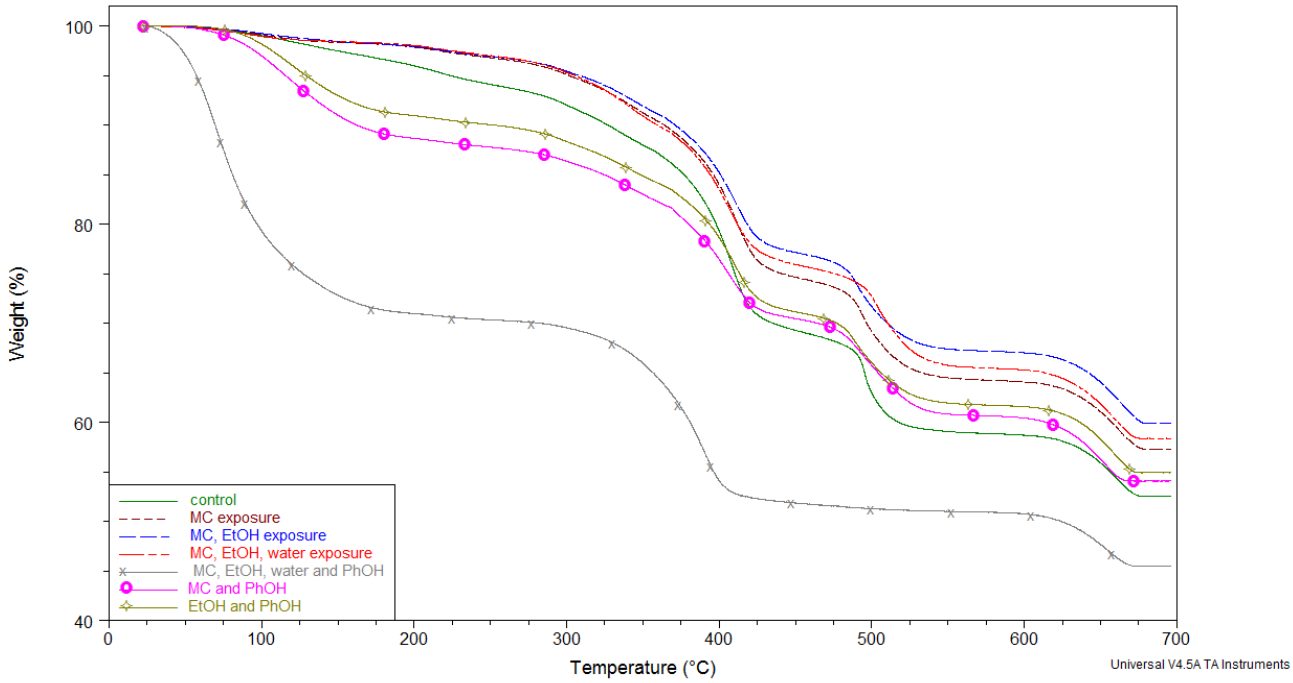

Figure 5-36. TGA overlay of MIL-DTL-53022 fully formulated film

Exposures to the phenol containing solutions (MC/EtOH/H_2O/PhOH, MC/PhOH and EtOH/PhOH) produce similar TGA results in the fully formulated coatings as well as in the clear coatings, mainly because of a substantial weight drop at the low temperatures while maintaining the same degradation profile as the control coating. For all the coatings except MIL-PRF-85285, exposures to the four component solution caused the greatest weight drop. In MIL-PRF-85285 the MC/PhOH solution created the largest weight decrease.

5.3.5 Comparison of clear, partially formulated and fully formulated films

DSC and TGA were also performed on partial formulations of MIL-DTL-53039 and MIL-PRF-85285. These film samples of partial formulations were made by ARL without any flattening agents but with pigments. These film samples were analyzed before and after exposure to a subset of the control solvent mixtures: methylene chloride; MC/EtOH/H_2O; and MC/EtOH/H_2O/PhOH listed in Table 4-1. The resulting glass transition temperatures show the same trend seen in the analysis of clear coatings with limited difference unless the solvent solution contains phenol, in which case a significant decrease in T_g occurs as shown in Table 5-13.

Table 5-13. Glass transition temperatures of clear, partial and fully formulated coatings of MIL-PRF-85285 and MIL-DTL-53039

Glass Transition Temperatures (T_g) in °C						
Solvent Exposure	**Navy/Air Force PU topcoat MIL-PRF-85285**			**Army polyurethane topcoat MIL-DTL-53039**		
	Clear Coatings	**Partial Formulation**	**Full Formulation**	**Clear Coatings**	**Partial Formulation**	**Full Formulation**
Control (no exposure)	51	65	0	87	64	60
Methylene Chloride (MC)	46	65	15	67	67	76
MC /EtOH/H_2O	45	65	26	70	66	81
MC/EtOH/H_2O/ PhOH	DECOMP	-19	-38	-11	-25	-8

TGA response of the partially formulated coatings was as expected. They have similar thermal degradation patterns to the clear and fully formulated coatings of the same military specification as illustrated in Figures 5-37, 5-38, 5-39, and 5-40. The finial weight of the partial formulated coatings lies between that of the clear (approaching zero) and the fully formulated coatings. The fully formulated coatings have a large amount of inorganic material as they contain pigments and flatteners where the partial formulated coatings have only flatteners.

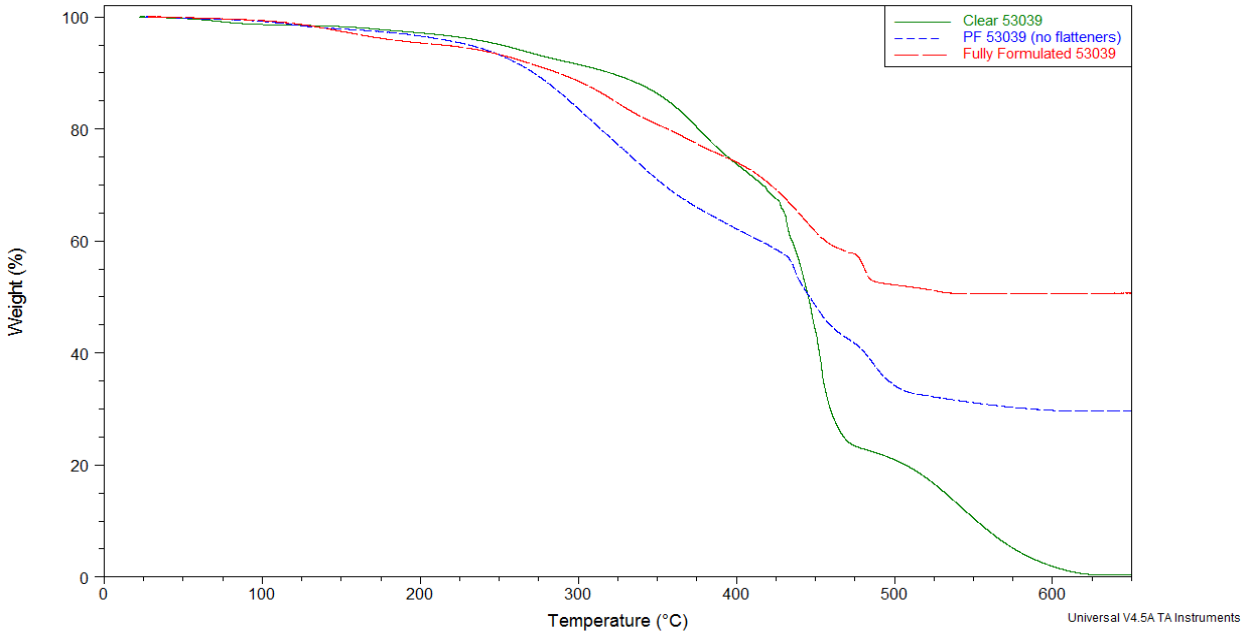

Figure 5-37. TGA overlay of the three formulations of control (unexposed) coatings of CARC polyurethane topcoat (MIL-DTL-53039)

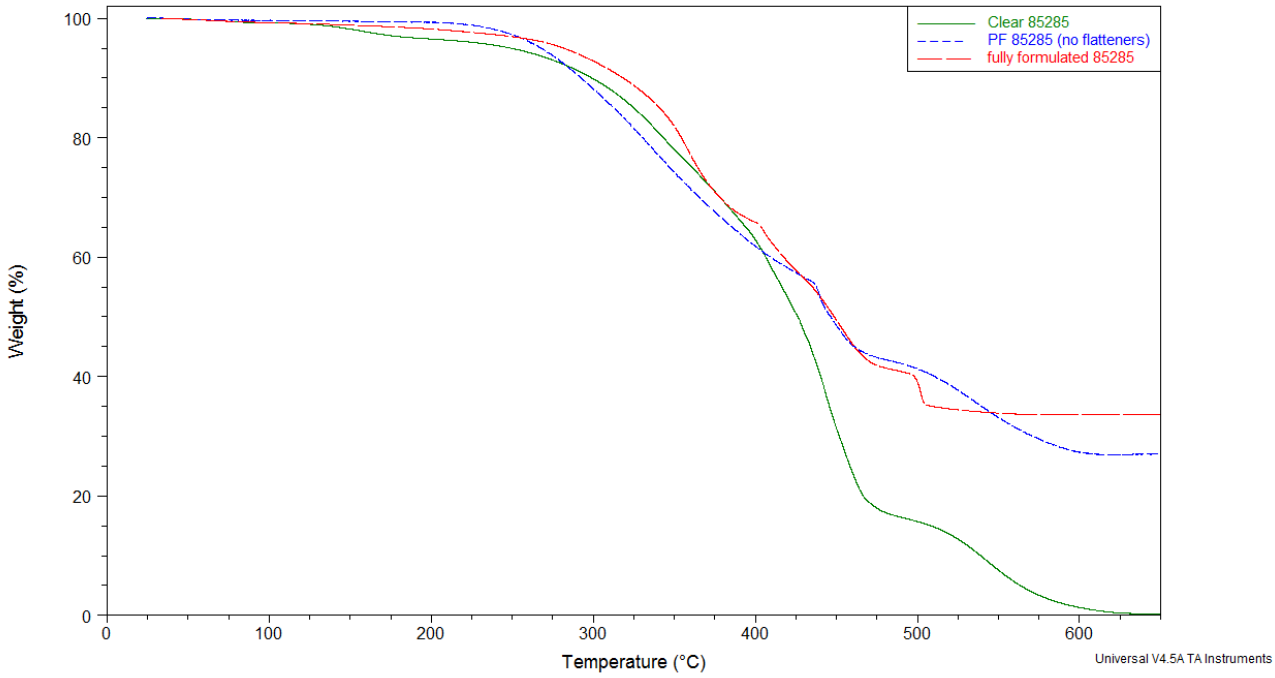

Figure 5-38. TGA overlay of the three formulations of control (unexposed) coatings of NAVY topcoat (MIL-PRF-85285)

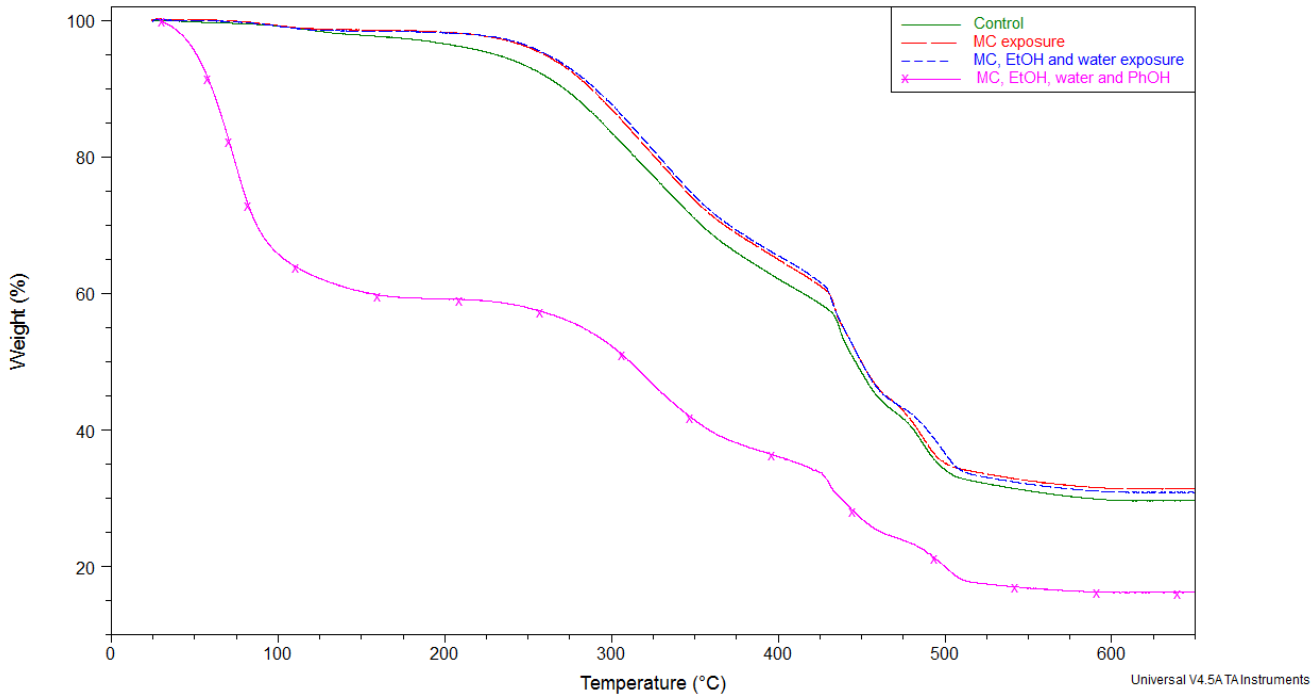

Figure 5-39. TGA overlay of Partial Formulated CARC polyurethane topcoat (MIL-DTL-53039) exposed to different solvent mixtures

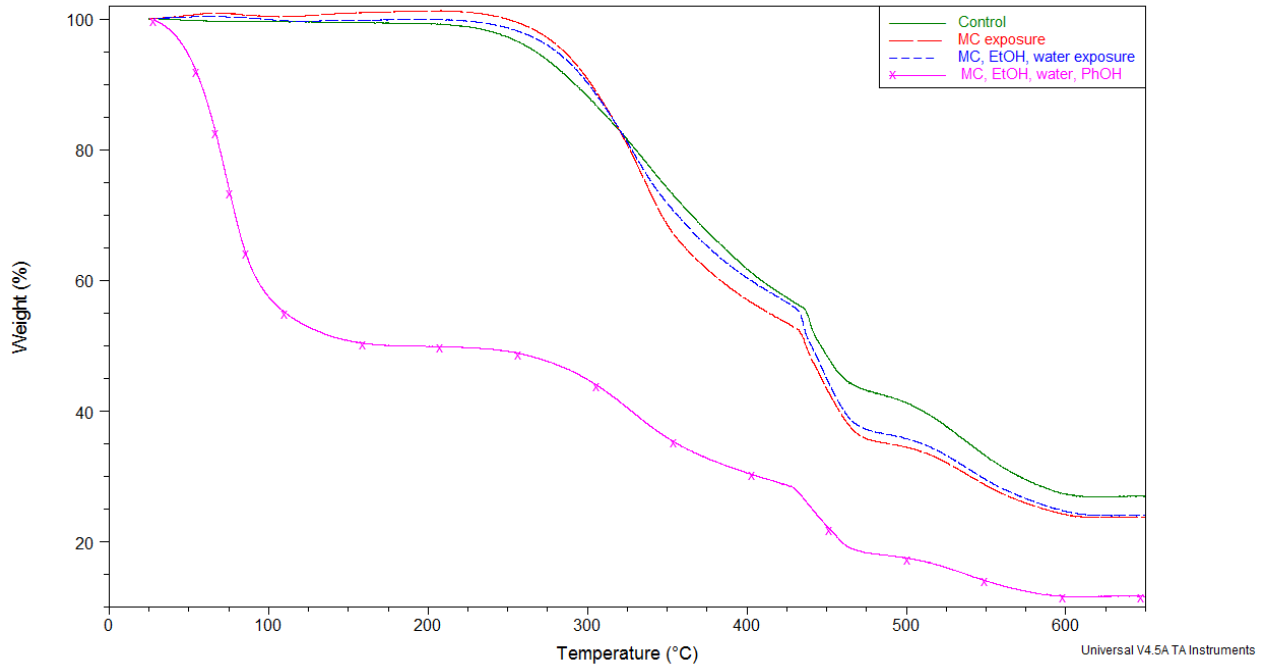

Figure 5-40. TGA overlay of partial formulations of NAVY polyurethane topcoat (MIL-PRF-85285) exposed to different solvent mixtures

The results of thermal analysis of clear films before and after exposure to the control solvent mixtures, as compared to the fully and partially formulated films, clearly illustrate the usefulness of the simplified coating system. Although the presence of pigments, filler and flatteners have an effect on the basic value of the glass transition temperature, the trends and changing of the T_g upon exposure is independent of the presence of this inorganic particles. The weight of incombustibles remaining at the end of the TGA run is, understandably, altered by the presence of pigments, fillers and flatteners but again the changes after exposure do not appear affected.

5.4 Vibrational Spectrometry

In order to create a mechanistic model, the chemical changes induced by solvents drawn from the MIL-R-81294 control formulation were evaluated using Raman and FTIR spectroscopic analyses. FTIR and Raman spectra have been obtained for each sample before and after exposure to the selected solvent mixtures. It was hoped that studying the coatings before and after solvent exposure would provide insight into any chemical changes. However, in some cases the solvent dried out of the sample and left the exposed coating in a very similar state to the unexposed coating. Use of the Raman spectrometer enables the study of the sample while it is saturated with solvent, which has led to some interesting results. The FTIR method employed here was attenuated total reflectance (ATR), which analyzes the top few microns of a sample. Through this experiment significant surface effects as a result of exposure were observed. In

order to better understand these changes, XPS was employed, which provides spectral information of the top few nanometers.

Spectroscopic analysis of military coating systems can be hampered significantly by the presence of fillers and pigments. Raman spectroscopy is a visible light technique, wherein pigments dominate the resulting spectrum, while polymeric fillers overlap significantly with the small amount of binder present in a given sample spot. While the effect is not as pronounced when studying samples with FTIR or XPS methods, the significant contribution of these components compared to the binder makes analysis of the latter quite difficult. In order to overcome this problem, clear versions of each coating were required. Later, partially-formulated coatings were investigated after the changes to the binder had been studied.

5.4.1 Dilation of Polymer Hydrogen Bonding

The clear films of the two polyurethane topcoats, MIL-PRF-85285 and MIL-DTL-53039, were subjected to equivalent exposure conditions and vibrational spectra were taken from both. While exposed to methylene chloride, both film samples exhibit an increase in flexibility and are swelled. The Raman shows significant broadening of the carbonyl (C=O) vibration while the film sample is solvated with methylene chloride, as seen in Figure 5-41, which shows the Raman spectra of the MIL-PRF-85285 clear film before and during exposure to methylene chloride. This broadening suggests that the solvent is affecting inter-chain dilation at the hydrogen-bonding links C=O…H-N. The carbonyl vibration peak broadening is more pronounced in the MIL-PRF-85285 clear film than in the MIL-DTL-53039 clear film. After being removed from the solvent, the effect on C=O peak disappears within 15 minutes, which is confirmed by a swelling collapse after solvent outgassing. Figure 5-42 shows the Raman spectra of the MIL-DTL-53039 clear film immediately following overnight exposure to methylene chloride. Three spectra are shown with increasing time from the coating's removal from methylene chloride. Physically the sample returns to approximately its original stiffness after removal from methylene chloride. Methylene chloride may not cause any permanent chemical changes to the polymer. However this induced dilation explains the ability of methylene chloride to facilitate the penetration into the coating of other components in the solvent mixture.

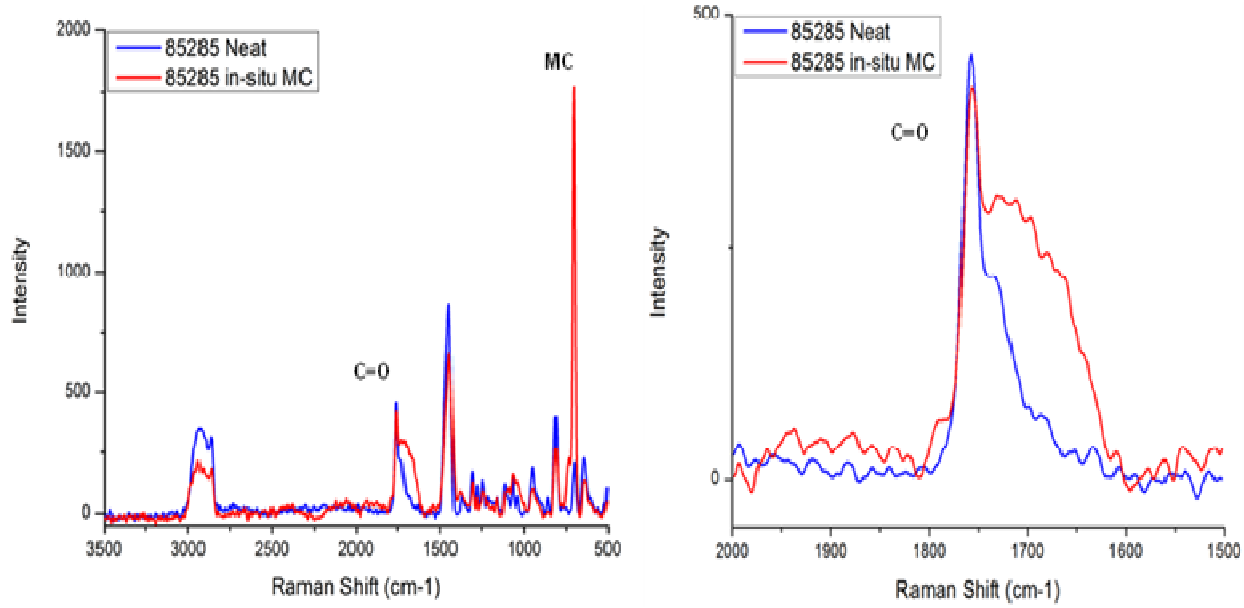

Figure 5-41. Raman spectra of the MIL-PRF-85285 clear film alone and saturated with methylene chloride (left) , zoom of C=O region (right)

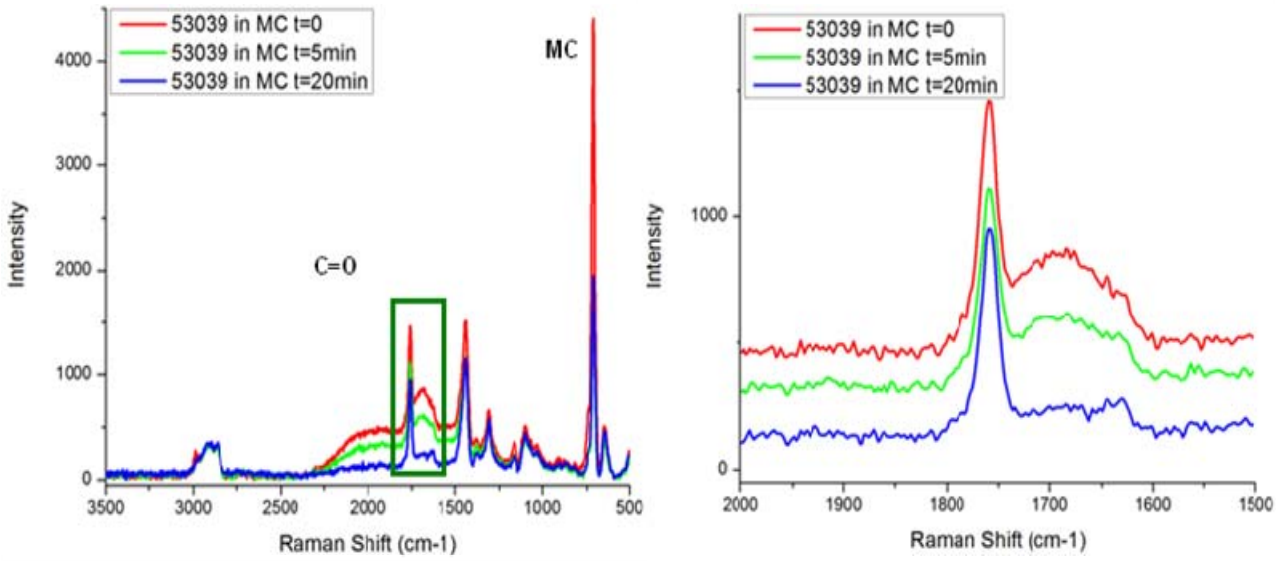

Figure 5-42. Raman spectra of the MIL-DTL-53039 clear film exposed to methylene chloride (left), zoom of C=O region (right)

Analysis of the FTIR spectra of the clear films before and after exposure to control solvent solutions of methylene chloride and MC/EtOH depicts no considerable changes as can be seen in Figure 5-43. In the spectrum of the MC/EtOH exposed coating there is a minor peak decrease at 1683 cm^{-1}, corresponding to the infrared-active C=O vibration. The carbonyl bond dilation is

unlikely to be present. It is reasonable that the solvents have evaporated from the top 2µm of the film and the dilation or other changes in the coating cannot be detected using FTIR.

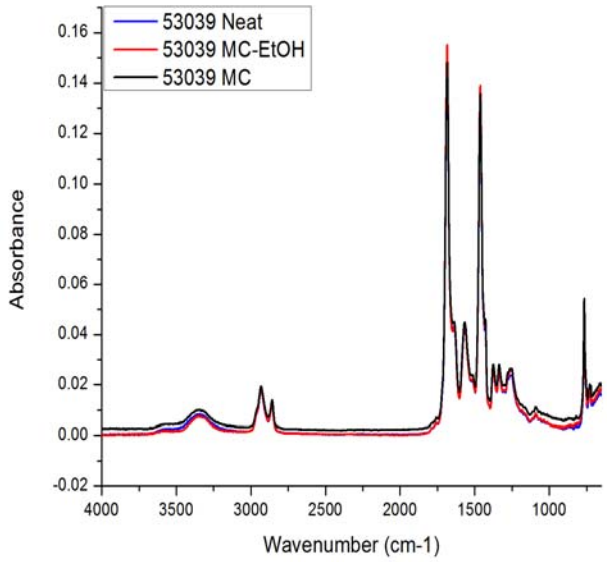

Figure 5-43. FTIR-ATR spectra of the MIL-DTL-53039 clear film before and after exposure to methylene chloride and MC/EtOH

Figure 5-44 shows the Raman spectra of MIL-DTL-53039 before and after exposure to methylene chloride and ethanol (82:8) as well as a magnified view of the carbonyl region of the spectrum at 1747 cm^{-1}. Several extra peaks are visible; these correspond to components of the solvents applied. Here, methylene chloride and ethanol are detected readily within the sample, even after extended periods of drying. Considering the comparatively short exposure time of the analyzed sample (15 minutes) as compared to drying time (two hours), the significant presence of solvent components within the film must be indicative of solvent entrapment by the matrix. The spectra shows a minor height decrease and shift in the carbonyl (C=O) peak at 1747 cm^{-1}, as a result of exposure to solvents containing methylene chloride; there is a broadening and shift of approximately 2 cm^{-1}. This confirms the dilation of the hydrogen bonds between the polyurethane chains (C=O---H-N) by methylene chloride, supporting the notion that methylene chloride acts to facilitate penetration into the coating of larger solvent molecules.

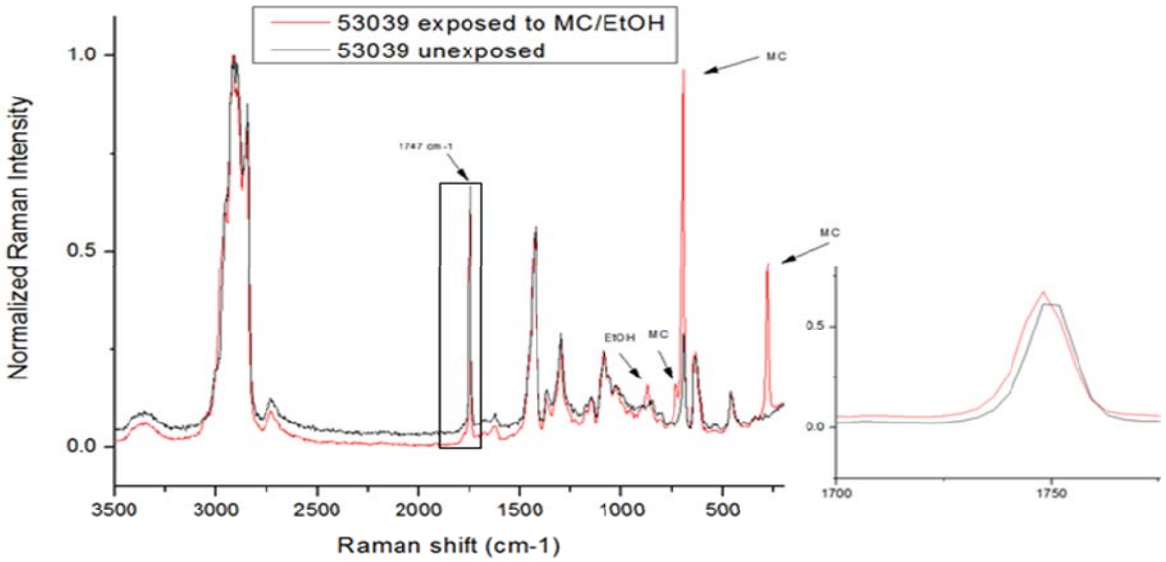

Figure 5-44. Raman spectra of MIL-DTL-53039 clear film before and after exposure to MC/EtOH including an expansion to resolve the carbonyl peak

The MIL-DTL-53039 clear film showed visible changes to relative opacity of the sample after exposure to the MC/EtOH/H_2O mixture; localized clear regions were observed. FTIR analysis of these clear regions has shown interesting chemical changes. With exposure to a solvent mixture of MC/EtOH/H_2O, FTIR shows a decrease in the carbonyl peak and evidence of new ether and alcohol groups. There is a dramatic decrease in the strength of the C=O vibration at 1683 cm^{-1}, with a corresponding formation of peaks at 1186, 1151, 1112, and 1061 cm^{-1}, representing a series of stretches occurring in a C-O-C system. These can be seen in Figure 5-45. A similar effect is seen in the MC/EtOH/H_2O/PhOH mixture; however, spectral overlap of phenol with many possible affected bonds has interfered with any mechanistic analysis. The presence of phenol within the sample after a very long drying period indicates that phenol is bound within the sample somehow, via either steric hindrance or chemical bonding to the surrounding resin.

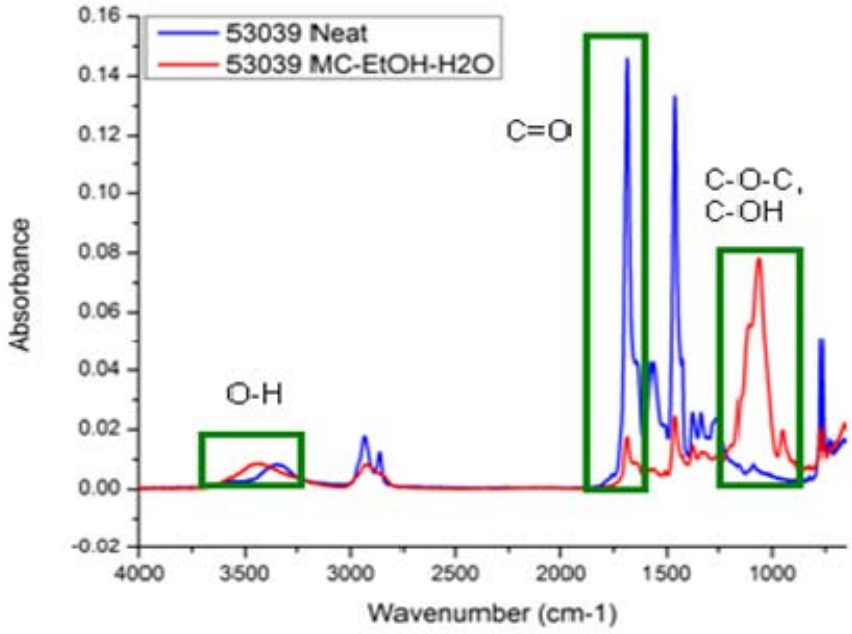

Figure 5-45. FTIR of MIL-DTL-53039 clear film before and after exposure to MC/EtOH/H_2O

5.4.2 Chemical Change: Hydrolysis

XPS was used to investigate the effects of exposure to the MC/EtOH/H_2O on the clear coating MIL-DTL-53039 clear film. XPS analysis highlighted distinct changes in the carbon (1s), nitrogen (1s) and oxygen (1s) spectra of the film following exposure that match well with previous results. In Carbon 1s (shown in Figure 5-46) the peak indicative of C=O is greatly diminished, which is also seen by ATR-FTIR analysis. The lack of broadening in the main Carbon 1s feature shows that any newly-formed bonds are of similar binding energy to the pre-existing carbon-nitrogen and carbon-oxygen bonds. In FTIR, this is seen by the formation of C-O-C and C-OH.

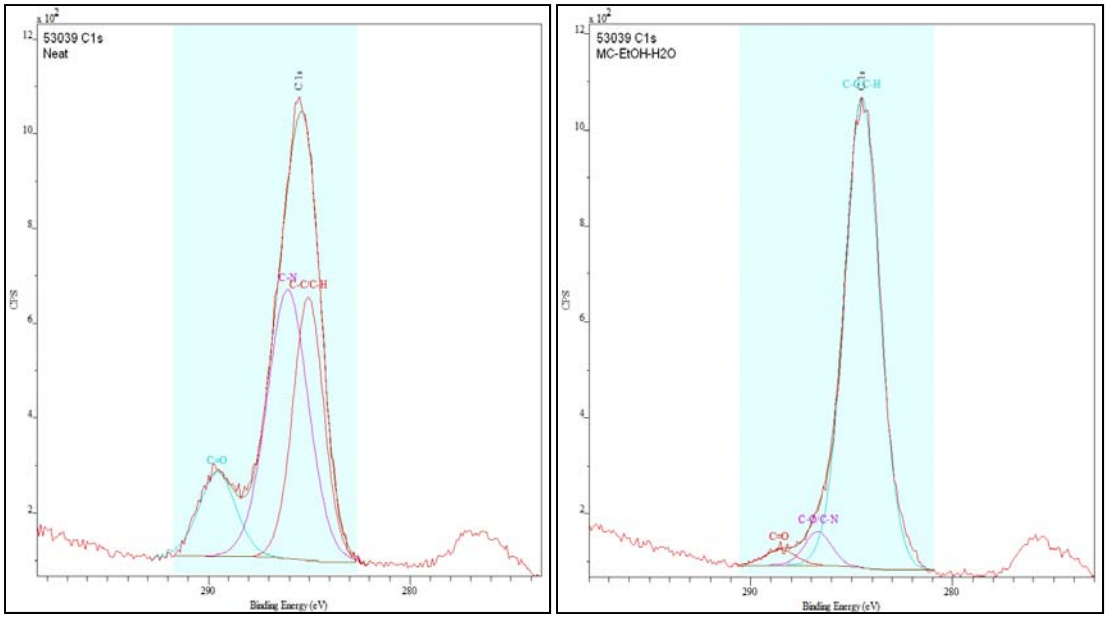

Figure 5-46. XPS of carbon (1s) in MIL-DTL53039 clear film before and after exposure to MC/EtOH/H_2O

The oxygen 1s spectrum further corroborates these changes, see Figure 5-47. Broadening of the main feature indicates the presence of the O-C and OH peaks seen by FTIR.

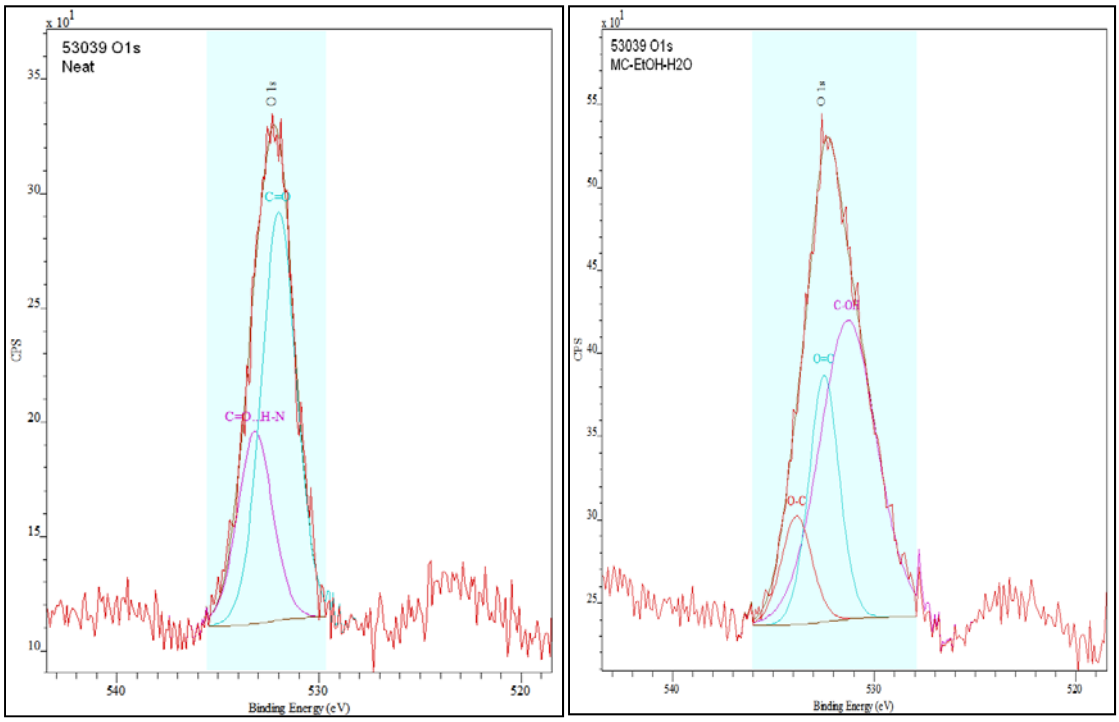

Figure 5-47. XPS of Oxygen (1s) in MIL-DTL-53039 clear film before and after exposure to MC/EtOH/H_2O

The nitrogen (1s) spectrum is severely diminished by solvent exposure (shown in Figure 5-48). This indicates that the solvent either induces a conformational change that depletes nitrogen from the surface, or the reactions that result in the formation of the new bonding states seen above also result in the elimination of nitrogen from the polymer. It should be noted that these changes are not visible using Raman spectroscopy. We speculate that it is because the changes are all occurring at the surface, and the Raman instrument used has a very high sampling depth in clear materials, while ATR-FTIR and XPS are highly surface-sensitive (2μm and 10nm, respectively).

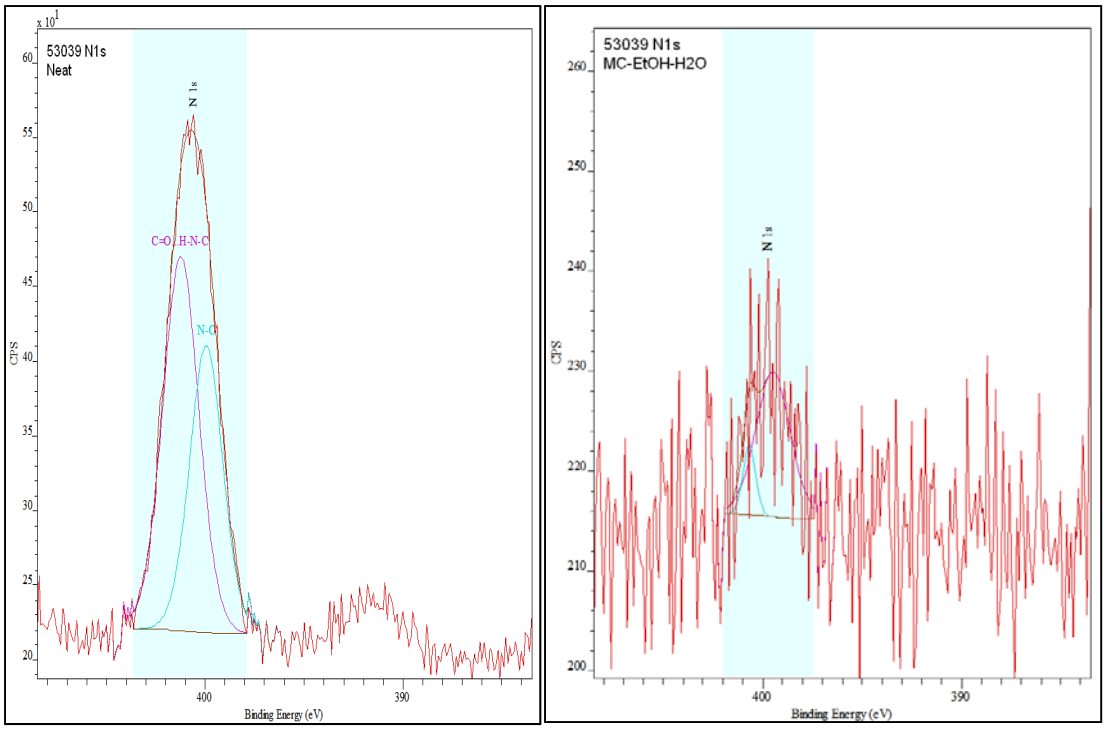

Figure 5-48. XPS of Nitrogen (1s) in MIL-PRF-53039 clear film before and after exposure to MC/EtOH/H_2O

We speculate that the evolution of C-O-C and C-OH at the surface of the coating is caused by a hydrolysis reaction, given that these peaks only form in the presence of water. The presence of Methocel as a thickener could also account for this surface chemistry, so further steps were taken to verify its absence. Samples were washed extensively in MC/EtOH after exposure in order to remove any trace of surface contamination. After this cleaning, the visible changes to the coating remained, indicating that a chemical reaction had occurred. SEM analysis of the MIL-PRF-85285 clear film after exposure to methylene chloride or to MC/EtOH/H_2O shows no damage after exposure to the former and visible surface degradation after exposure to the latter as illustrated in Figure 5-49.

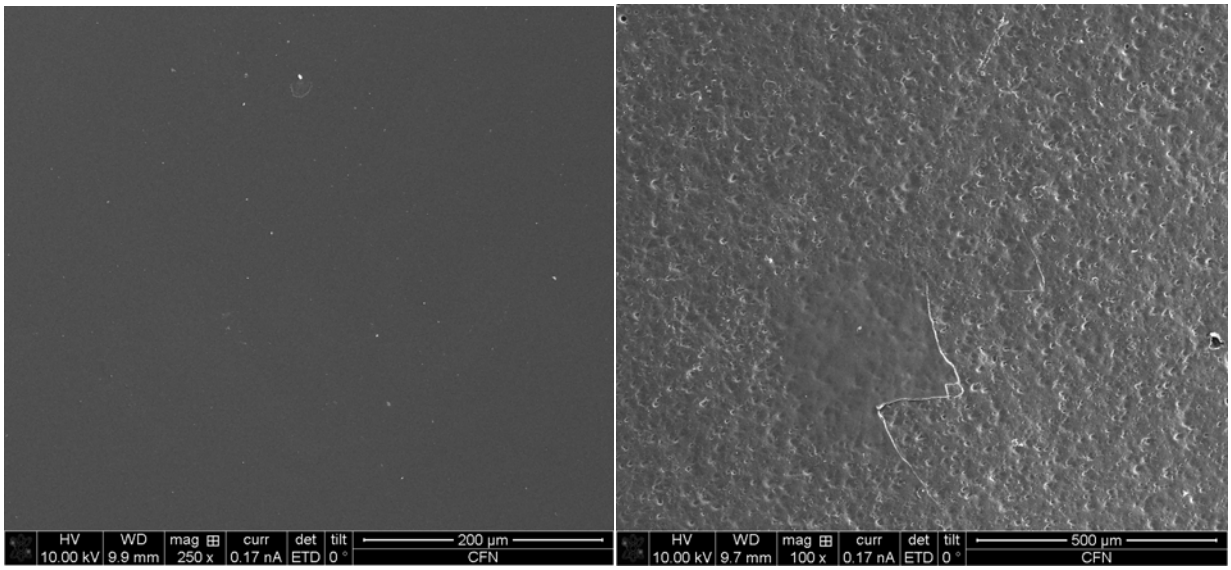

Figure 5-49. Electron micrographs of MIL-PRF-85285 clear film exposed to (left) methylene chloride and (right) MC/EtOH/H_2O, demonstrating significant surface changes as a result of exposure

Exposure to liquid phenol also results in significant swelling and softening of the coating which does not diminish even after extensive drying. The sample acquires a slight color indicative of the presence of impure solid phenol. The spectrum of phenol dominates the FTIR spectrum, obscuring the peaks of the polymer, making the evaluation of chemical changes extremely difficult. This is consistent with the previously noted color change and GC/MS headspace analysis. In Figure 5-50, phenol and methylene chloride are clearly present in the sample long after drying.

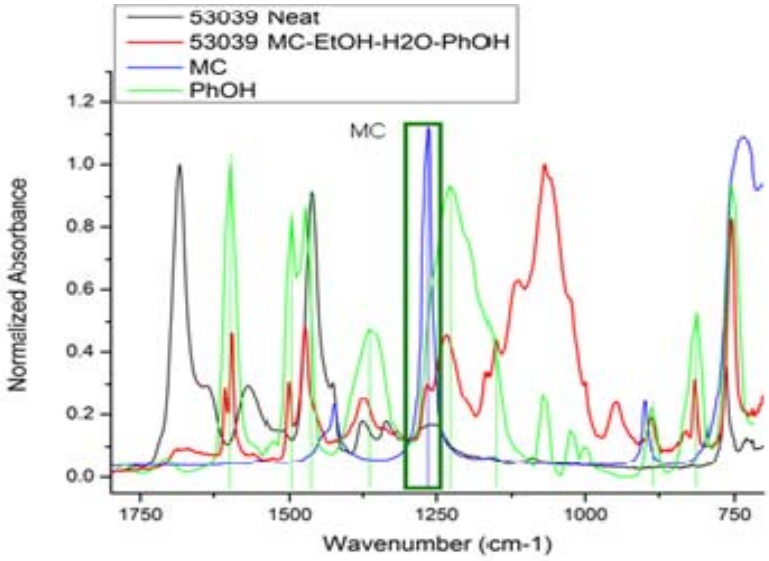

Figure 5-50. FTIR spectra demonstrating solvent persistence in MIL-PRF-53039 clear film after drying

Figure 5-51 depicts the Raman spectroscopic result of the exposure of the MIL-DTL-53039 clear film to the MC/EtOH/H_2O/PhOH mixture. Here, phenol is the dominant solvent component visible in the spectra; methylene chloride is not visible. The most significant effect of this solvent is the reduction in intensity of the peaks corresponding to C=O (1750 cm^{-1}) and CH_2/CH_3 stretching (around 3000 cm^{-1}). This indicates a reduction in presence of these components but precise quantitative conclusions cannot be drawn from these results. There is also a small increase in the region of 1060 cm^{-1}, corresponding to C-O-C ether stretching.

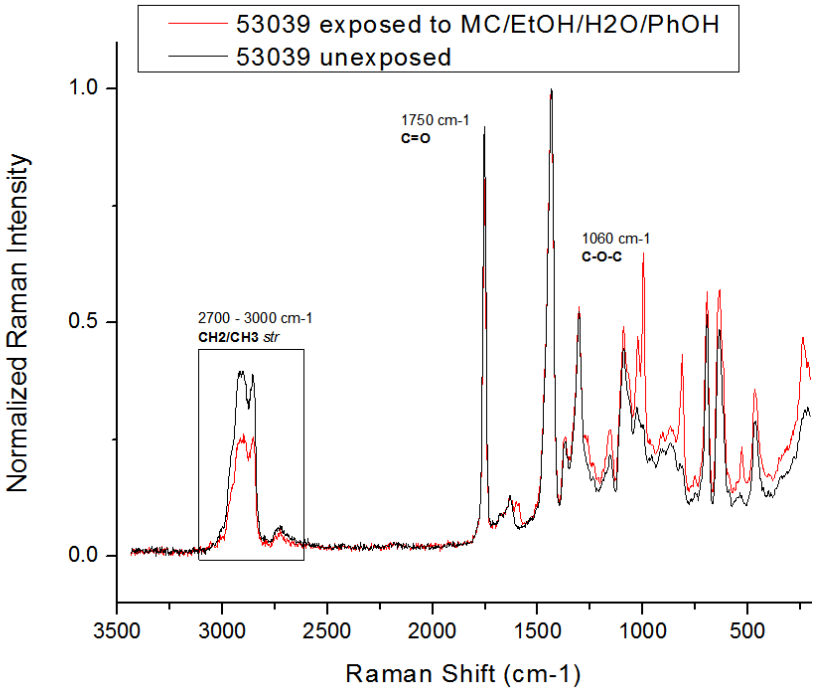

Figure 5-51. Raman spectra of MIL-DTL-53039 clear film before and after exposure to MC/EtOH/H2O/PhOH

The infrared spectrum of the same exposure, shown in Figure 5-52, provides even more interesting results. The peak representing C=O (around 1683 cm^{-1}) diminishes drastically, and a series of peaks indicative of ether C-O-C stretches (1167, 1152, 1117, 1069, 1025 and 1000 cm^{-1}) appear with moderate intensity. There is an obvious chemical change occurring.

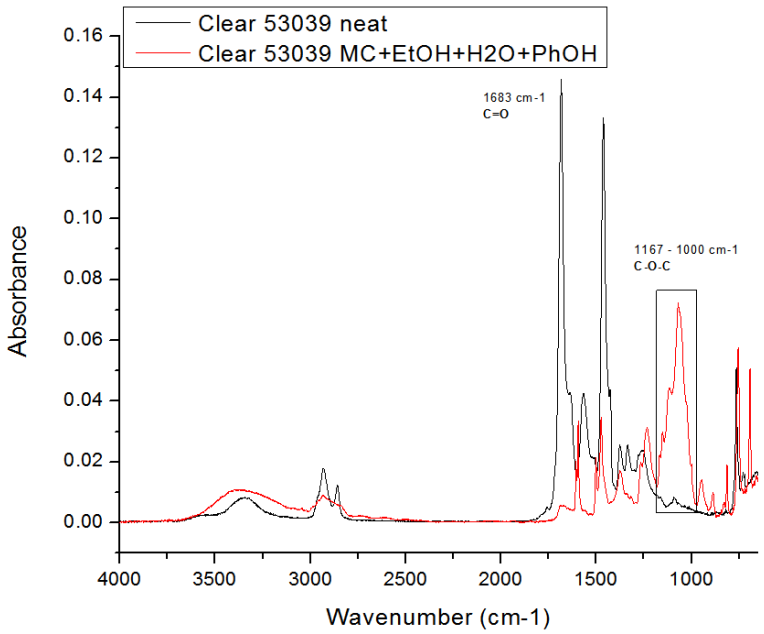

Figure 5-52. FTIR spectra of MIL-DTL-53039 clear film before and after exposure to MC/EtOH/H2O/PhOH

In light of the apparent effects of phenol, a separate experiment was performed; exposing the MIL-DTL-53039 clear film to liquid phenol (89 % PhOH, 11 % H_2O). Physically, the effects of this exposure are dramatic - the coating quickly dissolved into a shapeless mass after exposure. The Raman spectrum before and after this exposure is seen in Figure 5-53. Even after several days of outgassing, significant quantities of phenol remain within the sample. There is significant reduction in peak intensity and area in the region around 3000 cm^{-1}, corresponding to CH_3 and CH_2 stretching modes. Reduction is also seen at 1750 cm^{-1}, corresponding to C=O stretching. An increase is seen in the vicinity of expected ether stretches (1060 cm^{-1}) as well. Specific identification of the peaks is complicated by the presence of phenol as its vibrations overlap many of the likely regions for peak formation.

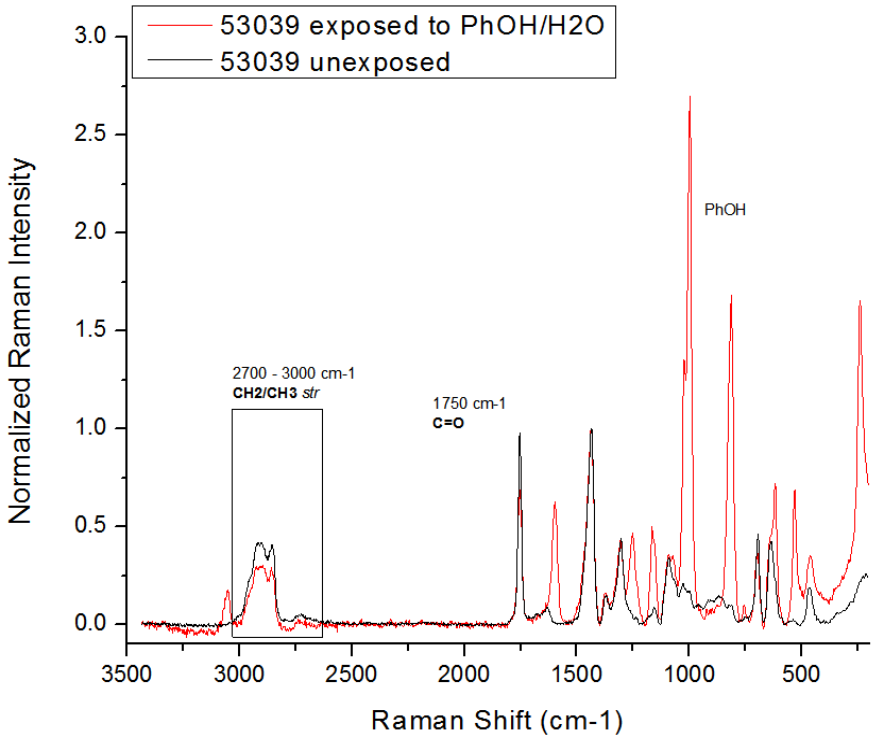

Figure 5-53. Raman spectra of MIL-DTL-53039 clear film before and after exposure to phenol/water

5.5 Solid-State NMR Analysis

In order to obtain molecular level information about the effects of solvents upon clear coatings using a very different spectroscopic approach, solid-state proton (^{1}H) and deuterium (^{2}H) NMR were employed. The ^{1}H NMR results provided information about the segmental dynamics of the polymer chains in the topcoat and epoxy as a function of temperature and solvent exposure. The ^{2}H NMR results provide molecular-level information about the solvent molecules themselves, by relying upon isotopic-labeling of the methylene chloride or phenol components.

In terms of deciding upon a strategy for using NMR spectroscopy, three nuclei; ^{1}H, ^{2}H, and ^{13}C; were considered as feasible candidates for this NMR study. For alkyd paint binders swollen overnight by deuterated chloroform, it was shown that reasonably high-resolution ^{13}C spectra were obtainable using a conventional liquid-state NMR spectrometer.[17] However, for the initial stages of solvent penetration such an approach would not succeed because the reduced mobility of the polymer chains would give more solid-like ^{13}C spectra requiring techniques such as cross-polarization magic-angle spinning (CP-MAS). These techniques have indeed been applied to monitor dynamics in water- or acetone-swollen ionizable polymer networks by monitoring ^{13}C relaxation times;[18] a number of ^{13}C and ^{1}H NMR studies have been reported on swollen polymer networks, but not in paint coating systems.[19-22] Although initial experiments yielded a ^{13}C CP-MAS NMR spectrum of a polyurethane topcoat film (data not shown), it was decided to concentrate on static (stationary) rather than CP-MAS for this NMR study because of the problems anticipated with the large centrifugal forces in the case of spinning samples that would

tend to expel the solvent from the polymer film and make spinning difficult as well. Static ^{1}H solid-state NMR is also a very convenient and sensitive way of monitoring the increase in segmental dynamics upon swelling. In terms of observing NMR of the solvent molecules themselves, ^{1}H NMR can be useful in more highly swollen cases such as chloroform in copolymer gel beads,[23] or in diffusion studies of organic solvents in polyisoprene.[24] However, labeling the solvent with deuterium provides greater selectivity (because of the low natural-abundance of ^{2}H, 0.015%) as well as greater sensitivity to and theoretical interpretability of molecular dynamics and orientation due to the dominance of the large nuclear quadrupole interaction. This is exemplified by ^{2}H NMR studies of D_2O in epoxy[25] and nylon[26] and deuterated small organic molecules used to probe stress/strain effects in polymers[27, 28] including d_5-phenol in nylon.[29] We found that in our systems solid-state ^{2}H NMR reveals a wealth of detailed dynamical information from changes in the spectral appearance and the spin-spin relaxation time (T_2) as a function of temperature. In particular, we observe marked reductions in the rate of molecular tumbling (i.e. increases in the rotational correlation times) for solvent molecules in the polymer matrix, compared to in solution, especially for lower degrees of swelling. Molecular tumbling of solvent molecules or nitroxide spin probes covalently attached to polymer backbones has previously been studied by electron paramagnetic resonance (EPR) spectroscopy[30-34] as well as ^{13}C NMR[19] and similar conclusions were obtained.

Solid-state ^{1}H NMR shows the effects of exposure to the control solvent mixtures on the segmental dynamics of the polymer chains. It also affords insight into the physical state of the solvent molecules of methylene chloride by indicating that the molecules are primarily in atomic-level contact with polymer molecules rather than in a larger pool of other solvent molecules. The changes as a function of temperature in the spin-lattice relaxation times (T_1), the spin-lattice relaxation times in the rotating frame ($T_{1\rho}$), and the spectra's peak line width at half-height (HHLW) after exposure to methylene chloride or phenol/water solutions are reported. Studies were done as a function of temperature to allow for comparison between dynamics induced from solvent exposure and those induced solely by increase in temperature.

5.5.1 ^{1}H Solid-state NMR of MIL-DTL-53039 Clear Film Exposed to MC

In the ^{1}H NMR spectra the full-HHLW is decreased by segmental dynamics of the polymer chain on time scales < 20 μs. The T_1 is governed by fast dynamics on a nano-second (ns) time scale (Figure 5-54). The $T_{1\rho}$ is affected predominantly by slow motions (having a ~ 15 μs time scale), of the type that may permit solvent diffusion into polymer (Figure 5-54). By performing these measurements as a function of temperature, dynamics induced by a rise in temperature can be compared with dynamics induced by solvent swelling.

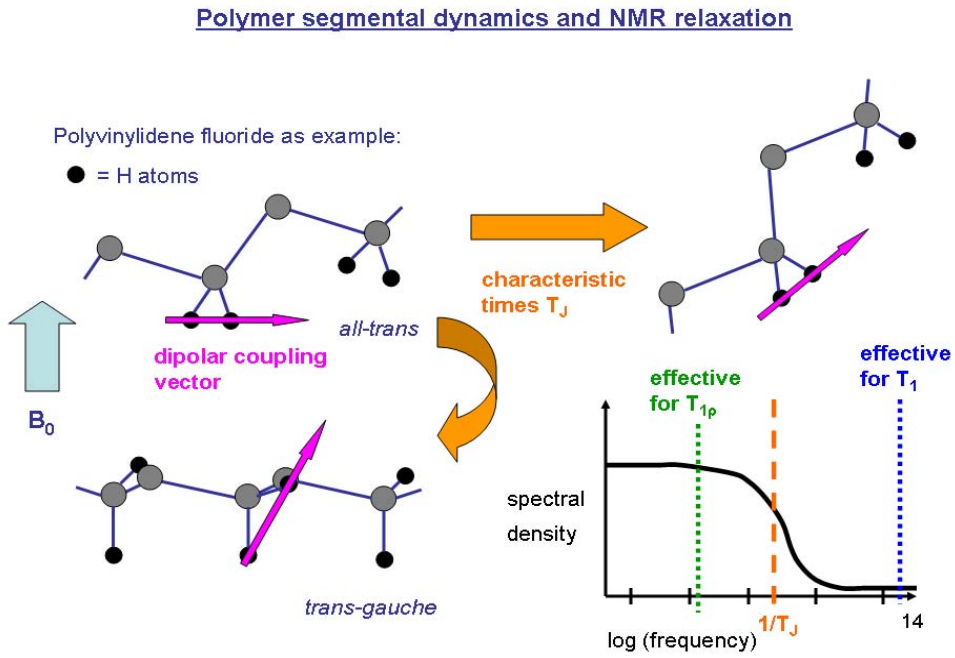

Figure 5-54. Schematic example of polymer segmental dynamics affecting ^{1}H NMR relaxation through modulation of proton-proton dipolar coupling

Figure 5-54 shows a schematic example of how polymer segmental dynamics (local conformational change in bottom molecule, longer-range reorientation of chain in top right molecule) modify the orientation of the internuclear proton-proton dipolar coupling vector with respect to the external magnetic field B_0. The resultant modulation of the dipolar coupling is responsible for NMR relaxation. The characteristic jump times (T_J) involved represent a correlation time for an assumed random process that can be related to a Lorentzian spectral density as shown in the log plot, with a cut-off frequency of $1/T_J$. For a dynamic process with the cut-off depicted, increasing temperature would raise the cut-off frequency while keeping the integrated spectral density constant, resulting in less-effective $T_{1\rho}$ relaxation (longer $T_{1\rho}$) and more-effective T_1 relaxation (shorter T_1).

The MIL-DTL-53039 clear film was selected as the first sample to examine using the strategy described in the materials and methods section. The ^{1}H NMR results from the unexposed sample were compared with those from the same sample exposed to methylene chloride for 5 minutes. Figure 5-55 shows T_1 vs. temperature for the film before and after exposure to methylene chloride, as well as the T_1 for the neat solvent alone.

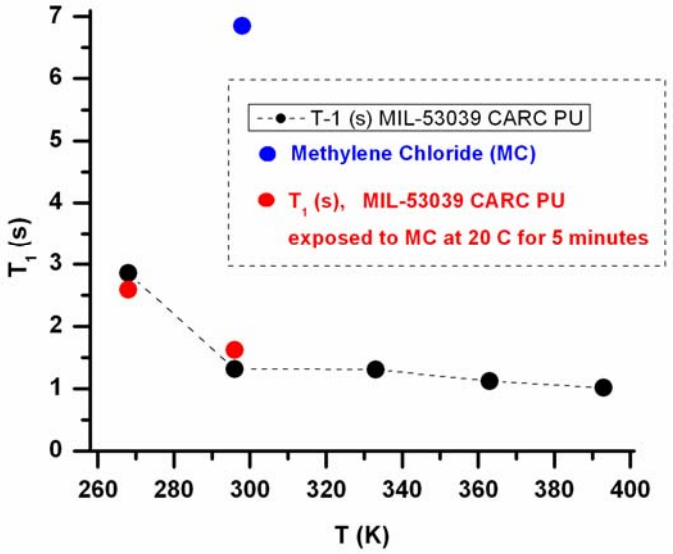

Figure 5-55. Proton NMR T_1 vs. temperature for MIL-DTL-53039 clear film before and after 5-minute exposure to methylene chloride at 20°C. Also shown is the T_1 of neat methylene chloride

Several conclusions can be drawn from these data. The T_1 of neat methylene chloride is long because it is an isotropic liquid with a short (ns) rotational correlation time, whereas the T_1 of the unexposed polymer film is significantly shorter and typical of non-rigid polymers. The near-equality of the two T_1 values of the polyurethane sample exposed to methylene chloride to those in the starting polyurethane film at the same temperature indicates that methylene chloride is in intimate atomic-scale contact with the polymer, since the proton NMR signal from the methylene chloride component contributes to the overall spectrum of the exposed sample. This intimate contact results in the methylene chloride having significant proton-proton dipolar coupling to the polyurethane polymer, which equalizes T_1 values by the process known as spin-diffusion. There is no evidence whatsoever for free methylene chloride in liquid-like pools of any size, which would yield a sharper proton NMR peak having a longer T_1.

In addition to these T_1 experiments on this same polyurethane film before and after exposure to methylene chloride, the $T_{1\rho}$ experiments as summarized in Figure 5-56 were conducted. The steep drop in $T_{1\rho}$ values for the unexposed film above the maximum around 330 K can be interpreted as due to the activation of relatively slow motions on an approximately 15 μs time scale (the optimum for $T_{1\rho}$ relaxation at the rf field strength used, corresponding to a T_J of 15 μs in Figure 5-56).

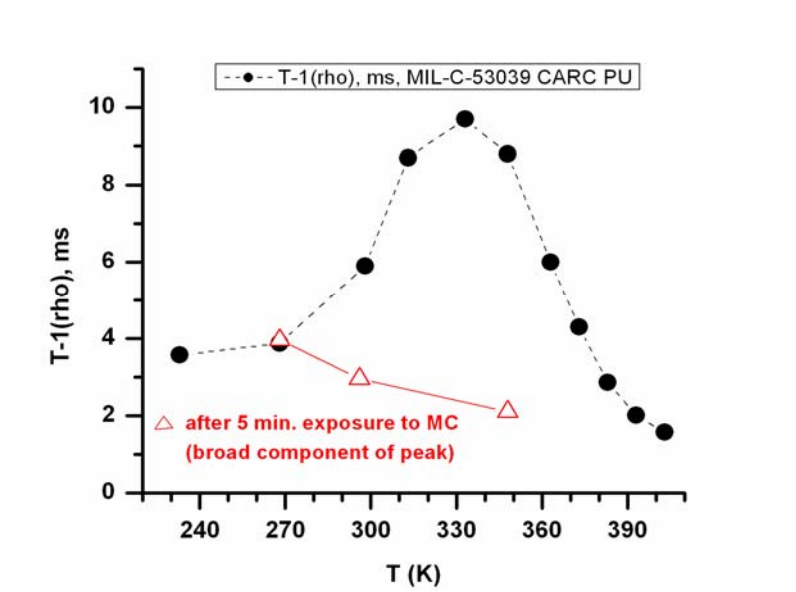

Figure 5-56. Proton NMR $T_{1\rho}$ vs. temperature for MIL-DTL-53039 clear film before and after 5-minute exposure to methylene chloride at 20°C

The proton NMR spectra of the MIL-DTL-53039 clear film are shown in Figure 5-57. The spectrum obtained at 296 K (23°C) is greatly broadened by homonuclear dipolar interactions (ca. 50 kHz HHLW), as expected for a crosslinked polymer with only limited segmental dynamics (the T_g measured above was 87°C). Heating the sample to near the T_g (363 K, or 90°C) results in a substantial reduction in the linewidth due to greatly increased segmental dynamics that partially average out the dipolar interactions.

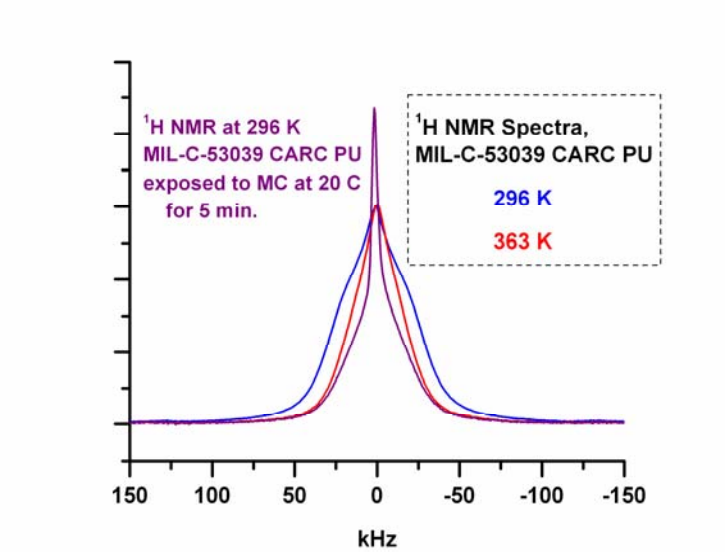

Figure 5-57. Wideline proton NMR spectra of MIL-DTL-53039 clear film at two different temperatures, and after exposure to methylene chloride

Similarly, exposure to methylene chloride for 5 minutes at 20°C results in a spectrum at 296 K that is greatly narrowed by an increase in the segmental dynamics, similar to the effects of increasing temperature alone. (The T_g reported above of this sample after 2 hours exposure to methylene chloride was 67°C.) The line shape also has the appearance of a sharper and a broader component, the former of which is still broader than would be the case for purely liquid-like pools of methylene chloride. It is reasonable to attribute the sharper component to methylene chloride that is so strongly dipolar-coupled to nearby polymer protons that it shares the same T_1 relaxation time (Figure 5-57).

5.5.2 ^{2}H Solid-state NMR of MIL-DTL-53039 Clear Film Exposed to CD_2Cl_2 (d_2-MC)

The deuterium NMR spectra of the MIL-DTL-53039 clear film after 10 minute exposure to deuterated methylene chloride are shown in Figure 5-58. The room temperature (24°C) CD_2Cl_2 narrow linewidth indicates rapid rotational motion, but not rapid enough to be liquid solvent. The spectrum reveals that all of the CD_2Cl_2 molecules are undergoing rotational motion sufficiently rapid enough (less than 10 μs) to average out the rigid-lattice nuclear quadrupole coupling constant (NQCC) (see the later section, Section 5.5.4, on ^{2}H NMR of d_5-phenol for a reference to published simulations of the effect of motions on the ^{2}H spectra). The 1.4 kHz HHLW is still broader than what is expected for the neat solvent.

Cooling the sample to 0°C resulted in a broader spectrum that could be fitted very well to a Lorentzian lineshape with a HHLW = 6.3 kHz, broader than the linewidth at 24°C. The T_2 value measured by varying the delay tau in the quadrupolar-echo sequence and fitting to a single-exponential decay was 67.2 μs, as shown in the figure. This value corresponds to a homogeneous linewidth of 4.74 kHz. The difference of 1.6 kHz from the (larger) measured linewidth seems too large to be accounted for by broadening due to magnetic susceptibility or field inhomogeneities. It may be due to a distribution of small residual quadrupolar splittings that somehow do not result in a deviation from a Lorentzian lineshape. The measured T_2 is many orders of magnitude shorter than that expected for pure CD_2Cl_2 (hundreds of milliseconds or greater). The relevant equation for the full HHLW of the Lorentzian in the motionally-narrowed regime is $\Delta\omega_0^2\ \tau_c / \pi$ (in Hz), where s $\Delta\omega_0^2$ is the second moment (in angular frequency units) characterizing the rigid solid linewidth and τ_c the rotational correlation time.[35] The latter depends upon the molecule or particle size and the viscosity of the medium, and is typically 10^{-11} s for a small molecule such as CD_2Cl_2 in a low-viscosity solvent. Thus, the measured T_2 and corresponding broad homogeneous linewidth indicate that the CD_2Cl_2 molecule in the MIL-DTL-53039 clear film at 0°C has a rotational correlation time of the order of three orders of magnitude greater than its value in neat CD_2Cl_2. Although one cannot assign a meaningful viscosity to the surrounding polymer matrix, it is clear that the rotational tumbling of the CD_2Cl_2 molecule is being restricted, quite plausibly by some sort of electric dipole-electric dipole interaction with polar groups on the polymer. The fact that the spectrum is not that of an immobilized solvent molecule indicates that the interaction energy is relatively weak compared to the thermal energy kT.

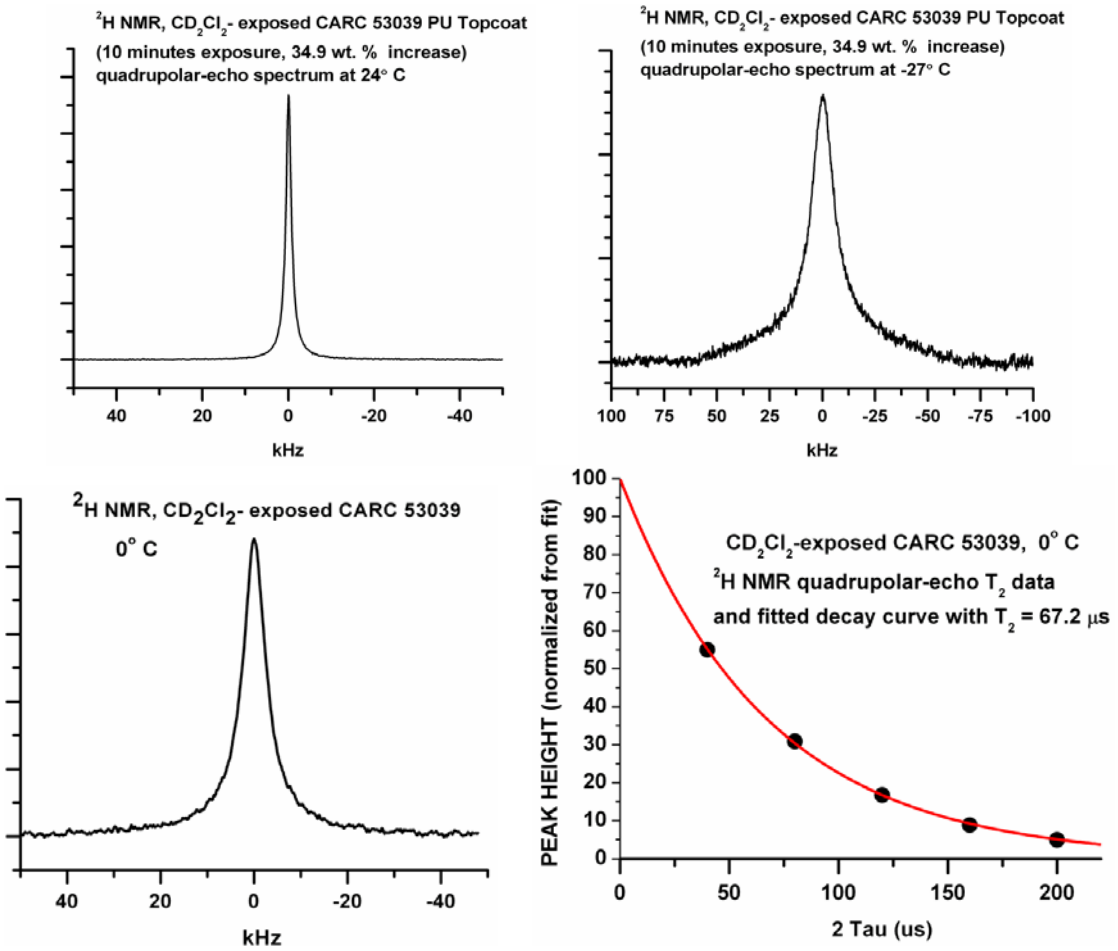

Figure 5-58. Deuterium quadrupole-echo NMR spectra of CD_2Cl_2 exposed MIL-DTL-53039 clear film at three different temperatures as indicated, and measurement of T_2 transverse relaxation time at 0°C

The spectrum at reduced temperature (-27°C) of deuterated methylene chloride after swelling the CARC polyurethane topcoat (MIL-DTL-53039) is significantly broader than the spectra obtained at either 24°C or 0°C (note the different frequency scale). The HHLW is 14.1 kHz, but also apparent is an even broader peak at the base. This indicates a further degree of restriction to the rotational motion of the solvent molecules upon further cooling, and possibly the existence of two different environments.

5.5.3 ^{1}H Solid-State NMR of MIL-PRF-23377 Clear Film Exposed to Phenol/Ethanol

An NMR strategy similar to that employed with the topcoat above was used to investigate the epoxy (polyamide) primer MIL-PRF-23377 clear film, whose T_g of 40°C reported above is much lower than that of the polyurethane topcoat (87°C). The ^{1}H NMR half-height linewidths as a function of temperature are shown in Figure 5-59. The solvent ^{1}H NMR signals did not appear as sharp peaks that would be the case for liquid-like pools, but instead as broadened indistinct features in the spectrum. Because they represent a minor proton-containing component in the exposed sample, their contribution to the linewidth can be neglected to a first approximation. It is interesting to note that although the polyurethane and the epoxy polymers do not have the same chemical structure, the effective number density of their hydrogen atoms may be

comparable, which in turn would yield comparable ^{1}H NMR linewidths for both in the rigid lattice limit (at low temperatures). Consequently, the approximately 50 kHz HHLW of the polyurethane film at 296 K is consistent with the fact that for the epoxy this broad linewidth is achieved only at approximately 230 K (-43°C), which in both cases is about 80°C below the respective T_g values.

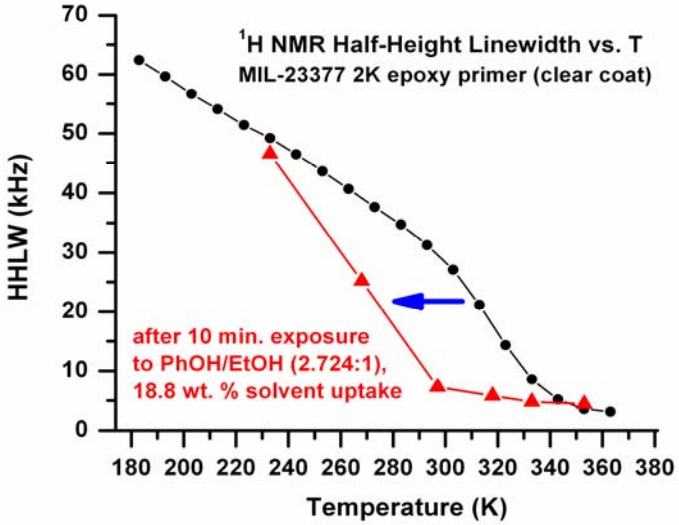

Figure 5-59. Proton NMR half-height linewidths vs. temperature for MIL-PRF-23377 clear film before and after exposure to phenol/ethanol

The effect of a 10-minute exposure to a phenol/ethanol mixture (2.724:1), which resulted in a 18.8 wt. % solvent uptake, upon the linewidth vs. temperature is shown in Figure 5-59. The solvent exposure has markedly shifted the temperature at which a marked decrease in linewidth occurs, by roughly 40°C. A somewhat larger decrease in the T_g, by 59°C, was observed by DSC after a two hour exposure to the same solvent mixture. It is clear that this solvent combination alone can significantly affect segmental dynamics of the epoxy MIL-PRF-23377 clear film even after a short 10-minute exposure.

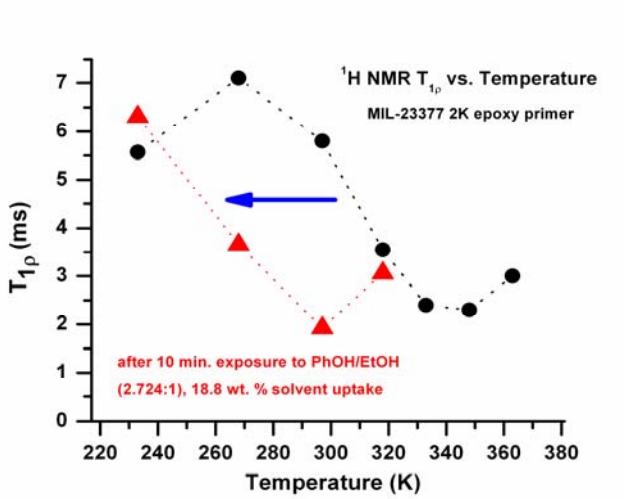

Figure 5-60. Proton NMR $T_{1\rho}$ relaxation times for MIL-PRF-23377 clear film vs. temperature, before and after exposure to phenol/ethanol for 10 minutes at 20°C

The ^{1}H $T_{1\rho}$ relaxation time vs. temperature for this same epoxy MIL-PRF-23377 clear film before and after a 10 minute exposure at 20°C to the same phenol and ethanol mixture (2.724:1) is shown in Figure 5-60. Several points are worth noting. For the unexposed film, a clear minimum in $T_{1\rho}$ is observed at approximately 340 K (67°C). As discussed above for the $T_{1\rho}$ results on the polyurethane MIL-DTL-53039 clear film, this implies that slow segmental dynamics on a (T_J) time scale of 15 μs have their maximum spectral density at this temperature. In other words, segmental dynamics occurring at a rate of 70 kHz are activated and maximized when the temperature is raised to 340 K., which is some 27°C above the measured T_g. The relationship deduced between the segmental dynamics associated with the polymer glass transition and the measured $T_{1\rho}$ values is supported by the (slightly extrapolated) $T_{1\rho}$ minimum for the polyurethane topcoat film at approximately 410 K in Figure 37, which would correspond to 37°C above its T_g.

The effect of exposure to the phenol and ethanol solution upon the temperature dependence of $T_{1\rho}$ shown in Figure 5-60 is to shift the curve roughly 50°C towards lower temperature. This results from the increased polymer segmental dynamics after solvent exposure, and is consistent with the similar shift of approximately 40°C noted above for the linewidths.

5.5.4 ^{2}H Solid-state NMR of Solid d_5-Phenol and of MIL-PRF-23377 Clear Film Exposed to d_5-Phenol/Ethanol Mixtures

The ^{2}H quadrupolar-echo NMR spectrum of solid d_5-phenol at 24°C, below its melting point of 41°C, is shown in Figure 5-61. Solid d_5-phenol, where the hydrogens on the phenyl ring have been replaced by deuterium, exhibits a very wide (129.4 kHz splitting of the "horns") spectrum characteristic of a 172.5 kHz NQCC and zero asymmetry parameter η. This arises from a rigid molecule that does not undergo the "flips" of the phenyl ring observed in other situations; the rigidity is reflected in the long recycle delay of 60 s needed to avoid saturating the signal. The sharp central peak seen in Figure 5-61 (HHLW = 130 Hz), which was observed to have a T_1 relaxation time substantially shorter than that of the broad quadrupole-split pattern, may arise from a small amount of highly mobile phenol molecules. A similar sharp peak was observed in previously reported ^{2}H spectra at 300 K and 295 K, but not 250 K.[32] Curiously, the "horns" of

our spectrum are much sharper than those observed in the previous study, which in addition to a nearly-identical splitting of the horns (131 kHz) also reported a sole single rather sharp peak at 310 K, which is 4° below the melting point. It remains unknown whether this is due to an error in measurement of the sample temperature, sample impurities and consequent melting point depression, an intensification of the central sharp peak relative to a broader peak that because of a shortened T_2 becomes unobservable in the quadrupolar echo, or complete nearly isotropic mobility of all phenol molecules in the lattice.

This previous study[36] also provided a series of simulations of the effect of "ring-flips," 180° rotations of the ring about the O-C bond at rates varying from $k = 10^3$ s^{-1} (slow exchange) to $k = 10^8$ s^{-1} (fast exchange). The appearance of the spectrum changes in a characteristic way that places more intensity in the center of the spectrum relative to the horns, and removes intensity beyond the horns (seen as weak shoulders in Figure 5-61). There appears to be a weak doublet with a splitting of 31.4 kHz in Figure 5-61, which interestingly resembles the splitting in the central portion of the theoretical simulations for phenol undergoing fast 180° ring flips (a similar small central splitting was also observed in low-temperature spectra of the epoxy primer exposed to the solvent mixture or 10 minutes, discussed below). In a pure compound one with molecules in the slow-exchange limit (i.e. not flipping), one would not expect to have a small subset undergoing flips in the fast-exchange limit. However, it is conceivable that impurities in the lattice might lead to a portion of the sample experiencing such flips.

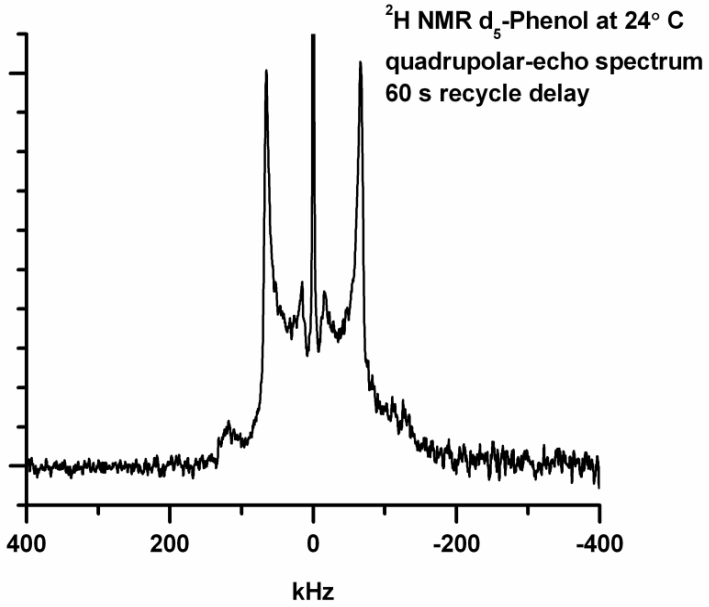

Figure 5-61. ^{2}H quadrupolar-echo NMR spectrum of solid d_5-phenol

The simulations of the effects of ring flips in phenol[36] are of value in interpreting the ^{2}H results we have obtained for the MIL-PRF-23377 clear film exposed to d_5-PhOH/EtOH (3.115/1.0). Figure 5-62 shows the ^{2}H quadrupolar-echo NMR spectra of the exposed sample for four different tau values in the echo sequence. The shortest echo time (10 μs) yields a spectrum having a peaked tent-like appearance, but as the echo time increases central peak is seen to

gradually disappear, leaving primarily a pattern very similar to that seen for bulk solid d_5-phenol (Figure 5-61), with a splitting between the horns of ca. 139 kHz. We thus conclude that there are at least two types of phenol molecules in the epoxy sample having very different T_2 values. The one with the longer T_2 is rather rigid and does not undergo 180° ring flips or any other substantial motion at a rate faster than about 10^4 s^{-1}, based on theoretical simulations.[36] The other type of phenol molecule has a much shorter T_2 as a result of restricted motion at a rate fast compared to the static quadrupole coupling constant, greater than perhaps 10^6 s^{-1}. This motion is not simply a 180° ring flip, since the theoretical spectra for such a process are quite different from what is observed.[36] The HHLW of the second component is of the order of 20 kHz, which if it were due to a homogenously broadened ^2H spectrum, as was observed for CD_2Cl_2 in MIL-DTL-53039 clear film above, would correspond to a T_2 value of ca. 16 μs. The relative proportions of the two types are difficult to determine, but from the 10 μs spectrum the mobile component appears to be dominant.

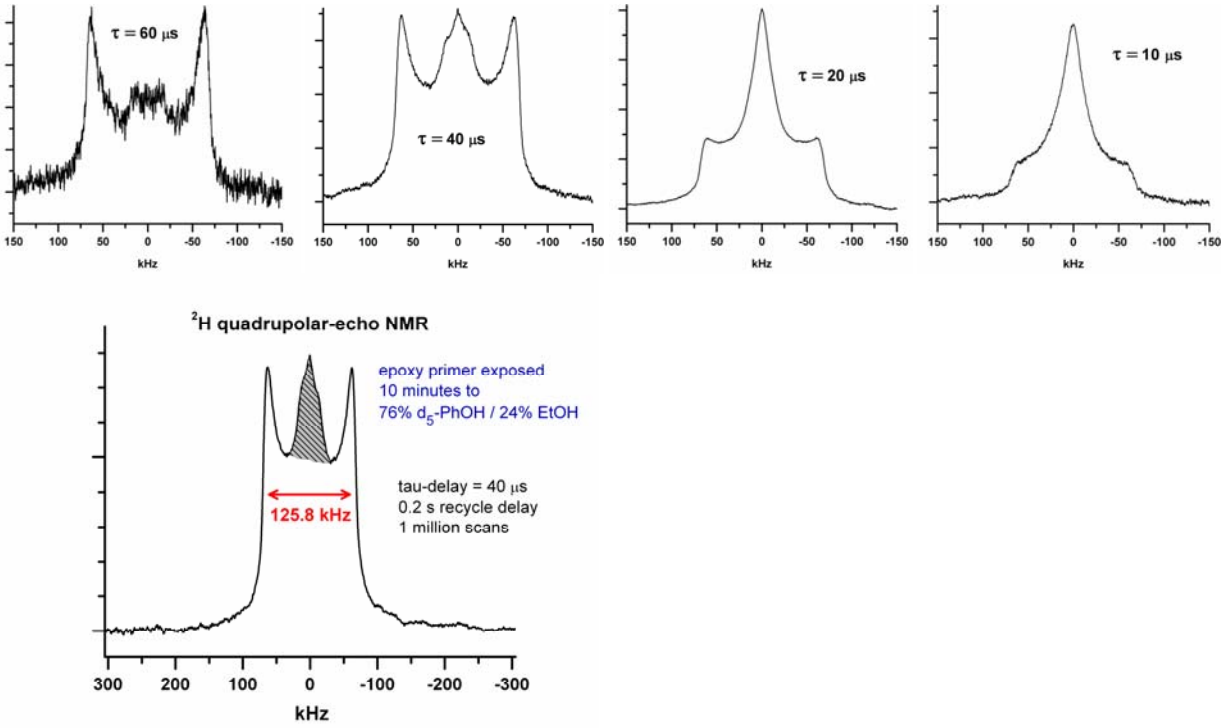

Figure 5-62. ^2H quadrupolar-echo NMR spectra at 24°C of MIL-PRF-23377 clear film exposed to d_5-PhOH/EtOH (3.115/1.0) for 10 minutes, at four different echo times tau as indicated. The differing signal to noise ratios reflect differences in the number of scans acquired. The recycle delay was 0.2 s and exponential apodization (linebroadening) was 300 Hz. A wider plot of the τ = 40 μs spectrum is also depicted with a shaded region arising from the more mobile second component having a shorter T_2

In order to obtain more information about the motional processes taking place, variable temperature quadrupolar-echo spectra were acquired and are shown in Figure 5-63. At the lowest temperature of -29°C, the spectrum obtained with the echo time τ = 20 μs (a shorter time was not used because of the indication of some artifacts in the previous τ = 10 μs spectrum)

showed a broad pattern characteristic of rigid phenol molecules not undergoing ring flips, with a splitting of the horns of 127.4 kHz. Changing the recycle delay from 0.2 s to 4 s did not change the appearance of the spectrum (data not shown). Curiously, a small central portion of the powder pattern is seen, with a splitting of 25.1 kHz, and resembling that seen for the bulk sample. As discussed above for that sample, it suggests that some fraction of the phenol molecules may be undergoing 180° ring flips. The spectrum at 24°C was discussed above (from Fig. 5-62).

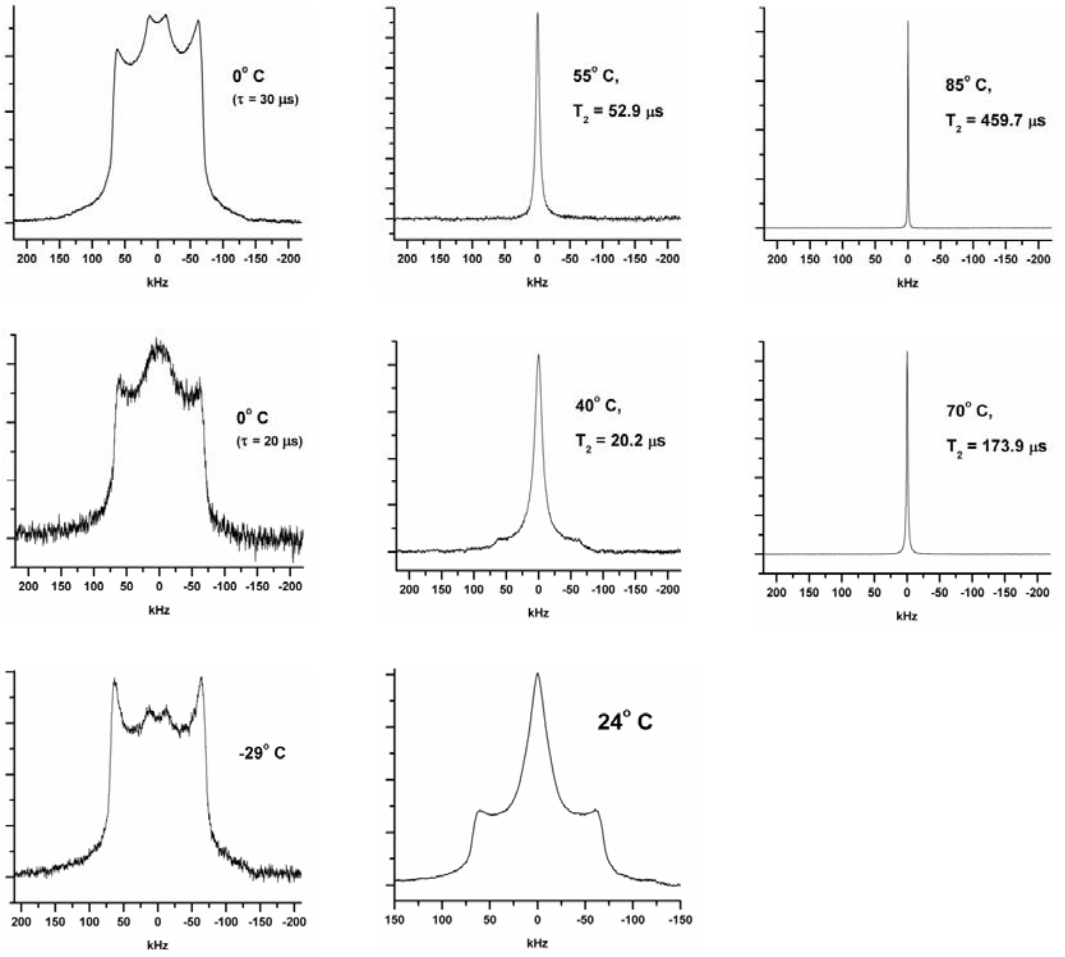

Figure 5-63. ^{2}H quadrupolar-echo NMR spectra of MIL-PRF-23377 clear film exposed to d_5-PhOH/EtOH (3.115/1.0) for 10 minutes, at different temperatures. The recycle delay was 0.2 s, exponential apodization (linebroadening) was 300 Hz, and τ = 20 μs except as noted

At 40°C, in addition to a broad pattern with a splitting of 125.2 kHz that may reflect fairly rigid phenol molecules not undergoing ring flips (despite being just below the melting point of the bulk solid), there is a much sharper single central peak with a HHLW of 15.1 kHz. The spectrum changes as the echo delay τ is increased from 20 to 80 μs (data not shown), at which point no signal is observable. The T_2 obtained from a single-exponential fit is shown on the plot,

$1/(\pi T_2)$ = 15.8 kHz, which is even slightly above the observed HHLW and indicates homogeneous broadening by T_2 relaxation as the source of the entire linewidth observed. Further sharpening is observed at 55°C, where as the echo delay τ is increased from 20 to 100 μs a decay with T_2 = 52.9 μs can be observed. The corresponding predicted homogeneous HHLW is 6.02 kHz, which is just slightly less than the observed HHLW of 6.31 kHz. Further sharpening is observed at 70°C, where as the echo delay τ is increased from 20 to 380 μs a longer decay with longer T_2 = 173.9 μs can be observed. Again, the predicted HHLW of 1.83 kHz is very close to the observed HHLW of 1.85 kHz. Yet further sharpening is observed at 85°C, where as the echo delay τ is increased from 20 to 580 μs a still longer T_2 of 459.7 μs is obtained, corresponding to a predicted HHLW of 0.69 kHz to compare with the experimental HHLW of 0.77 kHz.

The supposition that the central peak in these spectra at 40°C and above is from phenol that has attacked and is covalently attached to the epoxy polymer chain would predict that the peak would become sharper at higher temperatures as a result of increased segmental dynamics, as is observed, due to a combination of a decreased residual quadrupolar interaction as the phenol moiety experiences a wider range of orientations and a longer T_2 value due to increased rates of motion. Single-pulse ^{1}H NMR spectra were obtained on this sample at the various temperatures using the decoupling channel of the double-resonance probe. While not free of proton background signals, a marked decrease in HHLW was observed as the temperature increased from -29°C (~42 kHz) to 0°C (~33 kHz) to 40°C (ca. 11 kHz) to 55°C (ca. 8 kHz) to 85°C (ca. 7 kHz). This reduction in HHLW with increasing temperature compares well to the ^{1}H HHLW vs. temperature results in Figure 5-59 for the same polymer exposed for 10 minutes to the undeuterated solvent mixture, which had a very similar solvent uptake. The slightly greater reduction in HHLW observed for that sample in Figure 5-59 may have to do with the contributions of a sharper peak from the protonated phenol to the overall signal.

While the ^{2}H NMR linewidth narrowing at higher temperatures thus parallels in a crude sense the ^{1}H NMR linewidths, a direct comparison is not meaningful for several reasons. For one, chemical shift differences contribute significantly to the ^{1}H results, especially the 7 kHz (14 ppm) linewidth observed at 85°C. Also, even if the phenol group is covalently attached to the polymer, it would have additional degrees of motional averaging of its anisotropic (quadrupolar) interaction than the main polymer backbone. This could explain the absence of any quadrupolar splitting due to residual anisotropic interactions in the ^{2}H spectra above 40°C. Any interpretation of the ^{2}H NMR results that excludes this covalent attachment would have to account for the marked increase in T_2 as the temperature is increased from 40°C to 85°C. It is conceivable that strong molecular interactions, most likely involving hydrogen bonding, could take place with groups on the polymer and lead to significant temperature-dependences. It would also be valuable to investigate the T_2 temperature dependence of the molten d_5-phenol phase (whose melting point may differ slightly from that of the normal unlabeled molecule) to see if intermolecular hydrogen bonding might strongly influence the relaxation behavior.

The ^{2}H quadrupolar-echo NMR spectra of the MIL-PRF-23377 clear film exposed to d_5-PhOH/EtOH for 2 hours showed narrower peaks at comparable temperatures than those observed in the sample exposed for only 10 minutes (see Figures 5-63 and 5-64). At -7°C there is a ca. 6 kHz broad peak and a sharper peak with HHLW of ca. 260 Hz seen with an echo delay time τ of 20 μs, the latter being emphasized upon increasing τ from 20 to 400 μs. At 8°C the

HHLW is 1.9 kHz with τ of 20 μs, but a τ of 100 μs clearly shows the bimodal character, with a sharper component becoming more apparent. Further increasing the τ to 400 μs yields only the longer T_2 sharper component, whose HHLW is 244 Hz. At 24°C with a τ of 20 μs a peak with a HHLW of 640 Hz is observed. It appears that the bimodal character of the lower-temperature spectra is being made less conspicuous by the broad component becoming sharper at higher temperature. This interpretation is supported by the observed decrease in HHLW from 640 Hz to 530 Hz as τ is increased from 20 μs to 420 μs (data not shown). Going to 40°C and using a τ of 100 μs gave the sharpest peak in this series, with a HHLW of 400 Hz.

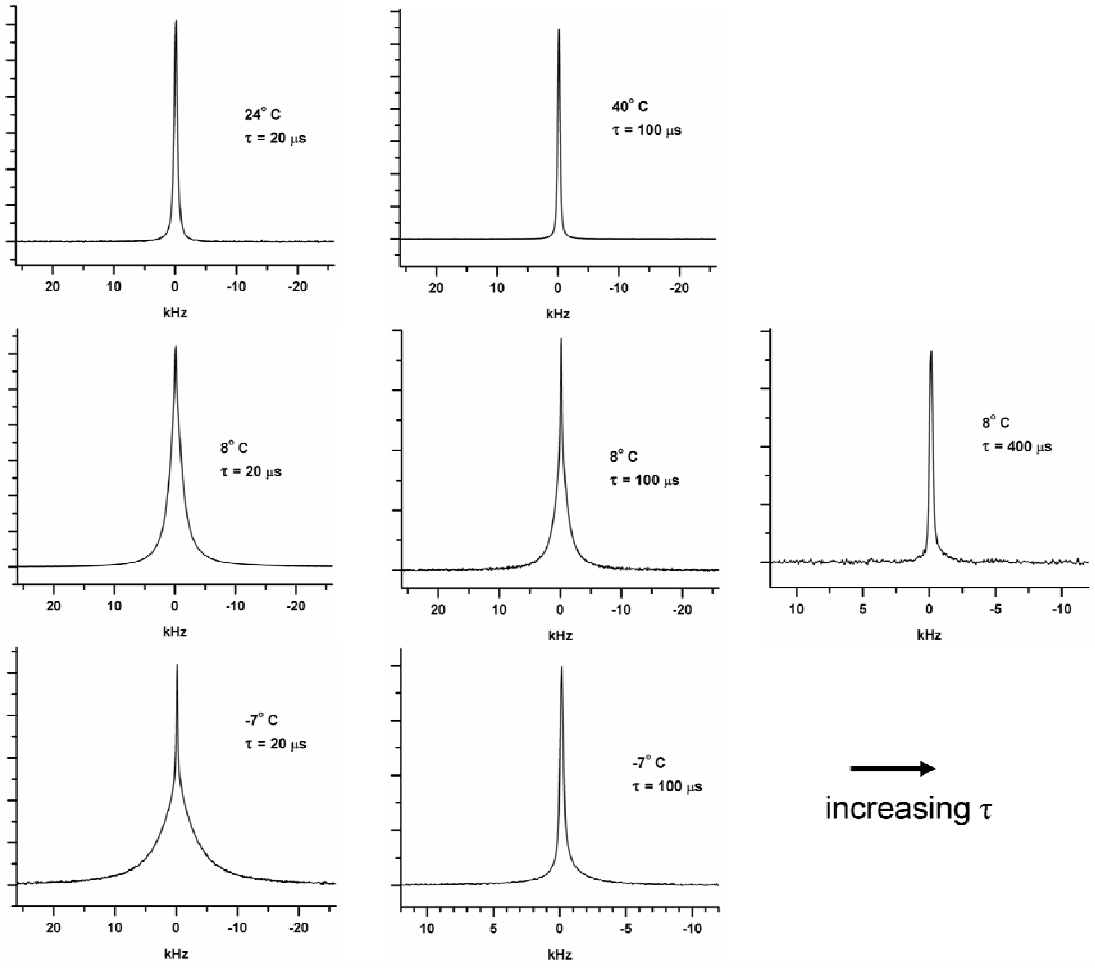

Figure 5-64. ^{2}H quadrupolar-echo NMR spectra at 24°C of MIL-PRF-23377 clear film exposed to d_5-PhOH/EtOH (3.115/1.0) for 2 hours, at four different temperatures and different echo times tau as indicated. The recycle delay was 0.2 s and exponential apodization (linebroadening) was 20 Hz. Note the expanded scale on two of the spectra at longer tau values

As with the results for CD_2Cl_2 discussed above, there are two possible sources of broadening of the ^{2}H NMR peaks. One is the presence of residual (partially-averaged) quadrupole coupling constants due to partial orientation of the molecules. Such orientation could result from molecules constrained in a non-spherical "cavity" within the swollen polymer, as well as from molecules that loosely bind in preferred orientations to groups in the polymer; distributions of

such residual quadrupole couplings would be likely. The second possible source of broadening is purely due to transverse relaxation of an isotropically tumbling molecule whose rotational correlation time is shortened over that in the pure solvent due to the polymer matrix where it finds itself inside. Weak interactions with groups on the polymer could also play a role in slowing down the tumbling rate.

In order to test which of these possibilities are operative, we carried out measurements of the transverse relaxation time T_2 in the sample at 24°C using two different types of echo pulse sequences, as shown in Figure 5-65. The quadrupolar-echo sequence yielded a single-exponential decay constant T_2 of 587.3 μs. This sequence is highly effective in refocusing ^2H nuclei with residual quadrupole couplings, as it is also for ^1H-^1H dipolar couplings betweens isolated pairs of proton nuclei (the sequence in fact was originally developed for the latter case, and is called a "solid echo" pulse sequence when applied there). However, it is not designed to refocus ^2H nuclei lacking residual quadrupole couplings. In contrast, the Hahn echo sequence (90º-τ-180º-τ-Acquire) is designed to refocus nuclei in the latter case, but may also refocus nuclei with suitably small residual quadrupole couplings. This may explain the systematic deviation from a good fit to a single-exponential for the Hahn-echo data in Figure 5-65. A biexponential however produces an excellent fit, with 89.3% of the signal having a T_2 of 573.0 μs and 10.7% having a much longer T_2 of 2996.2 μs. We note that the shorter T_2 value agrees well with that measured from the quadrupolar-echo data, and we thus attribute it to nuclei having small residual quadrupole couplings. The T_2 component of nearly 3 ms we can therefore attribute to more nuclei lacking such residual couplings and behaving as an isotropic liquid with, however, slower rotational tumbling than that of phenol in a normal solvent. We note that a more complicated procedure involving linear combinations of the signals from three pulse sequences of the solid echo and Hahn echo type have been used to cleanly separate the two types of nuclei in the case of ^1H in polymer networks having residual dipolar couplings,[37] and related approaches were earlier applied to ^2H NMR.[38] Such techniques could prove valuable in further NMR studies of these solvent/paint systems.

Interestingly, the shorter T_2 of 573 μs measured as the major component of the biexponential analysis of the Hahn echo results would predict a HHLW of a Lorentzian peak of 555 Hz, which is just slightly below the observed 590 Hz linewidth. Magnetic susceptibility differences and magnetic field inhomogeneities could easily account for the 35 Hz difference. Thus, for the majority of the phenol molecules in this sample it appears that the residual quadrupolar couplings, although appearing to be responsible for the signal observed in the quadrupolar-echo sequence, must be rather small, and the majority of the peak broadening observed is due solely to relaxation.

We can now try to consolidate this interpretation of the T_2 data with the temperature dependence of the spectra shown in Figure 5-64. The spectra obtained with the shortest τ value of 20 μs are the most quantitative, in the sense of representing the best relative proportions of broad and sharp components of the spectra. The -7°C spectrum clearly shows that the broad component dominates the sharper component, and is qualitatively consistent with the 89.3% fraction having the shorter T_2 in the biexponential analysis of the 24°C data above. The narrowing of the broader component observed as the temperature is raised to 8°C thus strongly suggests that the d_5-phenol group is covalently bonded to the polymer, the narrowing arising from increased segmental motion at higher temperature. The non-Lorentzian appearance of the broad

component indicates that it does not arise from an isotropically-tumbling free molecule, even one with a lengthened rotational correlation time. At 24°C and higher, the bimodal character is difficult to see because the broad component attributed to covalently-bound phenol sharpens so significantly. If this interpretation is correct, it appears that most of the phenol in the epoxy sample exposed for 2 hours, with its 124.5% weight gain, may be covalently bonded to the polymer. This would indicate a very extensive reaction, presumably of the phenolate anion with nucleophilic sites either on the polyoxymethylene backbone or on side groups and cross-linking groups as well.

Before discussing some ^{1}H NMR results for this sample, we want to mention the sole literature example we are aware of that studied the motions of d_5-phenol in a polymer by ^{2}H NMR. In a study of d_5-phenol absorbed from CCl_4 solution over 2 days by a rod of Nylon 6, a Lorentzian peak with a HHLW of about 2 kHz was observed, that broadened upon tensile deformation due to partial ordering.[29] The results cannot be compared with ours, except to note a similar reduction in linewidths from the static value due to dynamics.

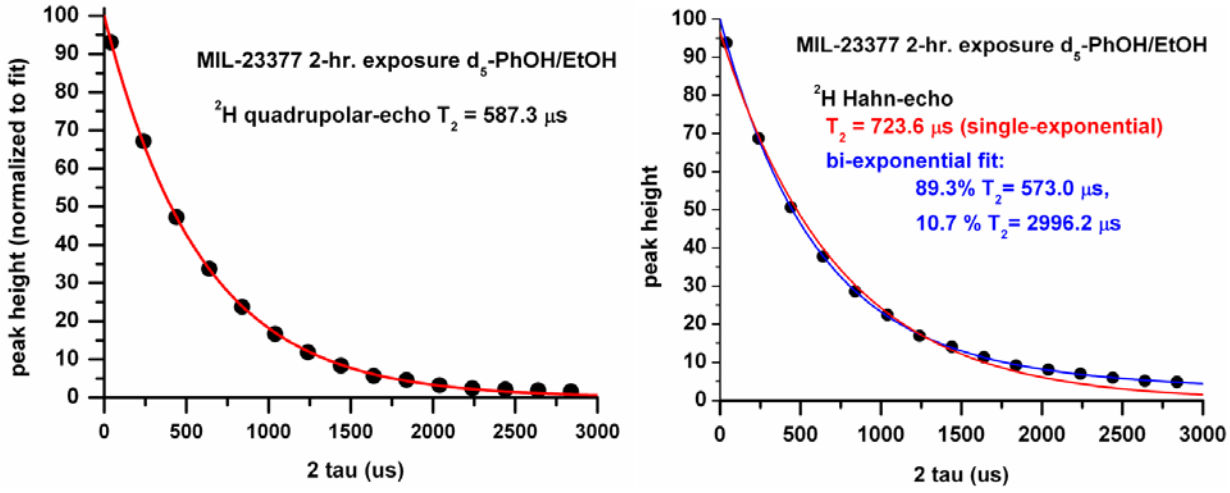

Figure 5-65. ^{2}H decay times at 24°C of MIL-PRF-23377 clear film exposed 2 hours to d_5-PhOH/EtOH, as measured by two different echo pulse sequences (see text). The single-exponential fit on the right is systematically lower than the experimental data points, unlike the biexponential fit

A limited number of ^{1}H NMR spectra of this sample were obtained at the same time as the ^{2}H experiments were performed. Figure 5-66 shows ^{1}H single-pulse NMR spectra of this epoxy MIL-PRF-23377 clear film exposed to d_5-PhOH/EtOH for 2 hours obtained at several temperatures while the sample was in the deuterium probe, by using the ^{1}H double-resonance channel. Although a substantial proton background signal was observed from this probe (unlike the proton probe used for the detailed studies above), quantitation indicated that the signals observed were dominated by the sample. Also, although chemical-shift referencing to a sample of ethanol had been carried out earlier, the slow magnet field drift over the two-week interval will introduce a small error on the order of a ppm into the chemical shift positions (but not the measured splittings depicted in the figure). The presence of two partially-resolved and fairly

sharp ^{1}H NMR peaks over the temperature range -7°C to 40°C is the most obvious feature of the spectra. The separation between the peaks varies in a non-monotonic way with temperature, due mainly to chemical shift changes of the left peak. (data not shown). The assignment of these two peaks to either solvent or polymer groups is not clear at this point. Ethanol itself shows methyl and methylene peaks at 0.96-1.25 ppm and 3.34-3.72 ppm in various organic solvents, with a separation of ca. 2.4 ppm.[39] The chemical shift of the OH peak of methanol in different solvents varies widely depending upon the degree of hydrogen bonding, and can range from at least 1.3 to 4.6 ppm.[39] (Higher temperatures generally disrupt hydrogen bonding and produce low-frequency shifts (to the right in the spectrum). The apparent absence of two peaks in a 3:2 ratio from the methyl and methylene protons (small J-couplings would not be resolved) that have an invariant chemical shift separation is rather puzzling. Ethanol, even allowing for some evaporation, should be a significant constituent in the sample: 13.5%, based on the uptake, and assuming that the 3.115/1 ratio of the d_5-phenol/ethanol solvent mixture is unchanged in the swollen polymer. It is possible that this latter assumption is not met, i.e. the proportion of ethanol decreases in the polymer; chemical spectroscopic analysis of extracted solvent would be a useful way to determine if this is the case. The contribution from residual aromatic protons on the phenol ring should be minimal in view of the 98% deuteration level of these protons. Since the phenol OH was not deuterated, it is tempting to suppose that the fairly sharp peak on the left might be due to hydrogen-bonded OH groups, which would have a temperature-dependent shift. The polymer backbone is likely to contribute to the broader peak at the base, which appears to narrow at higher temperatures as expected for increasing segmental dynamics. It is also possible that methyl groups somewhere in the polymer itself give rise to the peak on the right. A more detailed study of the ^{1}H NMR behavior of this system could clear up these ambiguities.

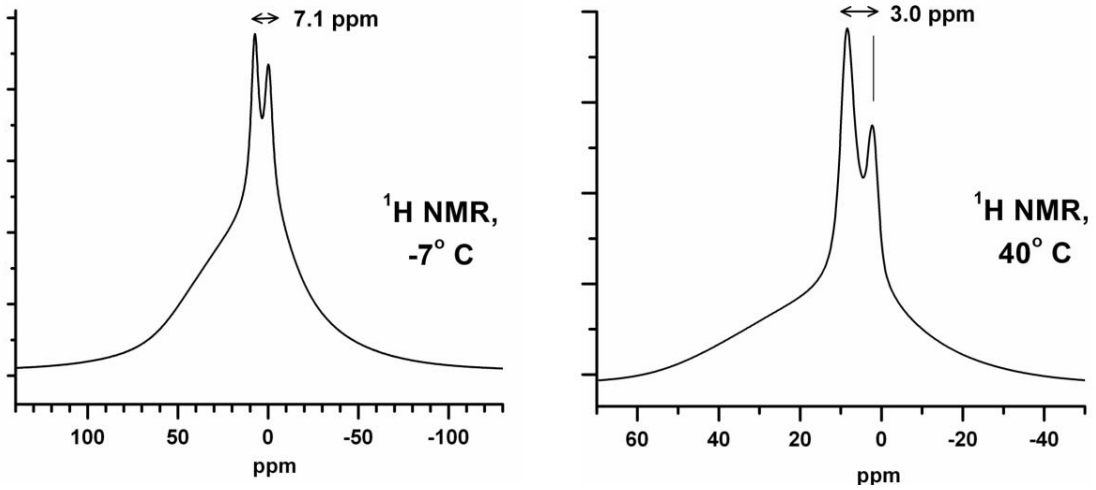

Figure 5-66. ^{1}H NMR spectra of epoxy primer MIL-PRF-23377 clear film exposed 2 hours to d_5-PhOH/EtOH at two different temperatures

5.6 Coating Removal

Coating removal experiments were performed with the MIL-PRF-23377 clear and fully formulated coatings on chromate conversion coated 2024 aluminum panels. These coated panels were aged at 150°F for 7 days prior to the coating removal experiments. The thickness of the MIL-PRF-23377 coatings was measured on 10 different locations using Elcometer 456 for non-ferrous substrates. Thickness measurements for the clear and fully formulated coatings fall between 1.60–1.84 mils (40.64–46.74 μm) and 0.84–1.10 mils (21.34–27.94 μm) respectively.

Three columns were set up on the test panel with the MIL-PRF-23377 clear coating as illustrated in Figure 5-67. The coating was exposed to MC for 4 minutes and 19 seconds, MC/PhOH for 4 minutes, and MC/PhOH/H_2O for 2 minutes and 25 seconds. After the columns were removed, the coating on the panel was checked visually. No visual change was observed on the coating exposed to methylene chloride. The coating exposed to MC/PhOH or MC/PhOH/H_2O was removed as illustrated in Figure 5-68. The difficulty to observe the changes of the clear coating through the glass columns while the coating was exposed to the test solvents, did not allow us to determine coating removal times, but it shows that MC/PhOH and MC/PhOH/H_2O removed the coating faster than methylene chloride.

In an attempt to determine the methylene chloride coating removal time using a different experimental method, in which a solvent was continually dropped onto the coating to keep the area of the coating wet, re-adherence of some of the removed coating was observed as methylene chloride was evaporating. In contrast, for the coating exposed to MC/PhOH/H_2O, re-adherence of the separated coating was not observed. This suggests that at least a role of water or aqueous phenol in a paint stripper is to prevent re-adhering of removed coatings, which has not been reported. It is also noted that separation of the coating wetted with methylene chloride only started in 6 minutes and 58 minutes and quickly spread as illustrated in Figure 5-69. Since there is no other chemical such as water (deemed to break the bonds between a primer and the CCCed substrate) or phenol than methylene chloride was used for this experiment, the solvation stress is only a possible cause of the coating separation from the CCCed substrate. This result also indicates that the bond between the coating and the substrate is weaker than inter-polymer bonds.

Figure 5-67. Experimental Set-up for MIL-PRF-23377 Clear Coating Removal

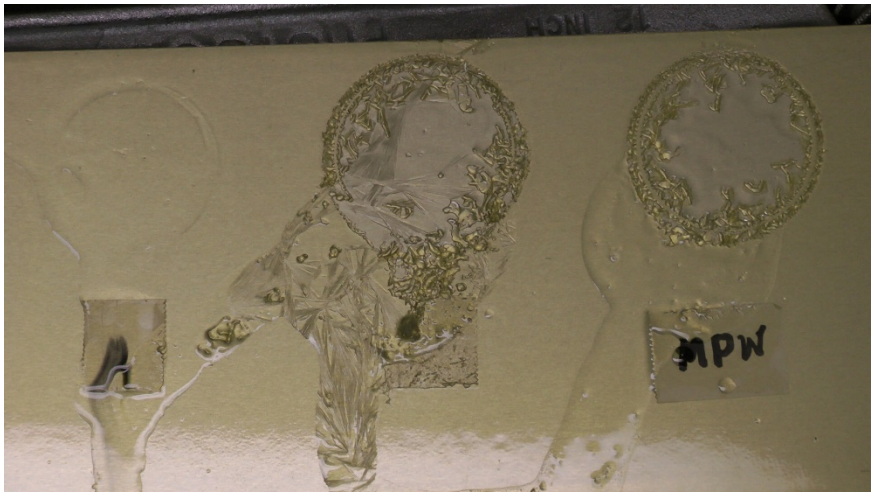

Figure 5-68. MIL-PRF-23377 Clear Coating Exposed to MC, MC/PhOH, or MC/PhOH/H_2O

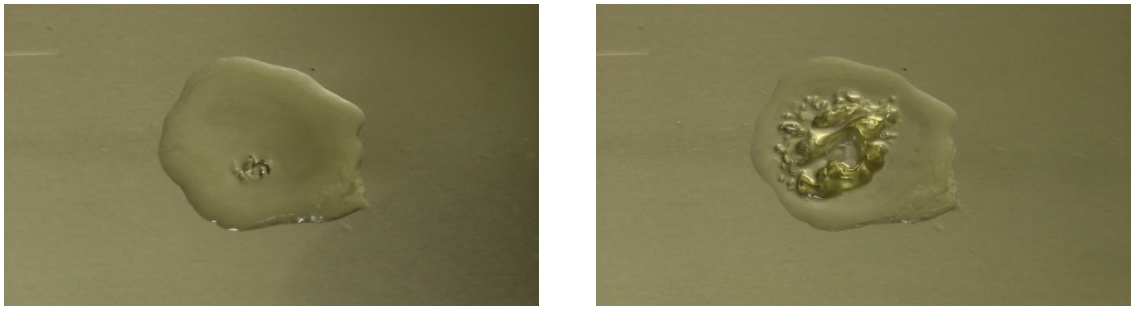

Figure 5-69. Separation of MIL-PRF-23377 Clear Coating Exposed to MC: At 6 Minutes and 58 Seconds (Left), 6 Minutes and 59 Seconds (Right)

The column experiment was performed with the MIL-PRF-23377 fully formulated coating. The coating was exposed to one of three solvents; metylene chloride, MC/PhOH, and MC/PhOH/H_2O for 20 minutes. No visual change was observed in the area exposed to methylene chloride. Gentle wiping with a laboratory towel partially and completely removed the coating exposed to MC/PhOH and MC/PhOH/H_2O as illustrated in Figure 5-70. The results from this experiment indicate that the MIL-PRF-23377 fully formulated coating is more difficult to remove than the MIL-PRF-23377 clear coating. The results also indicate that water, approximately 2% by weight, is an important component of the methylene chloride based paint stripper to remove MIL-PRF-23377. However, this coating removal test doesn't provide information on the role of water in coating removal. Since the weight increase of the MIL-PRF-2337 fully formulated sample exposed to MC/PhOH/H_2O at the sorption equilibrium, 93%, is not much different from the same sample exposed to MC/PhOH, 85%, the solvation stress in the sample is not likely

increased enough by 2% water to make the difference that we saw from the coating removal test. Then, the water induced interfacial delamination[40] may be the reason for faster removal of MIL-PRF-23377 coating exposed to MC/PhOH/H_2O.

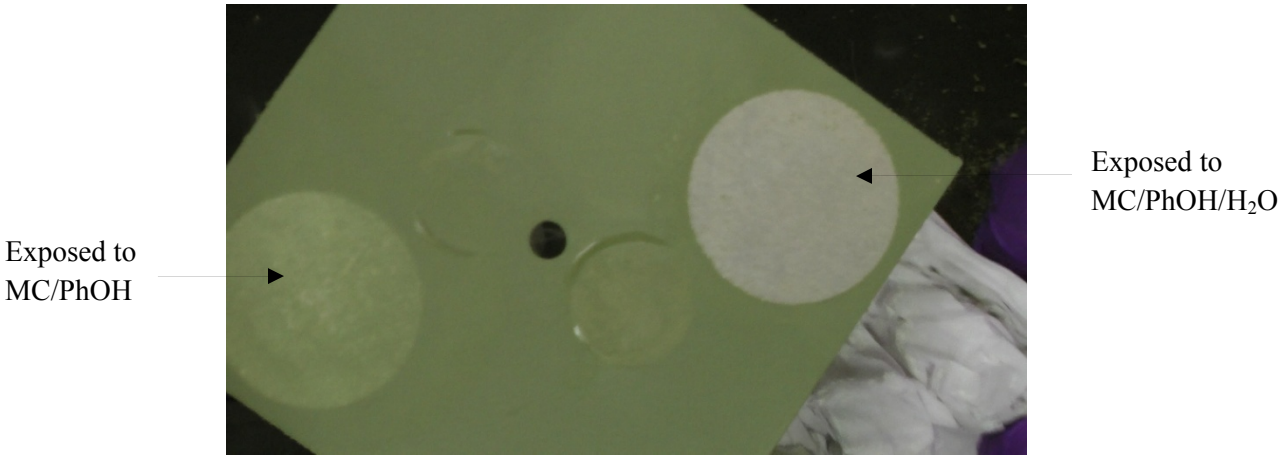

Figure 5-70. MIL-PRF-23377 Fully Formulated Coating Exposed to MC/PhOH and MC/PhOH/H_2O

6. Conclusion

Diffusion cell test results indicate that the high diffusivity of methylene chloride enables it to penetrate quickly through polymeric binders and create diffusion channels for slower-diffusing, polar co-solvents and activators which are present in solution. Methylene chloride also swells coatings as evidenced by the solvent sorption test, Raman, and ^{1}H and ^{2}H NMR. ^{1}H NMR results show that methylene chloride solvates the coating and is in close contact with the polymer chains. ^{2}H NMR shows restriction to the tumbling of methylene chloride, which is likely due to the dipole-dipole interaction between methylene chloride and the polar groups on the polymer. Raman spectroscopy suggests dilation of coating binders by solvating the carbonyl groups of the polymer chains.

Unlike methylene chloride, phenol is not a good penetrant; however, it does substantially swell the polymeric binders when it solvates polymers as gravimetric solvent sorption studies indicate. When the internal stress created by solvation is not effectively relieved, coatings find its way to release the stress. For the coated panels, the internal stress seems to cause coating removal. DSC shows significant depression of the glass transition temperature of all the coatings after exposure to solvent mixtures containing phenol, but little change after exposure to methylene chloride. This DSC result indicates the effectiveness of phenol in coating solvation. The possibility of polymer chain scission by phenol or hydrolysis is suggested based on the results of the FTIR-ATR, XPS, and NMR studies.

Water alone cannot easily penetrate through the military coating system. Yet, when it is formulated with other components such as methylene chloride, phenol, and ethanol, water diffuses into coatings and helps remove organic coatings as demonstrated by the coating removal experiments. The solvent sorption experiment performed with the MIL-PRF-23377 fully formulated sample shows water does not change the weight or volume of the sample significantly as compared to the sample exposed to MC/PhOH. Therefore, it seems that water helps break distressed bonds between the epoxy primer and the chromate conversion coated substrate due to polymer solvation.

(This page intentionally left blank)

7. Literature Cited

1. J.H. Cantrell, *J. Appl. Phys.*, **96**, 3775 (2004)
2. J. Kozol, D. Conrad, S. Hartle, G. Neumeister, and S. Spadafora, Techinical Report, NAWCADPAX-98-236-TR, (1999).
3. Material Protection Report, P-171, Naval Air Warfare Center Aircraft Division (NAWCAD), (1999).
4. P. Michelin and E. Ollivier, "Impact of VOC Regulations on Paint Adhesion", 5th European Adhesion Conference, September 18-21, (2000).
5. W.E. Kosik, "Mechanism of Military Coatings Degradation: Surface Characterization via X-ray Photoelectron Spectroscopy", Part of SERDP PP-1133 Final Report, (2003).
6. Phase 3 Low VOC CARC Stripping and Disposal, Final SERDP Report, Prepared by Southwest Research Institute for Coating Technology Integration Office Wright-Patterson Air Force Base, OH, April 2000.
7. P. Morrissey and D. Vesely, *Polymer*, **41**, 1865, (2000).
8. D. Vesely, *Int. Mater. Rev.*, **53**, 299, (2008).
9. M.R. Vanlandingham, R.F. Eduljee, and J.W. Gillespie, *J. Appl. Polym. Sci.*, 71, 787, (1999).
10. J. Asaad, E. Gomaa, and I.K. Bishay, *Mat. Sci, Eng. A*, **490**, 151, (2008).
11. D. Vesely, *Polymer*, **42**, 4417, (2001).
12. R. Parthasarathi, V. Subramanian, and N. Sathyamurthy, *J. Phys. Chem. A*, **109**, 843, (2005).
13. T. Alfrey, E.F. Gurnee, and W.G. Lloyd, *J. Polym. Sci.*, **12**, 249, (1966).
14. J.E. Ritums, M.S. Hedenqvist, T. Prodan, and I. Emri, *Polym. Eng. Sci.*, 1194, (2005)
15. C.N. Young and C.R. Clayton, "Spectroscopic analysis of the effects of methylene chloride- and phenol-based paint stripping solvent exposure on model coating systems", 2010 Partners in Environmental Technology Technical Symposium & Workshop, poster 69, abstract #313 (2010)
16. J. Graham, T. Yamada, W. Culhane, and E. Nyarko, "A fundamental study of the activity of selected paint stripping components with epoxy and polyurethane coatings", 2010 Partners in Environmental Technology Technical Symposium & Workshop, abstract #167 (2010)
17. G.L. Marshall and J.A. Lander, *Eur. Polymer. J.*, **21**, 959 (1985)
18. R.A. Scott, B.A. Cowans, and N.A. Peppa, *J. Polym. Sci. Part B*, **37**, 1953 (1999)
19. W. T. Ford, M. Periyasamy and H. O. Spivey, *Macromolecules*, **17**, 2881 (1984)
20. L. Calucci, C. Forte and E. Ranucci, *Biomacromolecules*, **8**, 2936 (2007)
21. I. Devotta, V. Premnath, M. V. Badiger, P. R. Rajamohanan, S. Ganapathy and R. A. Mashelkar, *Macromolecules*, **27**, 532 (1994)
22. R. A. Orza, P. Magusin, V. M. Litvinov, M. van Duin and M. A. J. Michels, *Macromolecules*, **40**, 8999 (2007)
23. K. Ogino and H. Sato, *J. Appl. Polym. Sci.*, **58**, 1015 (1995)
24. S. Schlick, Z. Gao, S. Matsukawa, I. Ando, E. Fead and G. Rossi, *Macromolecules*, **31**, 8124 (1998)
25. L. W. Jelinski, J. J. Dumais, A. L. Cholli, T. S. Ellis and F. E. Karasz, *Macromolecules*, **18**, 1091 (1985)

26. L. S. Loo, R. E. Cohen and K. K. Gleason, *Polymer*, **41**, 7699 (2000)
27. B. Deloche and E. T. Samulski, *Macromolecules*, **14**, 575 (1981)
28. P. T. Callaghan and E. T. Samulski, *Macromolecules*, **36**, 724 (2003)
29. L. S. Loo, R. E. Cohen and K. K. Gleason, *Macromolecules*, **32**, 4359 (1999)
30. Z. Veksli and W. G. Miller, *Macromolecules*, **8**, 248 (1975)
31. A. Guyot, A. Revillon, M. Camps, J. P. Montheard and B. Catoire, *Polym. Bull.*, **23**, 419 (1990)
32. S. L. Regen, *J. Am. Chem. Soc.*, **96**, 5275 (1974)
33. S. L. Regen, *J. Am. Chem. Soc.*, **97**, 3108 (1975)
34. S. L. Regen, *Macromolecules*, **8**, 689 (1975)
35. J.P. Yesinowski, *J. Am. Chem. Soc.*, **103**, 6266, (1981)
36. M.A. Janusa, X. Wu, F.K. Cartledge and L.G. Butler, *Env. Sci. Tech.*, **27**, 1426, (1993).
37. P.T. Callaghan and E.T. Samulski, *Macromolecules*, **30**, 113, (1997).
38. J. Collignon, H. Sillescu and H. W. Spiess, *Colloid & Polymer Science*, **259**, 220. (1981)
39. H.E. Gottlieb, V. Kotlyar and A. Nudelman, *J. Org. Chem.*, **62**, 7512, (1997)
40. H.B. Fan, E Chan, C. Wong, and M. Yuen, *J. Adhesion Sci. Technol.*, **20**, 1937 (2006).

8. Appendices

8.1 List of Scientific/Technical Publications

Watson, K.E.; Wynne, J.H. Yesinowski, J.P.; Han, Y.; Young, C.N.; Clayton, C.R. “Mode of action of chemical paint strippers in removing robust polymeric coatings” 242nd ACS National Meeting and Exposition, August 31, 2011, Denver, CO, poster 14553.

Watson, K.E.; Wynne, J.H. Yesinowski, J.P.; Young, C.N.; Clayton, C.R. “Role of Methylene Chloride and Phenol in Chemical Paint Strippers” 41st Annual ACS Mid-Atlantic Regional Meeting, April 11, 2010; paper 212.

Wynne, J.H.; Watson, K.E.; Yesinowski, J.P.; Young, C.N.; Clayton, C.R.; Nesteruk, N.; Kelley, J.; Braswell, T. "Interim Report on Scientific Basis for Paint Stripping; Mechanism of Methylene Chloride Based Paint Removers" NRL Memorandum Report # NRL/MR/6120-10-9303.

Watson, K.E.; Wynne, J.H.; Lundin, J.G.; Yesinowski, J.P. "Novel Environmentally Friendly Approach to Paint Strippers Based in Interfacial Mechanistic Studies" 240th Annual ACS National Meeting, August 25, 2010; Boston, MA, poster 281.

Watson, K.E.; Wynne, J.H.; Yesinowski, J.P. "Progress Toward Understanding the Mechanism of Action in Methylene Chloride/Phenol Based Paint Strippers" 2010 Partners in Environmental Technology Technical Symposium & Workshop, December 1, 2010, Washington, DC, poster 50, abstract #42.

Young, C. N.; Clayton, C.R. “Spectroscopic analysis of the effects of methylene chloride- and phenol-based paint stripping solvent exposure on model coating systems” 2010 Partners in Environmental Technology Technical Symposium & Workshop, December 1, 2010, Washington, DC, poster 69, abstract #313

Han, Y. et al., “Scientific basis for paint stripping mechanism of methylene chloride based paint strippers” December 1, 2010, Washington, DC, abstract #138

Han, Y. “Scientific basis for paint stripping mechanism of methylene chloride based paint strippers", 2010 Air Vehicle Conference, June 27-30, Washington, DC.

(This page intentionally left blank)